Visual Perception and Processing of Radial Motion

Niia Emilova Nikolova

Doctor of Philosophy (PhD)

City University of London

School of Health Sciences

June, 2018

Contents

List of Figures

List of Tables

Acknowledgements

I am grateful to many people for their guidance and support for this thesis. As my supervisor, Michael Morgan has been a source of guidance and wisdom, and has been constantly supportive of me being a mother as well as a researcher. I am thankful to my second supervisor Josh Solomon for his ideas and encouragement, however sporadic our visits have been.

A further thank you to the lab members at the Max Planck Institute; Sabine Raphael, for helping me get to terms with Matlab, Kai Schreiber, for sharing his invaluable experience with MRI, and Barbara Dillenburger for support and discussions. Thank you also to the MRI technicians and numerous administrative staff.

I extend my appreciation to all those who sat as observers in my lengthy experiments and dedicated many hours to collecting data!

A big thank you to my family, both close and those spread over the planet for their enduring support. To Alberto for his love, support and helping me be a happier and better person, to Pepe for his excitement to start each day, to my parents for their advice and motivation, and to my grandparents for their support. All of you are a great inspiration.

Declaration

I herewith declare that I have produced this thesis without the assistance of third parties and without making use of aids other than those specified; notions taken over directly or indirectly from other sources have been identified as such. This work has not previously been presented in identical or similar form to any examination board.

The work presented in this thesis was conducted from 2011 to 2016 under the supervision of Dr. Michael Morgan and Dr. Josh Solomon.

I grant powers of discretion to the University Librarian allowing the thesis to be copied in whole or in part without further reference to myself. This permission covers only single copies made for study purposes, and is subject to normal conditions of acknowledgement.

London, United Kingdom

Abstract

As we navigate the environment, images flow over our retinae and produce complex moving patterns including contraction and expansion. These in turn serve to inform us about our movement in the world, as well as about the positions and relative motions of the objects around us. The processes underlying the perception of radial motion were explored using psychophysics, eye tracking and functional magnetic resonance imaging (fMRI). The initial experiments studied how adaptation to radial motion affects discrimination using partially-coherent dot stimuli. Adaptation increased absolute detection thresholds in the adapted direction, but had no effect on the discrimination of higher pedestals. The change in sensitivity is consistent with a divisive inhibition mechanism, as well as with one based on proportion estimates. An orientation discrimination experiment adds support for the latter. Directed attention to one component of a motion-balanced transparently-moving stimulus impairs sensitivity to a level comparable to that following adaptation, although there were large inter-subject differences. A novel approach using relative velocity adjustments of transparently-moving dot fields was used to investigate the reference frame of motion adaptation, which is shown to be mainly retinotopic and diminished by gaze modulations. Finally, fMRI was used to probe the neural substrates of radial motion perception, including retinotopic mapping, localisation of MT/MST, and selectivity for contraction and expansion within the MT+ complex.

To Alberto and Pepe - my home.

Publications

Some of the work described in this dissertation has been previously published in poster or presentation form at scientific conferences.

- Nikolova, N. E. and Raphael, S. (2012). The reference frame of the motion aftereffect examined using velocity adjustments, *Perception* **41**(S): 180.
- Nikolova, N. E. and Morgan, M. J. (2013). Changes resulting from adaptation to radial motion, *British Neurosci. Assoc. Abstr.* **22**: 664
- Nikolova, N. E. and Morgan, M. J. (2013). Discrimination functions for radial motion and for orientation, *Perception* **42**(S): 184
- Nikolova, N. E. and Morgan, M. J. (2013). Mechanisms for discrimination following adaptation to radial motion, *Neuroscience Meeting Planner* **06**: 458
- Nikolova, N. E. and Morgan, M. J. (2014). Discrimination following adaptation to radial motion, comparison of spatial and temporal two-alternative forced choice tasks, *AVA X-Mas Meeting*
- Nikolova, N. E. and Morgan, M. J. (2016). Representation of radial motion in the visual cortex, *Scientific Advisory Board Meeting, Max Planck Society*
- Nikolova, N. E., Solomon, J. A. and Morgan, M. J. (2018). Asymmetrical responses to contraction and expansion in human MT+ complex, *Scottish Vision Group Meeting*

Glossary

1D, 2D, 3D one, two, three dimensional

aMRI anatomical magnetic resonance imaging

BOLD blood oxygenation-level dependant

CRT cathode ray tube monitor

CSF cerebral spinal fluid

DT detection threshold

EEG electroencephalography

EPI echo-planar imaging

fMRI functional magnetic resonance imaging

GE gradient echo

hMT+ human area MT including parts of adjacent areas (MT+)

HRF hemodynamic response function

IPS intraparietal sulcus

MAE motion after-effect

MEG magnetoencephalography

MRI magnetic resonance imaging

mse mean square error

MT middle temporal area (V5)

MVPA multi-voxel pattern analysis

PET positron emission tomography

PFC prefrontal cortex

PIT posterior inferotemporal area

ROI region of interest

s2AFC spatial two-alternative forced choice

SNR signal to noise ratio

t2AFC temporal two-alternative forced choice

TE time to echo

TMS transcranial magnetic stimulation

TR repetition time

V1 primary visual cortex, located on posterior pole of occipital cortex

V2 visual area V2, secondary visual cortex (prestriate cortex)

V3 visual area V3, third visual complex

V4 visual area V4, extrastriate visual cortex, located on posterior inferotemporal area (PIT)

V5 visual area V5/MT (middle temporal)

VOI volume of interest

voxel three dimensional pixel

Chapter 1

Introduction

This chapter outlines the scientific background related to this dissertation. First, the basic physiology of the visual system is described. The general background for psychophysics and the perception of visual motion are given, with an emphasis on the motion aftereffect and different measures thereof. Attentional processes and specifically their effect on motion perception are outlined. Finally, the basics of functional magnetic resonance imaging are described along with an overview of studies applying it to the study of motion processing.

1.1 Basic physiology of vision

1.1.1 The retina

The pathway that processes visual information about the outside world begins in the eye. As light falls on the retina, it is detected by individual photoreceptors sensitive to varying wavelengths and intensities of the electromagnetic spectrum. There are two classes of photoreceptor; rods and cones. Rods are highly sensitive light intensity, they pool over large areas and can detect a single photon, whereas three types of cones are sensitive to different ranges of wavelengths. The photoreceptors are not on the outer retinal surface - rather, light has to pass through the thickness of the retina before

reaching them. Light first passes through a dense layer of glial cells which, beside performing support and maintenance for neurons, act to channel the light onto the photoreceptors. This arrangement appears to be a result of optimisation; green and red wavelengths pass through the glial cell layer easier and are concentrated onto the cones 5 - 10 x more than blue wavelengths. As there is excess blue light in the atmosphere, this adaptation allows cones to function well with less light. The rods and cones then perform phototransduction, the transformation of light into neural signals. These signals take the form of fluctuating membrane potentials that combine onto horizontal and bipolar cells. The horizontal cells provide feedback to photoreceptors, allowing them to adjust to differing light conditions.

Bipolar cells meanwhile, receive input from either rods or cones and synapse onto retinal amacrine cells (rod bipolar cells) and ganglion cells (cone bipolar cells). The receptive fields of bipolar cells vary in size, and they may thus be selective to spatial scale. Those with smaller receptive fields are sensitive to fine structures (high spatial frequency), and those with larger receptive fields respond to rougher structures (low spatial frequencies). When the photoreceptors in its receptive field are exposed to light, an ON bipolar cell becomes active, while an OFF bipolar cell is inhibited. The information from photoreceptor cells converges onto bipolar cells and there are thus many more of the latter (80-110 million rods, 4-5 million cones) than the former (36 million BP cells). There is a one-to-one relationship between cone photoreceptors and bipolar cells, meaning that the 11 types of cone bipolar cells (Strettoi et al. 2010) are much more common in the foveal retina, while more rod bipolar cells are found in the periphery. On- and off-centre ganglion cells are present in roughly equal numbers, and their RFs have overlapping distributions so that every spot on the retina is covered by several ganglion cells of different arrangements.

There is evidence in non-human primates that motion processing begins as early as the retina, namely in one of around forty types of amacrine cell called the starburst

amacrine cell (SAC) (Taylor & Smith 2012). Receiving signals from the rod bipolar cells, SACs are a type of interneuron whose dendrites spread out in all directions in a typical 'starburst' pattern. They respond to stimuli which move from their cell body (soma) towards the distal dendrites. They are therefore sensitive to centrifugal motion, but not to motion in the opposite direction. The mechanism by which they compute direction of motion is similar to the Reichardt detector (see Section 1.3.1). SACs synapse onto retinal ganglion cells, some of which are also known to respond selectively for directions of movement (Barlow & Levick 1965).

Both horizontal and amacrine cells connect to the retinal ganglion cells (RGCs) on the retinal surface. Direction-selective (DS) ganglion cells are divided into three types. On/Off DS ganglion cells detect local motion, and fire at the onset and offset of a stimulus (light source). On DS ganglion cells respond only to the leading stimulus edge and Off DS cells respond only to the trailing edge (Borst et al. 2011).

Other types of RGCs have 'centre-surround' receptive fields which are defined by the geometry of connections leading to them from amacrine and bipolar cells. Each RGC is sensitive to local luminance variations between the centre of their receptive field and a concentric annulus surrounding it (i.e. on-centre ganglion cells prefer light spots and off-centre ganglion cells prefer dark spots), and responds to the net sum of its excitatory and inhibitory inputs. Whereas photoreceptors generate membrane potentials, ganglion cells generate action potentials along their axons which travel down the optic nerve to the brain. Single-cell recordings from RGCs in animals have long been used to study their receptive field properties. For example, when a light is shone in the centre of an on-centre ganglion cell's receptive field, its firing rate increases suddenly. If the light is positioned in the surround instead, the cell is suppressed and its firing rate decreases from the baseline. It is interesting to note that, when the light is switched on in the surround, the response increases briefly as it is released from inhibition. Because of these properties, ganglion cell output to the brain contains information on edge contrasts of

various spatial scales, their phase and location, as well as direction of motion.

Retinal ganglion cells can be subdivided into different kinds - M (magnocellular) ganglion cells receive input from both rods and cones and are most sensitive to black and white, while P (parvocellular) RGCs receive only cone input and are sensitive to colour. The M and P cells project to distinct layers in the LGN (lateral geniculate nucleus, see Section 1.1.2) of the thalamus, and this division propagates into the cortex.

Before moving on, it is important to mention that in addition to these feed-forward connections, there are also feed-back connections from the cerebral cortex to ganglion cells, as well as from bipolar and horizontal cells back to photoreceptors in lizards and salamanders (Jackman et al. (2011), Werblin & Dowling (1969)). This feed-back likely modifies photoreceptor responses based on prior experience. Furthermore, mammalian ganglion cells can be subdivided into 10 - 15 distinct morphological types, and there are 10 or more different kinds of bipolar cells. Considering the connectivity of the retina, it is possible that it may contribute to some visual processing which is classically attributed to the brain (Wässle 2004).

1.1.2 The central nervous system

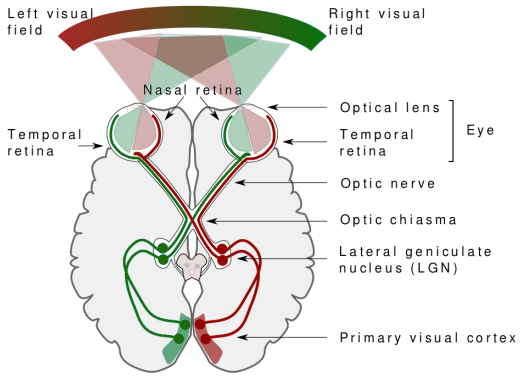

Figure 1.1: Schematic of the human visual system Axons from the nasal and temporal retina travel through the optic nerve to the LGN in each hemisphere. The nasal fibres cross at the optic chiasm before reaching the LGN, while the temporal fibres stay on the ipsilateral side. The optic tracts then carry the fibres from the LGN to the respective primary visual (striate) cortex, preserving neighbourhood relations. - *modified from Wikipedia*

In mammals, the optic nerve carries the axons of the retinal ganglion cells in each retina, and makes the first synapses to the brain in the lateral geniculate nucleus (LGN) in each hemisphere (see Figure 1.1). Before this, the optic nerve fibres from the nasal half of the retina cross at the optic chiasm, and thereby send their signals to the cerebral hemisphere on the opposite (contralateral) side. The lateral fibres stay on the same (ipsilateral) side of the brain. The result of this crossing over is that, after the LGN, the optic tract fibres carry information about the contralateral visual field to the first cortical visual area - the striate cortex (V1). Throughout the visual pathway, from retina to V1 and higher visual areas, the neighbourhood relations between adjacent ganglion cells are preserved, resulting in a retinotopic map. The central part of the retina (the fovea) is over-represented in the retinotopic maps of each hemisphere, which reflects the relatively high proportion of cells in the striate cortex allocated to analysing the foveal region of the visual field. Rather than terminating in the LGN, some optic nerve fibres connect to the left and right superior colliculus, which appears to be involved in mediating visual attention.

Some 'simple cells' in V1 are binocular, meaning that they receive input from both eyes in such a way that the V1 in each hemisphere represents the contra-lateral visual field. They are sensitive to orientation and spatial frequency (Huebel & Wiesel 1959), and selective as to the position of a stimulus on their receptive field. They may also have phase-shifted fields in the two eyes making them sensitive to binocular disparity. The output from the simple cells converges onto 'complex cells'; while they share many properties, the receptive fields of complex cells are not divided into excitatory and inhibitory regions (Huebel & Wiesel 1962). They prefer moving stimuli and are space- and phase-invariant (de Valois R. L. & de Valois K. K. 1988), meaning that it does not matter where an optimal stimulus falls on their receptive field. V1 also contains 'hypercomplex' cells which are additionally selective for stimulus length. Furthermore, neurons in the striate cortex are organised into orientationally-tuned columns and

alternating ocularity bands.

After V1, the visual pathway connects to extrastriate areas where cells are selective for increasingly complex features. According to the two-stream theory (Goodale & Milner 1992), upon leaving the occipital cortex the pathway divides into a ventral ("what") and a dorsal ("where") stream. The ventral stream is implicated in object recognition and travels to the temporal lobe, while the dorsal stream terminates in the parietal lobe and processes motion and positional information. Early lesion studies showed that damage to temporal areas in monkeys resulted in deficiencies in identifying objects, while lesions to parietal areas caused problems in locating them. It is important to note however, that while this theory provides a useful framework, there is significant interaction between the two streams, and they are far from independent from one another. An fMRI study has in fact shown that the regions that respond to form coherence, a global processing measure in the ventral stream, are located close to those responding to motion coherence and are scattered over many posterior cortical regions (Braddick et al. 2000). Furthermore, the information processing stream is far from one-directional - there is for example evidence of top-down modulation from frontal cortex on the retinotopic visual cortex (Ruff et al. 2006).

1.1.3 Physiological mechanisms for motion perception

As mentioned in Section 1.1.1, the M and P RGCs of the retina project to distinct magnocellular and parvocellular layers in the LGN. Compared to P ganglion cells, M cells have large receptive fields, are selective to luminance contrast, and respond quickly to changes in stimulation. These properties make the M cells good candidates for the first step in motion perception (Livingstone & Hubel 1988). This selectivity is maintained in the M and P layers of the LGN, with the magno cells there being more sensitive to stimulus changes and luminance contrast, and less sensitive to fine spatial detail and colour than the parvo cells. The magno cells go on to project to layers in V1

which connect to areas MT and MST, both of which are involved in motion processing.

The first specifically motion-selective cells are found in area V1. What makes these cells truly motion-selective and not only sensitive in stimulus changes over time, is that their response changes as a function of stimulus direction, responding the most to stimuli moving in their preferred direction and least to stimuli moving opposite the preferred direction. The outputs that then project to area MT are involved in the integration of individual local motions into the percept of coherently moving fields and objects. A class of stimuli which has been instrumental in showing integrative motion processes have been plaid gratings. These are composed of two superimposed gratings which move in different directions, and are usually perceived as a plaid pattern moving in the composite direction of the two components, rather than in the directions of the individual gratings. Movshon et al. 1985 have shown that some cells in MT respond to the individual component motions in plaid gratings (component cells), while pattern cells respond to the composite of the two motions. The later only make up about one quarter of all MT cells, indicating that integration largely occurs further on in the motion stream.

While early visual areas respond to simple motion stimuli such as unidirectional pattern motion, the neurons in areas further along the visual stream respond to increasingly complex features such as form-from-motion and optic flow patterns (Yu, Page, Gaborski & Duffy 2010). Neurons in area MT are selective for direction of translation. Area MST receives input from MT cells and has been shown to be sensitive to patterns of complex motion: contraction, expansion, rotation, and spiral movement (Mineault et al. 2012, Orban et al. 1992). In monkeys, particularly the dorsal portion of MST (MSTd) contains neurons that respond to particular patterns of motion in their large receptive fields; patterns that are often a result of self-motion, and are therefore useful for navigation and for visually guided behaviour. Such 'optic flow' provides rich information about our movement through the environment, about object motion, posture stabilization, as well

as about our bodily movements (see also 3.2). In 1950, Gibson suggested that higher order mechanisms must be responsible for the estimation of optic flow information in order to guide our behaviour within the surrounding world.

Cells in MT have relatively small receptive fields only a few degrees in diameter and generally respond to simple planar motions in one direction (Maunsell & Van Essen 1983*a*). Meanwhile, neurons in MST have much larger receptive fields (around 60 degrees) which can extend into the ipsi- and contralateral visual fields, and their receptive field sizes do not increase significantly with retinal eccentricity (Duffy & Wurtz 1991*a*,*b*, Orban et al. 1992, Tanaka et al. 1989). As they have been shown to respond selectively to contraction, expansion, rotation, spiral, and multi-component motions (Graziano et al. 1994, Saito et al. 1986, Tanaka et al. 1989, Wurtz & Duffy 1992), cells in MST are much more likely to be involved in optic flow computations than those in MT. MST is not the only cortical area that responds to complex motion, for example area 7a in the ventral intraparietal cortex is also highly selective for optic flow (Read & Siegel 1997, Schaafsma et al. 1997), and V3a has recently been shown to be involved in the computation of the focus of expansion (Strong et al. 2017).

1.2 Psychophysics

1.2.1 Thresholds

Thresholds are one of the fundamental measurements in the study of sensory perception, defining the minimal stimulus change that can be detected on a particular dimension (e.g. contrast, orientation or motion). Gustav Fechner, in his *Elemente der Psychophysik* (1860) first accurately described and compared three standard methods of measuring thresholds - the method of adjustment, the method of limits, and the method of constant stimuli. In psychophysics, thresholds can be defined as the stimulus intensity at which the observer's probability of responding correctly reaches a certain level (often 75 percent). The reason that the probability of a correct response increases gradually instead of as a

step function is generally thought to be random noise which causes variations in the signal intensity. Both external noise (e.g. a fluctuating light in the environment) and internal noise (e.g. random variations in cell firing rates) contribute to the stimulus signal. The noise is often assumed to be Gaussian. The absolute, or detection, threshold is the smallest stimulus that can be perceived, while the smallest *difference* in stimuli that we can see is the just noticeable difference (JND). For example, if we present a small dot of increasing brightness from black to white on a black background, the luminance at which the dot just becomes visible to the observer is the absolute threshold. If we then measure the minimum luminance that can be distinguished from the background as we increase its luminance, that would be the JND. When the JND is plotted as a function of the baseline signal intensity, it is called a threshold-versus-contrast (TvC) function; these functions often have a characteristic dipper shape. They can be divided into two regions: an initial facilitation region where the JND decreases with increasing stimulus intensity below the detection threshold, and a masking region thereafter where the JND increases proportionately with the baseline intensity. Dipper functions have previously been reported for blur (Georgeson 1994, Watt & Morgan 1983) and motion (Morgan, Chubb & Solomon 2006, 2011) discrimination.

1.2.2 Signal detection theory

Signal detection theory (SDT) is a branch of mathematics which is concerned with the problem of detecting signals within a noisy world (Green & Swets 1966, Peterson et al. 1954). Originally formulated for the use in radar systems, it has been elaborated and is used in diagnostics, telecommunications, and biological systems. Applied to psychophysics, SDT replaced the single threshold with the concepts of a sensory process and a later decision process. In this way, it avoided confounding sensitivity with the response criterion (bias) of the decision process, as was often the case with classical psychophysical methods such as the method of limits. SDT further described experimental

methods (such as 2AFC, described below) based on its theoretical assumptions.

In order to differentially measure the sensitivity and the criterion in a single-interval 'yes-no' task, it is necessary to measure the conditional probability that the observer responds "yes" when the stimulus is present (the hit rate, HR), as well as the conditional probability that they respond "yes" when the stimulus is absent (the false alarm rate, FAR). In the framework of Gaussian signal detection theory, the HR and FAR can be used in order to estimate the detection sensitivity and the decision criterion.

SDT assumes that the sensory process produces a continuous output by combining the stimulus signal with random Gaussian noise. Sensitivity is based on the difference in the mean outputs of the noise distribution (when no signal is present) and the signal distribution. Assuming that the standard deviations are equal between the two distributions ($\sigma_n = \sigma_s = 1$), sensitivity can be represented as d'.

$$d' = -\frac{(\mu_s - \mu_n)}{\sigma_n} \tag{1.1}$$

The decision process is assumed to use one or several decision criteria, against which the output of the sensory process is compared in order to determine the response. If the output of the sensory process exceeds the criterion, the observer's response is "yes, there was a signal", while if the output is less than the criterion the response is "no, there was no signal".

Then, sensitivity can be determined from the observed HR and FAR conditional probabilities, and the decision criterion can be described by the critical output of the sensory process. Sensitivity is assumed to be a relatively stable property of the sensory process, while the decision criterion can change from task to task and over time. At least three factors affect the criterion; the instructions to the observer, the relative proportions of signal and no-signal trials, and the pay-off, meaning the relative cost for making each type of error (type I or type II) or benefit of making each type of correct response (hit or correct rejection). Due to these factors, the observer may use

different decision criteria at different times, which may be falsely interpreted as changes in sensitivity if an appropriate index of sensitivity is not used.

An alternative method for estimating the observer's detection sensitivity in a way that is relatively unconfounded with the decision criteria is the two-alternative forced choice (2AFC) task. In one form of a 2AFC task, the observer decides which of two stimuli contains the stronger signal, rather than whether a single stimulus contains a signal or not (1AFC). This method uses percent correct (or percent of trials on which the observer answered 'stimulus A') as an index of performance and essentially forces observers to adopt the same decision criterion. The threshold stimulus value is defined as the stimulus giving rise to a set level of detection performance.

In summary, SDT assumes that there is no set internal threshold (minimal sensory activation); rather, the decision process has access to the response distributions of all the detecting mechanisms it monitors. It then compares them to either a criterion level, or to responses for another stimulus as in 2AFC tasks. Measures of the sensitivity of the sensory process are based on the difference between the mean outputs in the signal and no-signal conditions. Performance on a task can then be measured by the *discriminability index* d', or by *percent correct* P(c).

Finally, the method of single stimuli (MSS) requires the observer to classify a single stimulus, for example, whether it is tilted clockwise or anti-clockwise of the vertical. Though often confused with 2AFC, the MSS has only one source of external noise (due to the stimulus) instead of two, but inevitably involves an internal standard (e.g. the vertical) which may or may not have appreciable noise relative to the sensory noise (Morgan, Dillenburger, Raphael & Solomon 2012).

1.3 Models of motion perception

At a most basic level, motion perception is a problem of identifying changes in position over time. In science, plausible models are crucial for defining hypotheses and guiding

experimental design. The algorithms proposed for motion detection fall into several categories - Reichardt detectors (Hassenstein & Reichardt 1959, Reichardt 1961), spatio-temporal energy models (Adelson & Bergen 1985), and gradient detectors (Fennema & Thompson 1979). Both gradient detectors and spatio-temporal energy models are supported by single cell electrophysiology and are widely accepted. Reichardt motion detectors predict aliasing in the visual system. While it is uncertain whether mammals exhibit aliasing (there are claims for it in the peripheral visual field), it has indeed been observed in insects. Zebra stripes may even have evolved to produce aliasing in biting flies, making them less susceptible to attack (How & Zanker 2014).

1.3.1 Reichardt detectors

Reichardt detectors are the simplest class of model; they compare responses from two retinal points with a certain delay. Say photoreceptor cell A is to the left of cell B, and there is a set delay on the output of cell A. Both cells then connect to a detector, which fires only if the outputs form cells A and B are both positive and arrive simultaneously (see Figure 1.2). If a stimulus moves rightwards and passes through the receptive fields of both photoreceptors, it will first activate cell A, then cell B. If the delay on cell A output is matched to the time the stimulus takes to travel between the two receptive fields, then the signals will arrive at the detector at the same time - the detector is thus selective for speed and rightward motion (its preferred direction). To reduce false firing due to the high noise in photoreceptor responses, detectors are often arranged in opponent pairs of detectors selective for opposing directions which inhibit each other. Physiologically, such cells may be found in the SACs of the retina and in the LGN (Levick, Oyster & Takahashi 1969), where responses from direction-selective retinal ganglion cells converge. Evidence suggests that this model accurately describes visual processing in flies (Haag, Denk & Borst 2004).

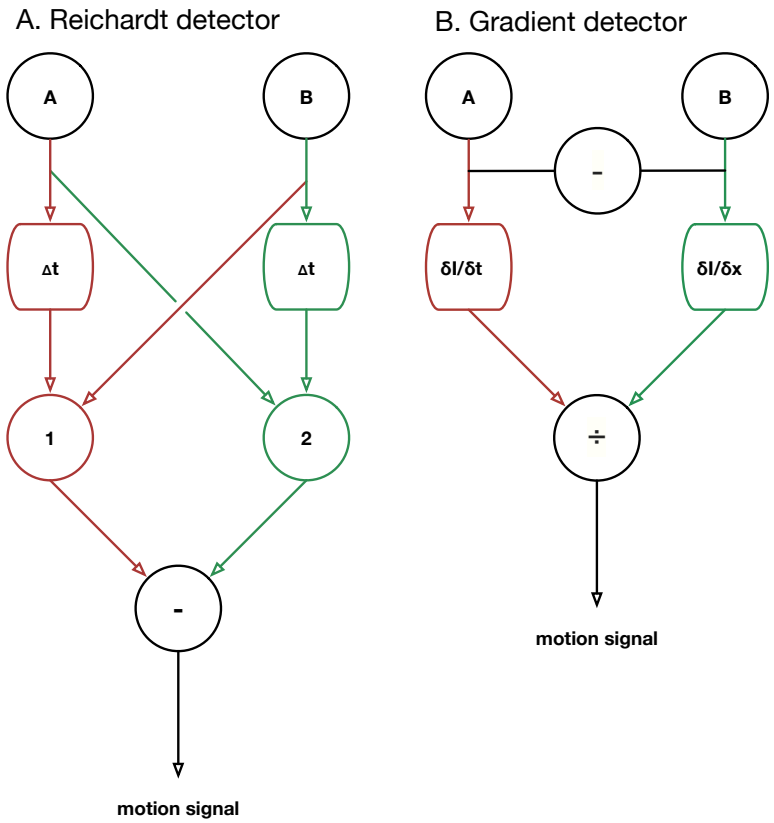

Figure 1.2: Reichardt and gradient detector models Basic representation of the reichardt and gradient detector models (see text).

1.3.2 Gradient detectors

To describe the gradient model, let us consider that motion is a change in position x over time t and speed is the rate of change of position, i.e. $\frac{\partial x}{\partial t}$. We can represent a 1D pattern I(x) moving through 1D space by $\frac{\partial x}{\partial t}$, where x and t define the position in 2D space-time. The derivative $\frac{dI}{dx}$ would define the rate of change or gradient at point x. As we move to the right across an image, our velocity is $\frac{\delta x}{\delta t}$. Therefore,

$$\frac{\delta x}{\delta t} = \frac{1}{\delta t} \times \frac{\delta x}{1} = \frac{\delta I}{\delta t} \times \frac{\delta x}{\delta I} = \frac{\delta I}{\delta t} \div \frac{\delta I}{\delta x} \tag{1.2}$$

Since in reality the image moves, rather than our detection mechanism, we can say that rightward motion over the image is equivalent to the image moving leftward. The temporal derivative of local luminance I_t is divided by its spatial derivative I_x. Therefore

image velocity becomes $V = -\frac{\delta x}{\delta t} = [-I_t \div I_x]$. The original algorithm proposed by Fennema & Thompson (1979) had the problem that the velocity estimate becomes large and noise-sensitive as I_x decreases towards zero. In order to deal with this problem, an alternative velocity estimate can be derived by using first and second derivatives since both I_{xx} and I_{xt} tend not to both be zero.

$$V = -\frac{I_{xt}}{I_{xx}}$$

These two velocity estimates have been combined by Johnston, Mcowan & Buxton (1992), adding a weighing factor w^2 and rearranging terms to form the multi-channel gradient model of velocity coding.

$$V = -\frac{I_x I_t + w^2 I_{xx} I_{xt}}{I_x^2 + w^2 I_{xx}^2} \tag{1.3}$$

1.3.3 Spatio-temporal energy models

In motion energy filters, motion is viewed as a tilt in space-time, just as orientation is a tilt in space. Defined by Adelson & Bergen (1985) (but see also Burr & Ross (1983) and Watson & Ahumada (1983)), it uses detectors that are oriented in space-time. Each motion-selective neuron thus has a spatio-temporal receptive field. While these cells are selective for specific velocities, they are also selective for contrast, i.e. they are phase-dependent. The solution proposed by Adelson and Bergen was to sum the squared outputs (or the "motion energy") of detectors that are out of phase with each other.

$$Motion\ energy = O_1^2 + O_2^2$$

The outputs from leftward and rightward oriented detectors are subtracted to get the opponent energy.

$$Opponent\ energy = E_R - E_L$$

The resulting energy signal would increase with image contrast, so it is finally divided by a static energy signal S^2 from neurons with non-directional receptive fields to get a measure of pure velocity.

$$Velocity = Opponent\ energy / Static\ energy = (E_R - E_L)/S^2$$

In this model, the squared linear receptive fields are a model of simple cells, and adding the out-of-phase outputs of the simple cells is a model of complex cells. Direction-selective complex cells in the cat V1 do indeed behave as the model predicts (Emerson, Bergen & Adelson 1992), and Qian et al. (1994) have found evidence for motion opponency in MT.

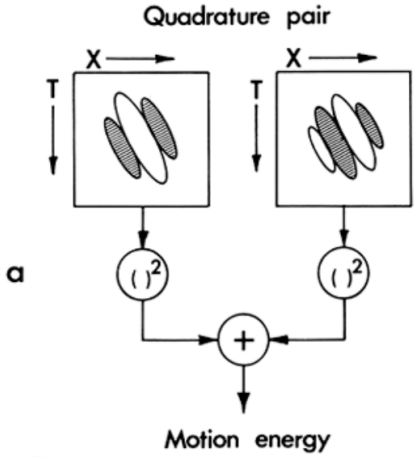

Figure 1.3: Motion energy model *from Adelson and Bergen, 1985*

While gradient detectors, Reichardt detectors and the motion energy models are conceptually different, they give similar predictions when it comes to motion adaptation. In fact, van Santen & Sperling (1985) showed that front-end filtering and multiplication of the two outputs predicts human responses better than addition. In this form they are shown to be essentially equivalent to the motion energy model (Adelson & Bergen 1985), in that the sensitivity of each channel adapts as a function of its response to the adapting stimulus. Morgan & Chubb (1999) later proposed that early Gaussian noise added

before the multiplication stage fits contrast thresholds for a direction discrimination task. Solomon, Chubb, John & Morgan (2005) further specified that an accelerating non-linear transducer better fitted psychometric function slopes than a linear transducer, but that the results of van Santen & Sperling (1985) were better fitted by a Reichardt detector with late noise. The following section describes the motion aftereffect and models thereof.

1.3.4 Motion psychophysics

Motion is likely processed in a hierarchical way, with outputs of early detectors converging in 'higher' areas, resulting in an increase in complexity of the optimal stimulus (Andersen et al. 1990). Local motions within small receptive fields (in V1 or later) are likely integrated at a later stage in order to determine the correct direction of motion of an object. Adelson & Movshon (1982) suggested a theory which combines the constraints of local motion detectors to estimate a global motion. Briefly, when an edge moves across a local receptive field, it's speed and direction are ambiguous because it could be moving in any of a set of directions given by a vector that lies along a constraint line in velocity space. But if two edges are assumed to be part of the same rigid object, then they must both be moving in the same direction. Therefore, the constraint lines of two edges with different orientations must have one vector in common, and this vector must be indicative of the object trajectory.

As with spatial acuity, the ability to detect motion decreases with retinal eccentricity. Barbur (1985) showed that motion displacement thresholds across a range of speeds are significantly higher at eccentricities of 25 degrees. Several other studies show that motion sensitivity declines with eccentricity (Baker & Braddick 1985, Johnson & Scobey 1980), consistent with the physiological findings that neurons corresponding to more retinally eccentric locations have larger receptive fields (Van Essen, Newsome & Maunsell 1984). Larger receptive fields affect the ability to discriminate motion; for

example, the detection of optic flow declines with increasing eccentricity. The reduction in sensitivity may be due to increased internal noise in motion direction estimates (Atchley & Andersen 1998). Furthermore, this reduction of sensitivity is much less present at small eccentricities (below 16 degrees) than at greater eccentricities, and appears to be independent of acuity (Bower, Bian & Andersen 2012). This suggests that the declines in sensitivity for acuity and global motion are likely not due to the same underlying processes.

Feature-tracking mechanisms, involved in the representation of image characteristics over the visual field, are involved in both luminance- and colour-defined motion. Drifting isoluminant gratings appear to move much more slowly than luminance-contrast defined gratings, and may even appear stationary. Adaptation to luminance gratings however, has been shown to produce a motion aftereffect when tested using an isoluminant grating (Cavanagh & Eizner Favreau 1985). Isoluminant stimuli have further been shown to induce an MAE (at least) as great as the MAE induced by luminance contrast (Mullen & Baker 1985). While the classical MAE is sensitive to chromatic composition (is colour-selective) (Favreau, Emerson & Corballis 1972), the positional MAE is not (McKeefry, Laviers & McGraw 2006). VEPs show cross-adaptation between colour- and luminance contrast-defined motion, indicating inputs to a common mechanism (McKeefry 2001).

1.4 The motion aftereffect

1.4.1 History and description

Biologists use micro-electrodes to measure responses of single neurons to stimuli; similarly, psychologists can study aftereffects in order to reveal the neural underpinnings of perception. In many cases, psychophysical measures prove to be more powerful than electro-physiological recordings of single cells, because they can uncover entire mechanisms and neural networks. Prominent among aftereffects in vision is the Motion

After-Effect (MAE) where, following a period of prolonged viewing (adaptation) of a moving stimulus, a subsequently viewed stationary or motion-balanced (test) stimulus will appear to move in the opposite direction.

The motion aftereffect has been a topic of curiosity and investigation since the time of Aristotle in 340 B.C., and has been an important tool in linking the percept of motion with its underlying physiology. Lucretius (ca. 56 B.C.) first accurately described the direction of the apparent motion, in viewing flowing water in a river. The effect was rediscovered multiple times in the nineteenth century. In particular, there are two descriptions, by Purkinje (1820 and again in 1825) and by Addams (1834). The later account named it the waterfall illusion; while viewing the Fall of Foyers in Scotland, he noted that after looking at the waterfall for an extended time and shifting his gaze, the adjacent rocky cliffs appeared to move upwards with a speed comparable to that of the waterfall. Later, it was also observed from moving railway trains, notably by S.P. Thompson who in 1877 reported:

> Thus, if from a rapid railway train objects from which the train is receding be watched, they seem to shrink as they are left behind, their images contracting and shrinking from the edges of the retina towards its centre. If after watching this motion for some time the gaze be transferred to an object at a constant distance from the eye, it seems to be actually expanding and approaching.
>
> *S.P. Thompson 1877, p.32*

Wohlgemuth in 1911 published a comprehensive review of the nineteenth-century reports on the MAE, replicating some studies, and adding many of his own. He compiled many of the known results on the phenomenon; that retinal motion is necessary, that the aftereffect immediately follows retinal motion, that its strength is increased by fixating on a point, that its location is restricted to stimulated retinal areas, that the MAE can be observed at different speeds, and that it can transfer between eyes, among

others. The MAE is a paradoxical percept, in that the observer is aware that the stimulus is not changing position, but nevertheless sees it as moving. This indicates that the visual system can process motion quite independently of other attributes. One of the common explanations for the MAE stems from Sigmund Exner in 1894. Exner had previously published his investigations of the motion aftereffect, including opposite aftereffects in each eye (Exner 1887, 1888), and linear combination of motion adaptation (Exner 1887). He speculated that direction-selective neurons are coupled into opponent pairs and that prolonged exposure to one motion direction recalibrates and/or fatigues one element of each pair. This leads to an unbalanced response, and gives rise to the aftereffect. The Reichardt detector described in Section 1.3 is an example of such an opponent system, and can thus subtend the MAE. This however, is a shallow explanation of motion adaptation; aftereffects are not simply mediated by independent pairs of direction-opponent mechanisms. Adaptation to two gratings drifting in different directions, for example, results in an aftereffect in the direction opposite the vector average of the adaptors. This suggests that motion is computed in a distributed way, across opponent pairs of motion detectors tuned to all different directions (Mather 1980, Mather & Moulden 1980). The MAE is then a result of a shift in the activity of these distributed opponent mechanisms. Adapting to expansion, the direction of motion is computed locally over all directions, and produces a contracting MAE. Two-stage models assume that detectors which are selective for opposing directions of motion at a first stage inhibit each other at the second stage. Neurophysiological data from Snowden et al. (1991) showed that this second stage is likely to be computed within area V5 in monkeys.

1.4.2 Neurological underpinnings

The MAE can be experienced when viewing either stationary or moving test stimuli following motion adaptation; these aftereffects have distinct properties and have been

termed the static and dynamic MAEs, respectively. The dynamic MAE is observed when a random-dot stimulus, RDVN (random dynamic visual noise), or counterphase grating is viewed following adaptation to motion. This dynamic MAE can be simulated with real motion, and observers cannot easily discriminate between the MAE when experienced with RDVN, and biased RDVN stimuli in which a percentage of dots (typically 30%) move coherently (Hiris & Blake 1992). Using flickering counterphase gratings, Bex, Verstraten & Mareschal (1996) further found that the dynamic MAE is tuned to the adapting spatial frequency, and is greatest when tested with low temporal frequencies below 0.25 Hz.

While the physiological basis of the MAE is still not fully understood, it appears to be mediated by the disinhibition and recalibration of opponent detectors sensitive to particular directions of motion. Opponent pairs of cells such as those described can be found as early as the retina in rabbits (Barlow & Hill 1963*a*, Fried, Münch & Werblin 2002). However, the dynamic MAE shows complete inter-ocular transfer (adaptation with only one eye produces a subsequent MAE in the unadapted eye) (Nishida, Ashida & Sato 1994), indicating that it is mediated, at the earliest, by binocular cells in the striate cortex, if not later. Several studies have identified directionally selective neurons responding to motion adaptation in the cat primary visual area (V1) (Giaschi, Douglas, Marlin & Cynader 1993, Hammond & Mouat 1988, Vautin & Berkley 1977) and Boynton et al. (2003) demonstrated that adaptation in area V5/MT in the macaque is likely inherited from V1, since adaptation in MT is spatially specific within the cells' receptive field. Further studies have shown selective adaptation independently in V1 and in MT+/V5, suggesting that the MAE is processed at several stages (Culham, Verstraten, Ashida & Cavanagh 2000, Verstraten, van der Smagt, Fredericksen & van de Grind 1999). While some functional imaging studies investigating the MAE have correlated increased activity in the human area MT+ with a subjective percept of the motion aftereffect (Culham et al. 1999, Hautzel et al. 2001, Taylor et al. 2000), others propose

that the MAE reflects a decrease in the responses of neurons selective for the adapting direction of motion (Huk, Ress & Heeger 2001).

1.4.3 Bias and sensitivity measures of adaptation

Most previous studies have examined motion adaptation using psychophysical observations which measure perceptual bias rather than sensitivity (Morgan, Chubb & Solomon 2006, Morgan, Melmoth & Solomon 2013). These observations focus on the inner *percept* of the stimulus.

Psychophysical measurements can therefore be divided into two classes. Class A are objective measures of sensitivity (or JND), while class B estimate bias and rely on tasks that have no correct answer. Illusions, which are nothing more than the introduction of a perceptual bias, are intrinsically class B phenomena. For class A evaluations, the observer is given a task such as deciding which of two gratings drift faster (note that there is an objectively right answer). We do not need the observer to respond to the correct stimulus; we can instead ask them to respond to the *appearance* of the stimulus. The resulting psychometric function contains two main sources of information: the central tendency, which determines the bias, and the slope, which gives the discrimination, a measure of the observer's internal noise. Using the method of single stimuli (see Section 1.2.2), the observer makes a decision along a continuous dimension of the stimulus and in order to do so, a criterion must be set. In this case, the midpoint of the psychometric function can represent one of two things - a change in sensitivity or a shift in the criterion (De Valois R. L. & De Valois 1991). This point was further illustrated by Morgan, Dillenburger, Raphael & Solomon (2012), who showed that observers can voluntarily shift their psychometric function with the method of single stimuli, without affecting its slope. As the two horizontal shifts in the psychometric function are indiscriminable within signal detection theory, it is important to distinguish them through methodology. Certain forms of two-alternative forced choice (2AFC) tasks

can overcome this problem, for example by using a roving pedestal (Morgan et al. 2013) or by making the real task opaque to the observer.

1.4.4 Theories of motion adaptation

Adaptation can be seen as a mechanism controlling the response of detectors to a persistent stimulus. The disinhibition theory of the MAE (Anstis, Verstraten & Mather 1998, Sekuler & Pantle 1967) suggests that motion-selective detectors inhibit the detectors selective for the opposite direction. Following adaptation, sensitivity of detectors selective for the adapted direction is reduced, and the detectors selective for the non-adapted direction are released from inhibition. Sekuler & Ganz (1963) showed a selective reduction in contrast sensitivity for gratings in the adapted direction of motion, supporting physiological evidence of sensitivity loss of directionally tuned detectors in the rabbit retina following prolonged stimulation (Barlow & Hill 1963*b*). It has been asserted that there are two stages to the disinhibition model; first detectors signal a direction of motion in area V1, and subsequently inhibit each other in area V5/MT (Verstraten et al. 1999). Further evidence in support of this model comes from Boynton et al. (2003), who showed that adaptation in the preferred direction reduces the responsiveness of MT neurons, in a manner consistent with an increase in divisive inhibition.

Morgan, Chubb and Solomon (2006, 2011) demonstrated an additional recalibration component to the MAE, shifting the balance point of a counterphase grating (the point at which the relative contrasts of the two gratings are such that they appear to be stationary) towards the adapted direction. The recalibration is manifested as a subtractive effect on the transducer function by which the input stimulus is translated into neuronal output, shifting it upwards and to the right, indicating a loss of sensitivity. In this model, the static MAE (stationary test stimulus) is brought about by a recalibration of the balance point, while the dynamic MAE (moving test stimulus) appears to be dependent on a disinhibition mechanism in addition to recalibration, effectively reducing the perceived

speed in the adapted direction. Nearly all response changes resulting from adaptation were a result of decreased sensitivity in directionally tuned mechanisms.

1.4.5 Adaptation to transparent motion

Most moving stimuli produce an MAE, but one class of stimuli fails to produce the expected aftereffect in the direction opposite the adapter. These are transparent motion stimuli, which consist of pairs of sinusoidal gratings or fields of dots moving in different directions, producing a percept of two superimposed drifting patterns. Mather (1980) performed such an experiment, in which he tested combinations of two moving random dot patterns drifting linearly with directions between 0° and 180° apart. The resulting MAE was unidirectional for all combinations of adapting motion. It did not comprise two superimposed aftereffects even though both motions were likely represented equally (Braddick, Wishart & Curran 2002), nor did it switch between directions. This suggested that an integrative process is involved, and that the specifics of this process could be studied. It was observed that a single MAE results in the direction opposite the combined vector average of the component fields. This aftereffect is susceptible to the influence of attention, which is known to strongly influence responses in the visual cortex (Gandhi, Heeger & Boynton 1999). Results by Raphael, Morgan & Dillenburger (2010) indicated that selective attention to one component of a transparent motion stimulus can bias the neural response to produce an adaptation effect, manifested as an MAE in the direction opposing the attended adapting stimulus component.

1.5 Attention

Attention is the process by which some features of the environment are selected for processing while others are ignored, and has been an interest of philosophers, psychologists and neuroscientists alike. While its effects are strongest on high-level cognitive process, attention has been shown to also affect perception. Attentional modulation

has been reported, among others, in area V4 (Moran & Desimone 1985), in the visual motion-selective area MT (Treue & Martínez Trujillo (1999), Treue & Maunsell (1999), Wall, Lingnau, Ashida & Smith (2008), Stoppel et al. (2011)) and even as early as V1 (Desimone & Duncan 1995, Gandhi et al. 1999, Motter 1993). One theory of attention, the cognitive load theory (Lavie 1995), posits that attention is a limited resource. If multiple stimuli are present and attention is uncontrolled, the stimuli will be processed equally. However, if a demanding task is being performed, then less resources will be available, and irrelevant information will not be processed. While some studies have found an effect of attentional modulation on motion adaptation (Beck et al. 2001, Chaudhuri 1990*a*,*b*), others have failed to do so (Morgan 2011, Rees et al. 2001). Most of these studies used bias-prone class B measures of adaptation (see Section 1.4.3).

1.6 Numerosity

The ability to estimate numbers has long been a subject of interest for biologists and psychologists, as there are clear evolutionary advantages in quickly and accurately gauging the number of conspecifics in an enemy group or of berries on a bush. Recently it has been suggested that the sense of number is a primary visual attribute, similar to contrast, colour, motion and size, because numerosity is susceptible to adaptation (Burr & Ross 2008) and number discrimination obeys Weber's law (Jevons 1871). By varying the number of elements in a set however, we inevitably also vary other parameters such as its size, density or contour, and it is thus difficult to isolate evidence for a distinct numerosity mechanism. Meanwhile, Dakin et al. (2011) and Morgan et al. (2014) suggested that relative numerosity is not estimated by a distinct process, but rather by a texture density mechanism sensitive to energy at high spatial frequencies.

Electrophysiological and neuroimaging studies have demonstrated that the intra-parietal sulcus (IPS) and surrounding regions in the parietal cortex are involved in estimates of absolute number (Dehaene & Changeux (1993), Nieder et al. (2002), see

Nieder (2005) and Nieder & Dehaene (2009) for reviews). Most physiological studies have looked at small quantities, usually < 10, so it is unclear whether the same regions are involved in the discriminations of greater numerosity. While we can accurately count sets of up to about 4 (this is called the subitizing range), greater quantities are either estimated or counted slowly, and even higher numbers are likely processed as textures (Durgin (1995), see Anobile, Cicchini & Burr (2016) for a review). Indeed, attentional requirements for subitizing are higher than for estimation of larger numbers (Burr, Turi & Anobile 2010, Vetter, Butterworth & Bahrami 2008*a*), indicating that differing mechanisms are involved at each range.

While absolute numerosity has been studied extensively, little is known about how the processes underlying number discrimination relate to those for proportions and ratios (Jacob, Vallentin & Nieder 2012). Recent studies used fMRI adaptation to examine the neural correlates of proportions; following repeat presentations of a given proportion (of dots or lines), presentation of a novel proportion was associated with a signal increase in the IPS and lateral prefrontal cortex (PFC), which varied with the distance between the adapting and novel proportions (Jacob & Nieder 2009). The interpretation of data from fMRI adaptation experiments is problematic however, as detailed in Section 6.2.4. This suggests that absolute number and proportions are processed in the same brain regions.

1.7 Functional magnetic resonance imaging

1.7.1 Magnetic resonance imaging

Magnetic resonance imaging (MRI) is a method of acquiring images of biological tissues using high intensity magnetic fields. In order to acquire these images, the phenomenon of nuclear magnetic resonance is exploited. When exposed to a magnetic field, some atomic nuclei can absorb and emit energy in the radio-frequency range. Hydrogen atoms are most commonly used to generate this signal, which is then picked up by magnetic

coils (antennae) close to the head. Since water composes 50 - 65% of the human body and about 75% of the brain, hydrogen atoms are abundant. Furthermore, the proportion of water varies between tissues so that by imaging it, we can delineate tissue boundaries. Hydrogen nuclei are electrically charged and spin around their axes, thereby evoking a magnetic field called the magnetic dipole moment (MDM). When they are exposed to a magnetic field, the MDMs tend to line up with the direction of the field. The stronger the magnetic field, the higher the proportion of MDMs that align. Next, the spin axes start to precess, and the frequency of this precession is directly proportional to the strength of the magnetic field. When a perpendicular radio-frequency pulse (RF) matching the precession frequency of hydrogen is applied, it causes the precession axis to tip. Following the RF pulse, the MDMs will once again align with the magnetic field, thereby emitting RF energy. This energy is termed the 'relaxation signal' and is measured by receivers around the head (the head coil). The different tissues in the brain (i.e. white matter, grey matter, cerebrospinal fluid) contain different proportions of hydrogen, have differing relaxation properties, and yield different contrasts in an MRI image.

1.7.2 Functional magnetic resonance imaging

Since its introduction in 1990, functional magnetic resonance imaging (fMRI) has become one of the most popular technologies for in vivo human brain imaging. It measures brain activity indirectly by means of hemodynamic responses (Belliveau et al. (1991), Kwong (1995), Ogawa et al. (1990, 1998), Williams et al. (1992), and Kim & Ogawa (2012) for a review) which are coupled to neuronal operations (Bandettini & Ungerleider (2001), Heeger & Ress (2002), Logothetis et al. (2001)). The most commonly used fMRI technique measures changes in blood oxygenation (the blood oxygen level dependent BOLD signal), which is activated by the metabolic demands of increased neuronal activity (e.g. Bandettini et al. (1992), Kwong et al. (1992), Ogawa et al. (1990,

1992), Turner et al. (1991)). The BOLD signal depends on the flow level, volume and oxygenation in blood, and is sensitive to the amount of oxygen carried by haemoglobin. Deoxyhaemoglobin is paramagnetic while oxyhaemoglobin is diamagnetic, therefore an increase in deoxyhaemoglobin introduces an inhomogeneity to the local magnetic field, reducing the BOLD signal. Following a brief increase in neuronal activity, the BOLD signal changes in time according to the hemodynamic response function (HRF). The HRF has three stages, 1) Neuronal activation is followed by a period of oxygen consumption, so there is an increase in deoxyhaemoglobin which causes a small decrease in BOLD signal intensity (called the 'initial dip', this phase is not always seen in the BOLD response), 2) A subsequent oversupply of oxygenated blood and an increase in BOLD signal (Raichle & Mintun 2006), and 3) A slow return to the baseline in the local blood supply and BOLD response, lasting approximately 24 seconds.

The fMRI technique has been popular because it has several advantages; 1) It has better spatial resolution than other methods based on hemodynamic signals (i.e. PET), 2) It is non-invasive and considered safe, allowing for extended testing on a single person, 3) It is possible to analyse the data in a relatively straight-forward way, compared to EEG or MEG, and 4) fMRI allows analysis of entire brain-networks involved in tasks. It is important to note that fMRI also has several limitations; 1) The BOLD signal is an indirect measure of neuronal activity, and is therefore susceptible to other influences, 2) The precise relationship between neuronal signals and the hemodynamic response is not understood, which affects the analysis and interpretation of fMRI data (e.g. BOLD signal may be driven by synaptic activity rather than action potentials, and may reflect either excitatory or inhibitory signaling, see Bandettini & Ungerleider (2001), Heeger & Ress (2002), Logothetis et al. (2001) and further discussion below), 3) The temporal resolution is limited by the blood supply to the brain, 4) The signal-to-noise ratio is low and fMRI is highly susceptible to motion artefacts, so data require careful preprocessing and statistical analysis, and lastly, 5) Experimental design is limited by the environment

of the MR scanner (i.e. subjects are immobilised in the loud and confined bore, and can only view stimuli using a mirror system). Despite these disadvantages fMRI has been enormously successful in neuroscience research.

What does BOLD activation actually represent? It is generally assumed that an area shows activation when it is involved in the *processing* of a task. However, the idea that brain areas are unidirectional information processing units can be misleading, and the relationship between BOLD activation and underlying neural functions is less than straightforward. In fact, cortical areas receive extensive feedback, and local connections are both excitatory and inhibitory (Douglas & Martin 2004). While the first experiments which compared BOLD activity to electrophysiological signals in the monkey visual cortex found a correlation between BOLD and action potentials (Heeger, Huk, Geisler & Albrecht 2000, Rees, Friston & Koch 2000), subsequent studies have correlated BOLD activity more closely with Local Field Potentials than multi-unit spiking (Logothetis 2003, Logothetis et al. 2001) and have shown that regional CBF changes can be independent of neuronal spiking (Thomsen, Offenhauser & Lauritzen 2004). Reuptake of post-synaptic glutamate by neurons (Attwell & Iadecola 2002) and astrocytes (Zonta et al. 2003) has been shown to dilate artelioles (see also Lauritzen (2005), Mulligan & MacVicar (2004), Peppiatt & Attwell (2004) and Gordon et al. (2008)). Changes in the BOLD response therefore appear to be coupled to postsynaptic intracellular activity rather than to action potentials, and likely reflect the input and intrinsic processing of neuronal populations rather than their output.

While the BOLD response can show an area's involvement in a task, it cannot easily differentiate between neuromodulation and task-specific signals, top-down and bottom-up processing, and neuronal excitation and inhibition. Regardless of these drawbacks, the BOLD signal remains one of the most powerful tools available today to study brain function. The relevance of results critically depends on the experimental protocol and careful statistical analysis as well as on the imaging technology. This highlights the benefits of multimodal approaches, combining fMRI with psychophysics,

computational modelling and other techniques for recording brain activity.

1.7.3 fMRI in vision research

fMRI has helped to make numerous contributions to the field of visual motion perception (see Courtney & Ungerleider (1997), Tootell, Dale, Sereno & Malach (1996), Wandell (1999) and Culham, He, Dukelow & Verstraten (2001)). It has allowed the verification and integration of results from other methodologies, such as psychophysics, lesion studies and electrophysiology. It has uncovered the locations and properties of previously known motion-selective areas such as MT and MST (Dukelow et al. 2001, Huk et al. 2002, Tootell & Taylor 1995), but it has also revealed unexpected new areas sensitive to movement such as V3A and KO (Oostende et al. 1997, Sunaert et al. 1999, Tootell et al. 1997). fMRI has shown that activity in nearly all visual areas is modulated by top-down processes, such as attention and prior expectations (Beauchamp et al. 1997, Chun & Marois 2002, O'Craven et al. 1997, Somers et al. 1999). Importantly, fMRI has also allowed for the precise delineation of visual areas by methods such as retinotopic mapping (Engel, Glover & Wandell (1997), within 1 mm). This allows the quantitative analysis of the organisation of the visual cortex. Not only can receptive field sizes and cortical magnification factors be estimated (Sereno et al. 1995), but results from humans and other primates can be compared (Brewer et al. 2002, Sereno 1998, Van Essen et al. 2001). By accurately describing visual areas, we can localise activations in functionally (rather than anatomically) defined areas. Additionally, it allows us to perform region of interest (ROI) analyses, i.e. assuming homogeneous processing within a region in order to average responses from the same anatomically- or functionally- defined region across sessions or subjects, greatly increasing the signal-to-noise ratio.

In humans, Heeger et al. (1999) showed that the response amplitude in MT+ was reduced by superimposing a second grating moving in the opposite direction of an initial translating grating. These results provide evidence for motion opponency and thus for directionally selective responses in MT+.

While there are some reports that perception of the MAE increases activity in MT+ (Culham et al. 1999, He et al. 1998, Taylor et al. 2000, Tootell, Reppas, Dale, Look, Sereno, Malach, Brady & Rosen 1995), the percept of the MAE is interesting and subjects may allocate more attention to the stimulus than when passively viewing the adaptor. When Huk et al. (2001) controlled for attention by asking the subjects to perform a 2AFC speed discrimination task during the adaptation period, the BOLD responses were equal on MAE and control trials. They proposed that adaptation actually decreases the responses of direction-selective neurons, and that previous studies found the opposite effect due to increased attention to the MAE.

1.8 This thesis

This dissertation details my work using the techniques of psychophysics and functional magnetic resonance imaging to study the perception and processing of visual motion. Of particular interest were the consequences of adaptation to radial motion.

An initial research question was that of whether selective attention can induce an MAE, as measured by dot coherence thresholds for radial motion. In order to better understand the response properties of systems involved in the processing of radial motion, it was important to characterise sensitivity above the absolute threshold (i.e. across the stimulus range). It could then be studied how adaptation affects the sensitivity. A class of partially-coherent dot stimuli composed of radial (contracting and expanding) and random movement were used to measure how dot coherence thresholds vary with baseline coherence (the discrimination function: see Section 1.2.1). Results from an early experiment suggested that observers' judgements may reflect judgements of relative proportions rather than motion energy, and a study of orientation coherence was performed to investigate this idea. It was then examined whether attention to one component of transparent motion results in a sensitivity change selective to that component.

While the physiological responses in early visual areas are generally encoded in a retinotopic frame of reference and cells respond to specific locations on the retina, our percept of the world is stable. As this observation suggests, some visual information appears to be represented in world-based coordinates in the brain, and a cortical area's frame of reference can therefore give an indication as to it's function. To gain insight to the level of visual processing of radial motion, a study was performed to test whether the radial MAE is retinotopic.

Finally, it was interesting to use functional imaging in order to examine the selectivity to radial motion within the motion-selective cortical areas MT and MST. More specifically, an intention was to test whether distinct fMRI responses could be elicited by contraction and expansion, and to investigate if any anisotropies were present and how these related to psychophysical sensitivity.

This introduction (Chapter 1) has described the background literature relevant to understanding concepts introduced within the thesis. In Chapter 2, the general methods used in the psychophysical and functional imaging experiments presented in this thesis are detailed. Chapter 3 describes a series of studies aimed at investigating the effect of directed attention on adaptation to radial motion. As part of these experiments, the effect of adaptation on discrimination functions for radial motion is studied using spatial and temporal 2AFC tasks. The question of whether adaptation to radial motion is retinotopic or spatiotopic is addressed in Chapter 4. The fifth chapter describes a set of fMRI studies designed to probe the cortical substrate of radial motion perception, including retinotopic mapping, an MT and MST localiser, and selectivity for contraction and expansion within area MST. Finally, the discussion summarises the findings presented in the thesis and relates them to other work. Every experimental chapter is prefaced by a statement on its motivation, followed by a description of each experiment performed as part of it (introduction, methods, results and discussion), and ends with concluding remarks on the chapter findings.

Chapter 2

General Methods

2.1 Introduction

This chapter describes the measurements, equipments, various stimuli, as well as experimental and analytical techniques used in this thesis.

2.2 Measures

2.2.1 Luminance

The luminance of a stimulus is the wavelength-weighted luminous intensity of the light emitted from the screen per unit area and is expressed in SI base units as Candelas per square meter (cd/m^2).

2.2.2 Contrast

The contrast of a stimulus is its luminance modulation, and is most commonly expressed as the Michelson Contrast

$$C_{Michaelson} = \frac{L_{Max} - L_{Min}}{L_{Max} + L_{Min}}, \tag{2.1}$$

where Lmax and Lmin are the maximum and minimum luminance values.

2.2.3 Visual angle

Objects viewed by the eye can be concisely described in terms of visual angle in order to avoid specification of the object size and viewing distance. The visual angle, or angular size, is the angle that a viewed object subtends on the eye. One degree of visual angle is equivalent to about 0.3 mm on the retina (de Valois R. L. & de Valois K. K. 1988), and approximately the width of the index finger held at arms length. In this work, units of visual angle will be referred to with the word *degree*, whereas degrees of orientation will be denoted by the degree symbol (°).

2.2.4 Speed

The speed of a stimulus or stimulus component is expressed as the number of degrees of visual angle per second (deg/s).

2.2.5 Orientation

The orientation of a stimulus is referred to with the degree symbol (°). To avoid confusion, degrees of visual angle are expressed with the word *degree*. The orientation of a horizontal stimulus is 0°, and increases anti-clockwise (i.e. a vertical stimulus is oriented at 90°).

2.2.6 Spatial frequency

The spatial frequency of a periodic stimulus is expressed as the number of cycles per degree of visual angle (c/deg). More complex stimuli can be specified by their power spectra; for example the $1/f^2$ function characteristic of many natural scenes (see Field (1987, 1994), Tolhurst, Tadmor & Chao (1992), and Burton & Moorhead (1987)).

2.3 Equipment

2.3.1 Monitors and stimulus presentation

The stimuli in all psychophysical experiments described in this work were presented on cathode ray tube (CRT) monitors. It is important to calibrate the display so that the luminance characteristics are specified. The CRT monitors were calibrated using measurements acquired with a photometer, so that linear increments specified in software result in linear increases in pixel luminance on the monitor (Brainard, Pelli & Robson 2002). The uniform black background of the screen was determined to have a luminance of 22 cd/m^2. The experiments were conducted in a darkened room. All experiments were carried out on an Intel HD Graphics 3000 512 MB graphics card of a MacBook Pro.

2.3.2 Software

All experiments were coded using a set of custom written functions, and made use of the Psychtoolbox (Brainard 1997, Pelli 1997) running in Matlab versions 2011b and 2013a (The Mathworks Inc.; Natick, Massachusetts).

2.4 Stimuli

2.4.1 Random dot kinematograms

While they had previously been used in studies of motion (see Julesz (1971)), random dot kinematograms (RDKs) were first used to measure the MAE by Blake & Hiris (1993) in order to sidestep existing issues in the measure of the MAE. Many early studies of the MAE have expressed its strength in terms of duration, the time between the cessation of the moving stimulus and the end of illusory motion. While this measure is straightforward to explain to subjects, it has several faults. First, it is a class B estimate as described in Section 1.4.3 earlier, and the sensitivity and bias are therefore

indiscriminable. Second, the time point when illusory motion from an MAE disappears is ambiguous and subjects often report that it fades and then reappears. Third, it only contains information about the length, but not the intensity of the aftereffect.

To avoid these issues, Hiris & Blake (1992) (see also Morgan & Ward (1980), Newsome, Britten & Movshon (1989) and Britten et al. (1992*b*)) proposed nulling the MAE by varying the proportion of coherently moving dots in an RDK. The observer adapts to a movie showing dots moving in a given direction, then views a segment with all dots moving in all possible directions. Adaptation causes the net motion of these dots to appear to move in the direction opposite the adapter. By presenting a movie in which a proportion of dots move opposite the aftereffect, we can perceptually null the illusory motion. The signal-to-noise ratio can be controlled by varying the proportion of dots moving coherently to those moving in random directions. This measure has several advantages. When used with the method of constant stimuli in a 2AFC task, observers cannot anticipate the correct response. The task is simple to follow for observers and the effect is convincing.

Random dot fields are now widely used as stimuli for the study of visual motion, and were used as stimuli in many of the experiments in this thesis. In those experiments, each dot was black and subtended 0.1 degree of visual angle, unless stated otherwise. Transparent motion stimuli contained both black and white dots on a gray (22 cd/m^2) background in order to separate the motion components. The average dot density was around 2 dots per degree^2, and their speed (except where otherwise noted) was 6.5 deg/s. The dots had the same properties, and only the level of coherence was varied.

It should be noted here that elevated motion coherence thresholds cannot discriminate between under-sampling of motion directions and poor estimates of dot directions. Dakin, Mareschal & Bex (2005) showed that equivalent noise paradigms can separate these issues by using added external noise to estimate internal noise in global direction judgements.

2.4.2 Gabor patches

The Gabor patch, a sine grating multiplied by a two dimensional Gaussian envelope, is among the most popular stimuli in vision research. These patches can vary along numerous dimensions, including phase, contrast, and orientation.

2.5 Procedures

2.5.1 Two-alternative forced choice

All psychophysical experiments followed two-alternative forced choice (2AFC) procedures. Two stimuli are presented on each trial; one of these stimuli, picked at random, contains a cue of a chosen intensity, while the other contains a standard stimulus. The standard is kept constant at a set level throughout the entire session. The two stimuli can either be presented in succession (temporal 2AFC, t2AFC), or simultaneously in separate areas of the visual field (spatial 2AFC, s2AFC). The observer presses a button to indicate the chosen stimulus, and feedback can be provided by a change in the colour of the fixation point.

2.5.2 Method of constant stimuli

Most of the studies described in this thesis used the method of constant stimuli (Woodworth & Schlosberg 1954). Stimulus levels are chosen along a spectrum, such that the observer's task is easy on some trials and increasingly difficult on others. Data is collected by presenting each level a set number of times in order to probe the width of the psychometric function, and the stimuli are presented in a pseudo-random order.

When the range of desired stimuli is known, the method of constant stimuli has several advantages over other methods (Guilford 1954). The number of trials is determined by the experimenter in advance, allowing them to avoid subject fatigue. Responses have a correct answer which allows performance to be determined objectively, and for the

response error distribution to be obtained. Since the stimulus levels can be presented in a pseudo-random sequence, observers cannot anticipate the correct answer based on previous trials. It should be noted that the method of constant stimuli is susceptible to range effects and can be inefficient when the stimulus range is not well-selected, an issue which can be avoided with the use of well-designed adaptive procedures.

2.5.3 Adaptive probit estimation

One experiment described in this thesis (Chapter 4) made use of an adaptive psychophysical procedure designed to increase efficiency in the probing of the psychometric function. Adaptive probit estimation, or APE, (Watt & Andrews 1981) uses the recent response history in order to select which stimuli will contain the most information about the psychometric function. Such a procedure is useful when we do not want to probe the entire psychometric function, in order not to tire the observer with many sub-threshold trials.

2.6 Psychometric functions

2.6.1 Threshold-level detection

The psychometric function is an essential tool in psychophysics, relating physical properties to their internal representation in the observer. It expresses the probability of a certain response as a function of the pertinent property of the stimulus, and can be described by a sigmoidal shape. Generally, these functions have four free parameters. The slope corresponds to how the observer's response varies based on the stimulus. The lower and upper asymptotes represent the guess rate and the 100 percent correct rate, respectively. Finally, the observer's sensitivity is reflected in the function's position on the abscissa. In the Weibull function,

$$f(x) = \gamma + (1 - \gamma - \lambda) \times (1 - exp(-\frac{a}{\alpha})^{\beta}). \tag{2.2}$$

These parameters are controlled by α (position), β (slope), γ (lower limit) and λ (upper limit). It is favourable to fix irrelevant parameters in order to obtain accurate thresholds. For 2AFC procedures, the lower asymptote can be set at 0.5 - the 'guess rate' with two stimuli, and the upper asymptote can be fixed at 1. In this way, the two remaining free parameters α and β can be estimated by fitting the psychometric function to observed data, and the threshold can be estimated as the stimulus intensity at which observer performance reaches a set level.

2.6.2 Palamedes

The Palamedes toolbox (Kingdom & Prins 2010, Prins & Kingdom 2009) was used for fitting psychometric functions for most experiments in this thesis. All were fitted with Cumulative Gaussian functions except where otherwise stated.

2.7 Eye tracking

In Chapter 4, an SR EyeLink1000 was used to record eye movements monocularly at a rate of 2000 Hz. The EyeLink1000 is a desktop mounted infrared reflection recorder, and has an average accuracy of 0.25 - 0.5 degrees. Saccades are some of the fastest movements the eyes can make, and their velocities reach up to 900 deg/sec, and about 500 deg/sec (for 30 degree amplitude i.e. angular distance), and at the size of our stimuli and expected saccade amplitudes (about 4 degrees), velocity is about 200-250 deg/sec. While eye tracker sampling rates of 60-350 Hz are sufficient for most experimental designs, higher sampling rates (1000 Hz) are needed for measuring saccade dynamics and micro saccades. Since the accuracy of gaze direction estimates depends on the demarcation of the pupil and the detection of the corneal reflection, accuracy degrades at large viewing angles where pupil demarcation becomes difficult. The experiments were conducted in a dark room. The observer's head was stabilised using an EyeLink chin and forehead rest, and observers positioned their fingers over the response keys prior

to the start of each experimental run. An EyeLink 9-point calibration was performed before each session in order to calibrate the system. Observers sequentially scanned a 3 x 3 array of white fixation points on a black background while the associated eye positions were recorded, and the fixations were accepted manually by the experimenter. The calibration was then validated (EyeLink validation procedure), by sequentially presenting nine points slightly offset from the calibration points (towards the centre of the screen) and accepting the fixations manually. Where the distances between expected and recorded validation positions was large, the calibration was repeated. The EyeLink parameters were set to 40 deg/s velocity threshold, 8000 acceleration threshold and 0.5 motion threshold, in order to exclude microsaccades (Collins, Semroud, Orriols & Doré-Mazars 2008). Prior to analysis, saccades that occurred less than 80 ms after the target jump, as well as blinks and outliers, were identified and excluded from the data. In some experimental conditions, the fixation point jumped to a new location at a rate of 1 Hz and observers were instructed to make a saccadic eye movement to the fixation point (target location) when they saw it move.

2.8 fMRI

2.8.1 Data acquisition

A Siemens Trio 3.0 Tesla MRI scanner was used to collect functional imaging data, with a 20-channel array head coil. Anatomical T1 and T2 weighted images were collected during a separate scanning session before the functional experiments began (192 sagittal slices, in-plane resolution 256 x 256, 1 mm isotropic voxels, repetition time = 2300 ms, echo time = 2.32 ms, flip angle = 8°, bandwidth = 200 Hz/pixel).

Prior to collecting functional data, the detection thresholds for contraction and expansion were measured psychophysically for each person, with the same stimulus parameters as those used in the MRI scanner. Participants came in on up to 6 days for scanning sessions of functional data acquisition using a gradient-echo, echoplanar

sequence (repetition time = 2000 ms, 34 axial slices, interleaved acquisition order, 3 mm isotropic voxels, in-plane resolution 64 x 64 voxels, field of view = 192 x 192 mm, flip angle = 90°, echo time = 30 ms, bandwidth = 1776 Hz/pixel).

For the functional scans, stimuli were presented on a 30" OptoStim LCD monitor positioned at the head of the scanner, viewed through a mirror system fixed to the head coil. Observer responses were recorded by a fORP932 response box. Functional scanning runs for the MT and MST localisers consisted of 122 and 244 volumes respectively, and therefore lasted 4m 12s and 8m 24s each. The runs for the population response scans consisted of 122 volumes and thus lasted 4m 12s each. In the preliminary psychophysical experiments, stimuli were presented on a Sony Trinitron monitor with a refresh rate of 60 Hz and mean luminance of 22 cd/m^2. Subjects were seated at a viewing distance of 70 cm and their position was stabilised using a chin rest.

2.8.2 Data analysis

The data were preprocessed and analysed using the FMRIB Software library (FSL) (Smith et al. 2004), Freesurfer (Dale, Fischl & Sereno 1999), and AFNI (Cox 1996). Functional data were corrected for head motion and distortions and were spatially smoothed before calculating the T2* maps using isotropic Gaussian kernels of 3 mm or 1 voxel (full width at half-amplitude). While some studies choose not to apply spatial smoothing in fear of losing resolution in small brain areas, Beissner, Deichmann & Baudrexel (2011) have shown that smoothing using a kernel of one voxel size is sensitive to activations in small brainstem nuclei. I additionally compared results without spatial smoothing and with smoothing using Gaussian kernels of 0, 1 and 1.5 voxels (or 0 mm, 3 mm, 4.5 mm), and found that kernels of 1 voxel gave the best signal-to-noise ratio in the Superior Temporal lobe (see Figure 2.1).

The most recent T1 anatomical image for each subject was used as the reference image to which all sessions were registered. The images were kept in the native subject-space

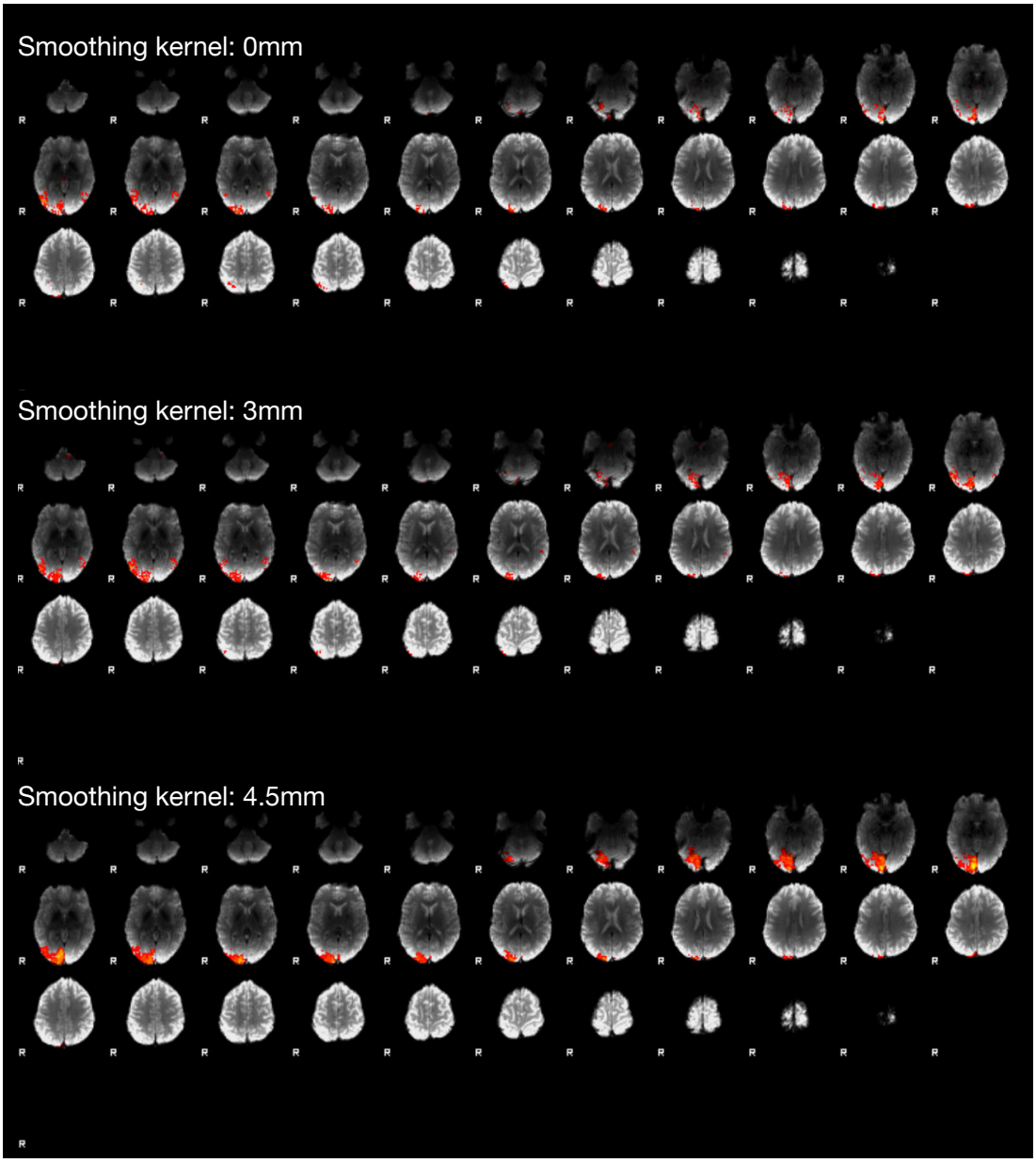

Figure 2.1: Comparison of different spatial smoothing kernels Example activations of one session of the MST localiser - stimulus left, analysed using three different spatial smoothing kernels: 0 mm, 3 mm and 4.5 mm. While 0 mm leaves single voxels defined as significantly active, and the boundary between V1 and MT+ is blurred in the 4.5 mm analysis, 3 mm results in an acceptable trade-off.

instead of registering to a standard space (i.e. Talariach) because there is inter-subject variability in the precise locations of MT and MST. The model regressors were defined based on the timing of the alternating moving and static dot fields. Additionally, standard parameters for breathing, heart rate and head motion were included as regressors. Average responses over the stimulus blocks and sessions were computed and the mean time-courses over the whole trial period were extracted as percentage signal change for each ROI.

Before the main experiment, each subject participated in several separate scanning runs in order to localise visual ROIs. A retinotopic mapping procedure was performed to make eccentricity and polar angle maps of the early visual areas V1, V2 and V3, and a localiser was used to separate the motion-sensitive MT+ complex into MT and MST. These runs used the same scanning protocols as those in the main experiment.

Based on the localiser data, the MT and MST ROIs were defined as clusters of motion-responsive voxels, located near the ascending limb of the inferior temporal sulcus (Dumoulin et al. 2000, Tootell, Reppas, Kwong, Malach, Born, Brady, Rosen & Belliveau 1995). The model regressors were defined as above, and the responses were averaged over sessions. Since MST is responsive to ipsilateral stimuli (Dukelow et al. 2001), while the MT+ complex is activated by contralateral stimuli, MST was defined by continuous sets of voxels which were active during ipsilateral motion stimulation. Conversely, MT was defined as the continuous set of voxels active during contralateral stimulation, excluding those voxels included in MST (Fischer, Büthoff, Logothetis, Bartels, Buïthoff, Logothetis & Bartels 2012, Huk, Dougherty & Heeger 2002, Smith, Wall, Williams & Singh 2006). MST is known to be situated anterior to MT (Dukelow et al. 2001, Huk et al. 2002, Smith et al. 2006), so voxels located anterior to the mean axial position of MST were discarded from the MT ROI.

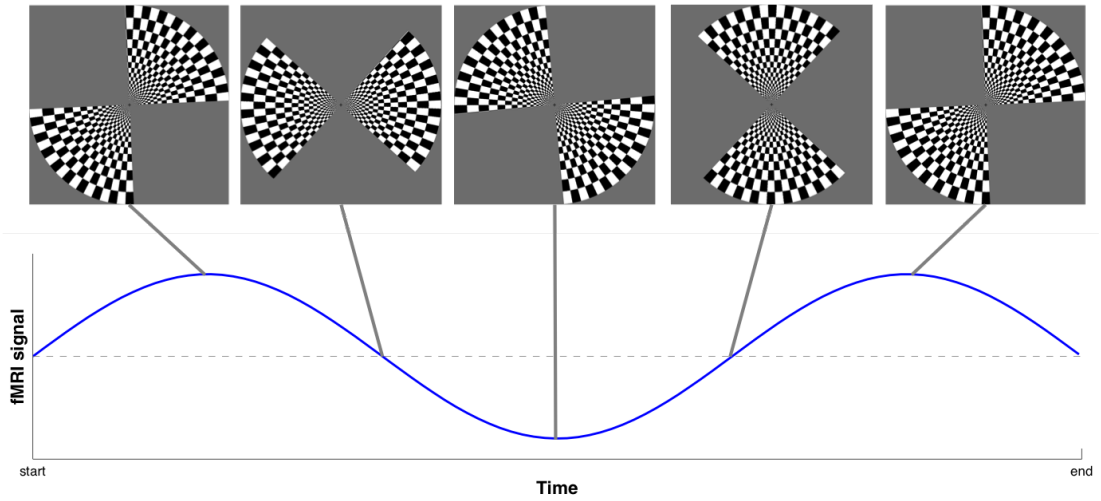

Figure 2.2: Retinotopy wedge stimulus as a travelling wave Schematic of the wedge stimulus used in order to produce polar angle retinotopic maps. Note that each stimulus angle maps onto a distinct part of a sinusoidal wave, which is fitted to each voxels response amplitude, and used to find its preferred angle.

Phase-encoded retinotopic maps were obtained by mapping each voxel's preferred angle (wedges) and eccentricity (rings), based on the temporal phase of a sinusoid

fitted to the travelling wave stimulus (Engel et al. 1997, Sereno et al. 1995) (see Figure 2.2). Mean responses over 2 - 3 sessions were calculated in AFNI (Cox 1996) and phase maps were determined in Freesurfer (Dale et al. 1999). The clockwise-rotating wedge and the contracting ring runs were then temporally reversed and averaged with the counter-clockwise-rotating wedge and expanding ring runs respectively. The time series were smoothed using a Gaussian kernel of 5 mm, and projected onto a flattened representation of the occipital lobes. The flattened representations were created by segmenting and reconstructing the border between white and grey matter in each hemisphere, inflating the surface and cutting along the calcarine sulcus, then flattening and correcting for linear distortions. These steps were performed using the Freesurfer software. Boundaries of the visual areas were drawn by hand along reversals of the direction of phase preference.

Chapter 3

Discrimination and the Effects of Directing Attention to Radial Motion

3.1 Motivation

As we shift our attention over the features in a visual scene, not all of the information from the retinal image is processed equally. Instead, we target our attention selectively to different parts or aspects of it over time. Attention can be directed globally to the whole image, to a particular object, or even to a specific property of an object such as its colour or texture. Attention can also be directed to track an object or group of objects, for example in ball sports or when driving a car. It has been suggested that this tracking function of attention is part of a higher-level motion system (Cavanagh 1991, Cavanagh & Mather 1989, Culham et al. 2000, Lu & Sperling 1995) which complements a more automatic low-level motion system. Using rotating counterphase gratings to adapt and test the MAE, Culham et al. (2000) showed an adaptation effect on dynamic, but not static, test patterns following attentional tracking of one motion component of

the adapting stimulus. This aftereffect is distinct from the low-level MAE seen using static test stimuli, in that it is not retinotopic and can override MAEs from low-level motion based only on luminance changes. They show that attentional tracking does not only enhance low-level motion signals, but instead produces adaptation at a later stage.

Several studies have examined the effect of attentional distraction, rather than tracking, on the MAE. While some report that this reduces the strength of adaptation (Rees, Frith & Lavie 1997, Rezec, Krekelberg & Dobkins 2004, Taya, Adams, Graf & Lavie 2009), others find no effect (Morgan 2011, 2012, Nishida & Ashida 2000, Wohlgemuth 1911). Most of these studies have measured the static MAE using the aftereffect duration, which is susceptible to top-down effects such as biases and expectations (Sinha 1952). As the stimulus parameters and experimental measures used in previous studies vary widely, the way in which attention interacts with motion processing remains not well understood.

While there are multiple reports on threshold-level performance using translating stimuli, no studies to date have examined discrimination using random dot motion. By studying the discrimination function, we can understand how the response functions of the detecting mechanism are affected by adaptation. This chapter details a series of experiments characterising the effect of adaptation on discrimination functions for radial motion, leading up to a study of how attentional tracking affects this MAE.

3.2 Experiment 1 - effect of adaptation on motion discrimination in a spatial 2AFC task

3.2.1 Introduction

In order to investigate the effects of adaptation on the response function for radial motion perception, we must understand how sensitivity changes as a function of increasing dot coherence. This study investigates the effect of adaptation on discrimination of radial

motion by measuring discrimination functions using a random dot test stimulus (Blake & Hiris 1993, Hiris & Blake 1992). A 2AFC task and partially coherent moving dot stimuli are used to measure the MAE, having the advantage of yielding a more objective response than a duration estimate. In this experiment, the two test alternatives are presented simultaneously on the left and right sides of the screen - the stimuli are arranged spatially (s2AFC task). The MAE is expected to affect both test stimuli equally, whereas if they were presented sequentially one after the other the MAE would be stronger for the first interval.

When navigating the environment, the visual system uses information from the patterns of motion formed on the retina in order to guide movement and avoid obstacles (Gibson 1950). Such complex 'optic flow' patterns include radial motion, rotation and spiral movement, are processed at a higher level than translating motion, and activate different areas in the brain (Smith et al. 2006, Wall et al. 2008). Viewing of radial motion further avoids the confounding influence of involuntary eye pursuit of the stimulus (the optokinetic reflex), and allows the probing of neurons in the MT+ complex - especially area MST (Smith, Wall, Williams & Singh 2006).

Edwards & Ibbotson (2007) have tested varieties of optic flow stimuli, varying the speed gradient along the radius of expanding and contracting dot fields. In these strict optic flow fields, forward motion creates expanding motion patterns with areas near the centre having slower speeds and areas near the periphery having maximum speeds. Rather than strict optic flow, here a fixed dot speed is used in order to maintain a constant dot density. Furthermore, a dot speed of 5.6 deg/s was used to match the known response properties of primate MT neurons (Maunsell & Van Essen 1983*b*).

3.2.2 Methods

Equipment and stimuli

Stimuli were presented on a Sony Trinitron monitor with a refresh rate of 60 Hz and mean luminance of 22 cd/m^2, connected to an Apple MacBook Pro with OS X 10.7 "Lion" running Matlab 2011b and the PsychToolBox software (Brainard 1997, Pelli 1997). Other variables were as detailed in Chapter 2. Subjects were positioned at a viewing distance of 70 cm from the screen using a chin rest. At this distance, individual stimuli subtended 8.2 by 16.7 degrees of visual angle. All observers used the same experimental set-up.

The adaptation and test stimuli were random dot fields with varying dot motion coherence levels. Two dot fields, each containing 300 dots, were presented simultaneously on the screen on either side of a central fixation point, forming two hemifields. Each dot had a limited lifetime of 0.6 seconds and moved at a speed of 5.6 deg/s. A limited dot lifetime avoids crowding of dots near the center (during contraction) or around the edge of the stimulus (during expansion) and prevents tracking of individual dots.

Procedures

Data were collected using a spatial two-alternative forced choice (2AFC) procedure. One hemifield contained the standard (baseline) stimulus, and the other contained the standard and an additional increment (signal) (see Figure 3.1). In adaptation conditions, a 45 second adaptation period was presented at the start of each session and every 20 trials thereafter, and a further 5 second top-up adaptation preceded all other trials. During adaptation, all dots (corresponding to 100% coherence) either contracted or expanded, and observers were asked to maintain their gaze on a central fixation point. On a given day, observers performed experiments with only one adaptation direction, and the non-adaptation sessions were carried out first. Data were collected over multiple days, and each session on a given day lasted between 1 and 1.5 hours.

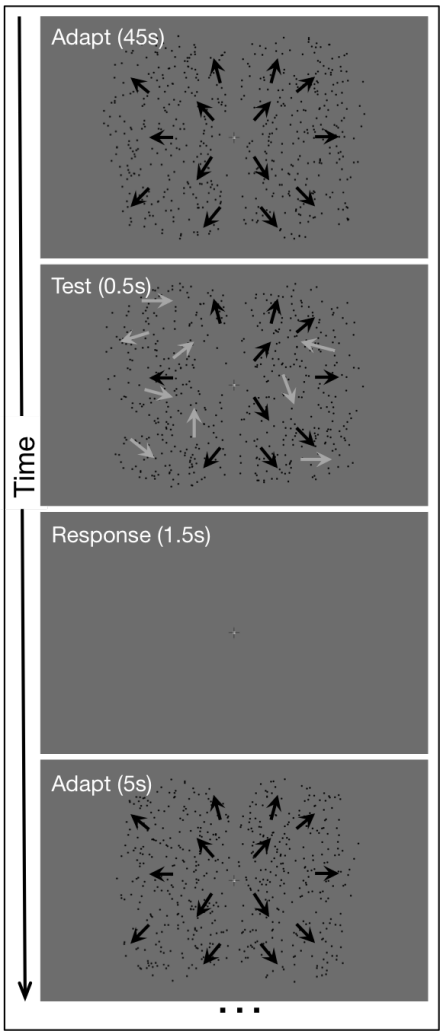

Figure 3.1: Stimulus representation - motion discrimination Protocol for Experiment 1. Subjects adapted to coherent expanding (or contracting) motion on both hemi-fields for 45 seconds. This was followed by 0.5 second test period, each of which was preceded by a 5 second top-up adaptation. Observers had up to 1.5 seconds to make a response using the left and right arrow keys of a keyboard.

To measure absolute thresholds, the standard contained only random dot directions, while for determining difference thresholds the pedestal was varied in multiples (0.25, 0.5, 1, 1.5, 2, 3) of each observer's respective detection threshold (expressed as the proportion of coherently moving dots). The observer's task was to identify which hemifield contained more coherent dot motion by pressing the left or right keyboard arrows for the left and right hemifields respectively, and feedback was provided in form of a colour change in the fixation point (green - correct, red - incorrect).

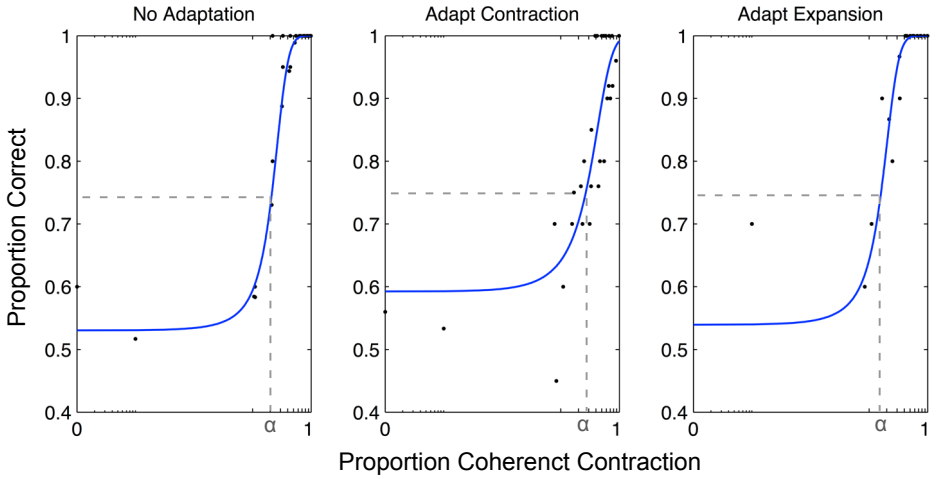

Figure 3.2: Example psychometric function fits to data A Cumulative Normal function has been fit to contracting test stimulus data from No Adaptation, Adapt to Contraction and Adapt to Expansion sessions for one observer. The threshold α is where the vertical line meets the x-axis, and corresponds to 75% correct.

Data were collected for the two radial motion directions - contraction and expansion - independently. Coherence thresholds were determined by the method of constant stimuli, with a minimum stimulus coherence of either 0 percent or the pedestal, a maximum of 99 percent and 10 levels spaced equally in between. Each session contained ten repetitions at each stimulus, presented in a pseudo-random order. The pedestal conditions were blocked, and each observer performed 3 to 5 sessions for each pedestal intensity in randomised order. The coherence detection thresholds were calculated for each session using a maximum likelihood criterion, allowing estimation of the mean and standard error across sessions. In a pilot experiment, the expansion and contraction conditions were interleaved within each session. The results from these two experiments showed no systematic differences, and the radial motion directions were tested separately throughout the main experiment. The data were collapsed across trials for each direction, and thresholds at the 75% correct point were estimated by a 2-parameter fit of a Cumulative Normal function to the p(correct) versus log increment as detailed in Section 2.6 in the General Methods (see Figure 3.2).

Observers

Absolute thresholds were determined for six observers, two experienced and four naive (JH, ME, MM, NN, SU and TS), five of whom continued to collect difference thresholds (JH, ME, MM, NN and TS). The observers were between the ages of 24 and 70 at the time the data was collected. A slight strabismus (undiagnosed) in the left eye was observed for observer TS. Vision was corrected when necessary and all experiments were conducted binocularly with natural pupils.

3.2.3 Results

Detection

Following adaptation in the detection task, both stimuli appeared to be moving in the direction opposite the adaptor. Even the zero-pedestal stimulus containing only incoherent motion thus appeared to contain coherent motion, and the observer's task was to identify which of the two stimuli contained *more* coherent motion. Detection thresholds varied from a proportion coherence of 0.18 to 0.43. There was no consistent difference between the detection thresholds for contraction and expansion (see Figure 3.3), neither before nor after adaptation. This is contrary to previous reports of a longer-lasting expanding aftereffect following adaptation with a spinning spiral (Bakan & Mizusawa 1963, Spitz 1966). This difference may be due to the differences in the stimuli used and the measure of the MAE. Both Bakan & Mizusawa and Spitz measured the duration of the aftereffect on a white square following adaptation to a flat rotating spiral. It is well-known that the duration of the MAE is susceptible to top-down effects (see Sinha (1952), also Morgan (2012)), and a spiral is likely to produce a different percept than the coherently moving dots used in the present study.

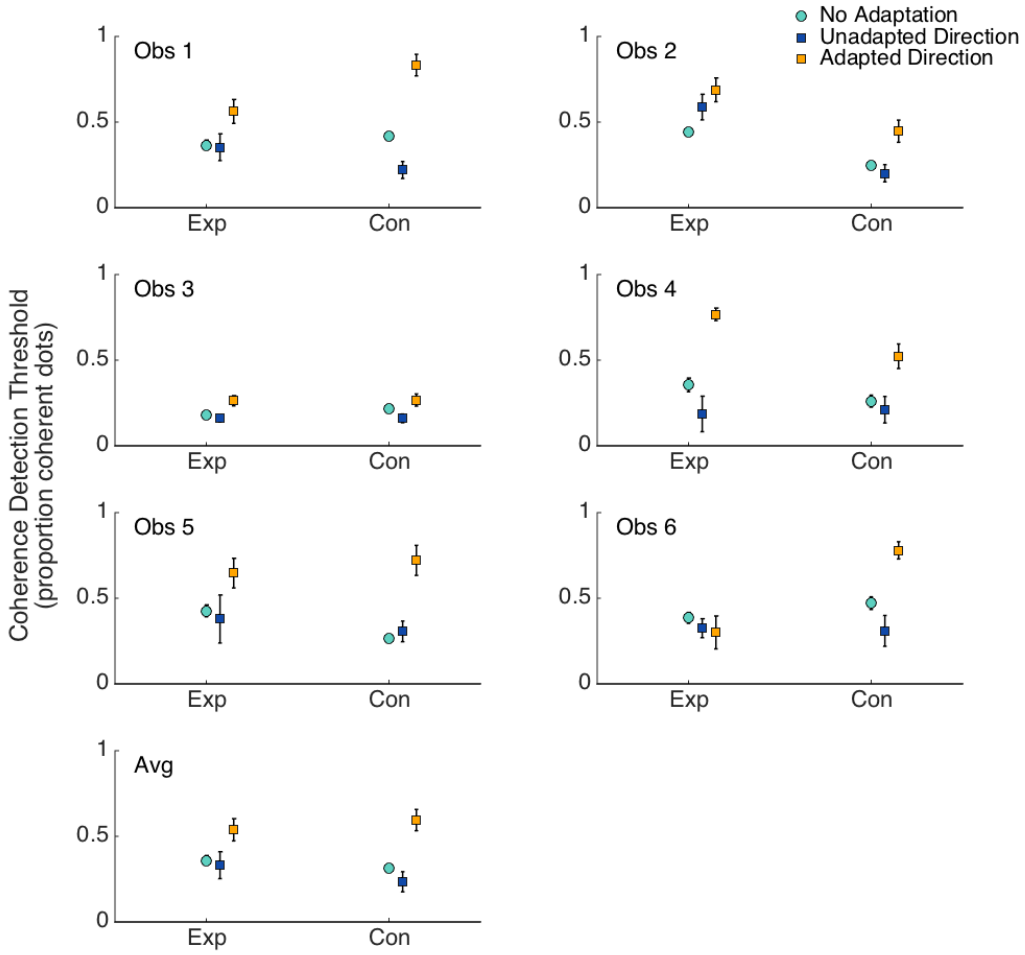

Figure 3.3: Motion: s2AFC detection thresholds for contraction and expansion Dot coherence detection thresholds for spatial 2AFC procedure for contraction and expansion were comparable for all observers, as well as for the group average. Data points are based on at least 3 sessions of 100 trials each in each direction and error bars represent bootstrapped standard errors.

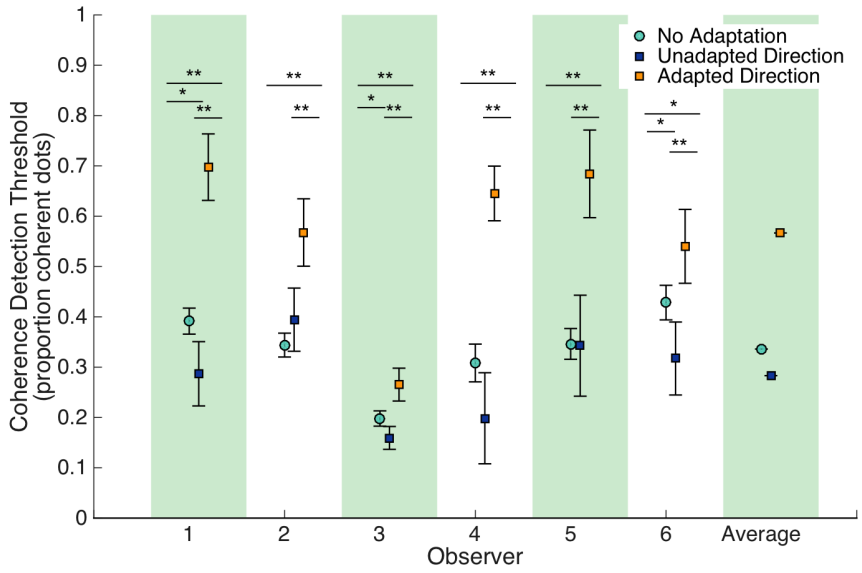

Figure 3.4: Motion: s2AFC detection thresholds Dot coherence detection thresholds for spatial 2AFC procedure pooled across direction (contraction and expansion) for each observer individually, and averaged across observers. Data points are based on at least 3 sessions of 100 trials each in each direction and error bars represent bootstrapped standard errors. Two-tailed t-test significance levels: * $p < 0.01$, ** $p < 0.005$. Upper stars show significance levels between No Adaptation and Adapted Direction conditions, lower stars between No Adaptation and Unadapted Direction, and bottom, starts between Unadapted and Adapted Direction conditions.

Figure 3.4 shows dot coherence thresholds (i.e. the proportion of dots moving coherently at which the observer detects radial motion on 75 percent of trials), collapsed across direction of motion (contraction and expansion) for all six observers, as well as the inter-subject mean. Data are shown for all three adaptation conditions (no adaptation, test in the adapted direction, test in the unadapted direction). Paired sample t-tests were performed for each observer to compare thresholds between the adapted direction, unadapted direction and no adaptation conditions. Thresholds in the adapted direction (yellow triangles) were significantly higher (two-tailed t-tests, $p < 0.01$) than those without adaptation (turquoise circles) or in the unadapted direction (blue squares) for all six observers. No consistent difference was found between thresholds without adaptation and those in the unadapted direction. Detection thresholds were variable between observers, from 19 percent coherence for observer 3, to above 40 percent for observer 6.

Adaptation to radial motion increased detection thresholds in the adapted direction, and had minimal effects in the unadapted direction compared to detection thresholds without adaptation. While this result is consistent with the work of Hiris & Blake (1992), the coherence thresholds we find are higher than the nulling percentages they report for translational motion. They report nulling percentages of 30-40% signal dots needed to null the MAE, while the range observed here is 25-70%, with the adapted direction thresholds for most subject falling between 55-70%. This experiment tested radial motion, likely resulting in adaptation at a different site than translational motion, which may account for this difference.

Adaptation is found to have no effect on detection thresholds for the unadapted direction. This supports results of Raymond (1993) and Raymond & Braddick (1996) who, by measuring complete psychometric functions (PFs) from 100% coherent leftwards motion through to 100% coherent rightwards motion, showed that adaptation flattened the adapted PF side (i.e. decreased sensitivity for the adapted direction), but did not affect either the zero-point nor the unadapted direction. Because an opponent mechanism for motion detection as suggested by Verstraten et al. (1994) would predict a shift in the PF, and thus reduced thresholds in the unadapted direction, the above result is considered incompatible with an opponent mechanism. It instead supports a distribution shift model (Levinson & Sekuler 1976, Mather 1980) in which perception is based on the weighted average of activity in independent motion-direction detectors, and adaptation causes desensitization and a redistribution of activity towards the opposite direction.

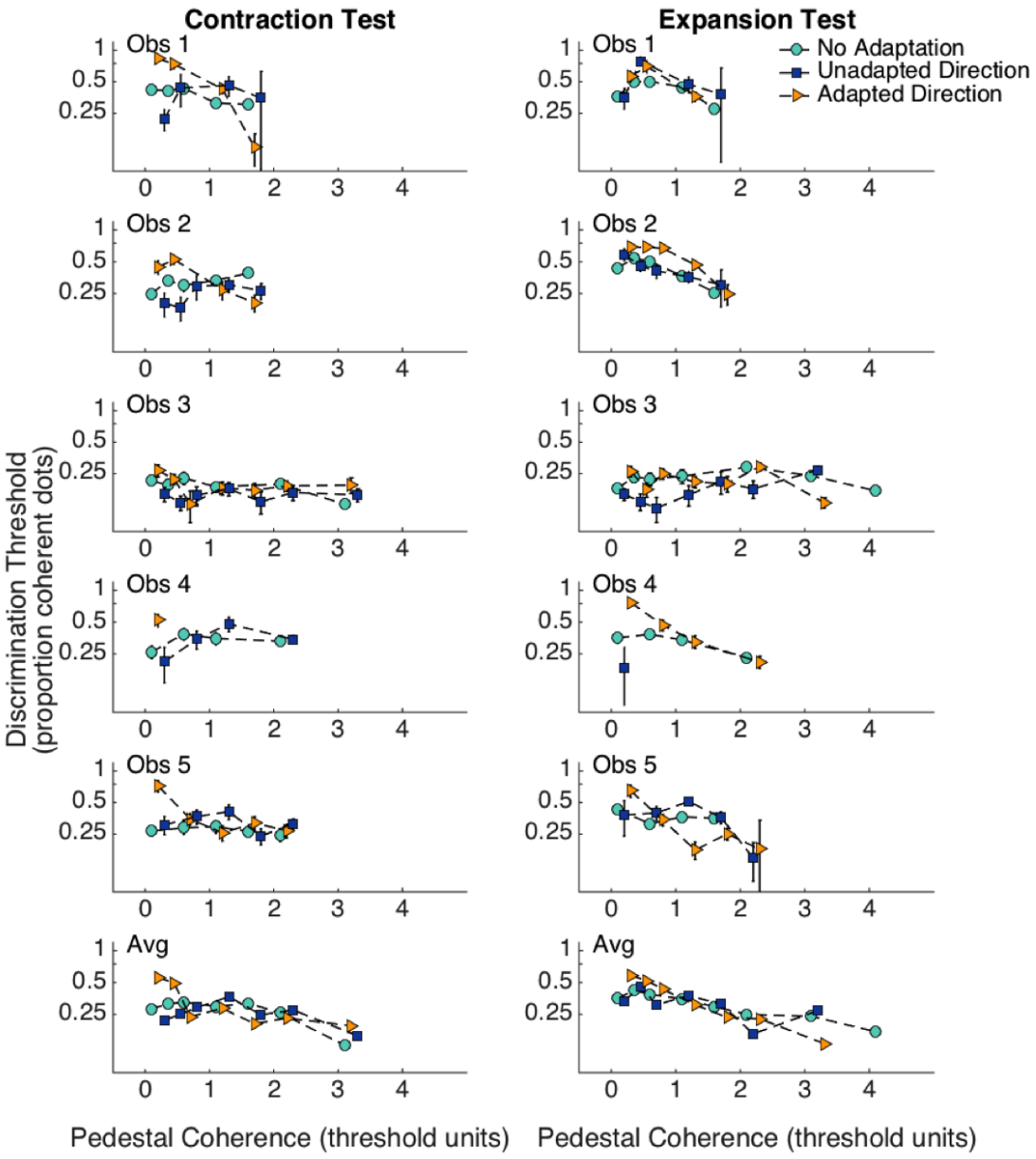

Figure 3.5: Motion: s2AFC discrimination thresholds Discrimination thresholds for contraction (Left column) and expansion (Right column) test directions, without adaptation (turquoise circles) and following adaptation in either the same direction (yellow triangles) or that opposite the test (blue squares) are shown as a function of pedestal coherence in units of detection threshold for all five observers. Data points are based on at least 3 sessions of 50 trials each and error bars represent bootstrapped standard errors. Note that markers are slightly offset for visibility.

Discrimination

Data was collected for both contraction and expansion test directions after adaptation to either of the two directions of radial motion. Discrimination thresholds were defined as the smallest detectable increment of dots moving coherently in order for a difference in contraction or expansion to be detected on 75 percent of trials. There were therefore four combinations of directional conditions; adapt and test for contraction, adapt to contraction and test for expansion, adapt and test for expansion, and adapt to expansion and test for contraction. Discrimination thresholds were determined for pedestals in multiples (0.25, 0.5, 1, 1.5, 2, 3) of each observer's absolute detection threshold without adaptation, and TvC functions were estimated (see Figure 3.5). On average, adaptation had no effect once the pedestals exceeded 1.5x the absolute detection threshold. The discrimination thresholds for the unadapted direction were not significantly affected by the addition of a pedestal (3-factor repeated measures ANOVA, $F(1,4) = 2.94$, $p = 0.16$), while those without adaptation and in the adapted direction tended to decrease slightly at high pedestals (3x or 4x the absolute threshold, not statistically significant). There was no sensitivity difference between contraction and expansion which was consistent between subjects. The results of this study show that the JND for radial motion is constant with increasing pedestal levels. While adaptation leads to an increase in detection thresholds in the adapted direction, it does not have an affect on motion discrimination at pedestals greater than 1.5x the absolute threshold.

3.2.4 Discussion

This study used radially moving partially-coherent dot stimuli to measure the MAE. The percentage of dots moving coherently was varied in order to determine thresholds following adaptation. The higher the percentage of dots needed to offset the MAE, the greater the presumed magnitude of the MAE (Blake & Hiris 1993).

The coherence thresholds observed in the unadapted direction in the present study

were slightly lower than the thresholds without adaptation. This supports a similar effect reported by Hirahara (2006) at low speeds (2 deg/s). The sensitivity for contracting motion matches that for expansion, and there is no significant difference between the two directions of movement in any of the conditions tested. This result supports the findings of Edwards & Ibbotson (2007), who report no consistent difference between dot coherence thresholds for the two directions of radial motion using strict optic flow stimuli. While earlier reports (Bakan & Mizusawa 1963, Spitz 1966) suggested an asymmetry in the level of adaptation to contracting and expanding motion, the methods used were less robust than those here and in Edwards & Ibbotson, as noted in the Results section above.

The way in which sensitivity varies with increasing baseline (pedestal) stimulus intensity has been studied in many modalities including contrast, blur, orientation and motion. The relation between pedestal intensity I and the Just Noticeable Increment ΔI often follows what is known as Weber's Law, stating that the JND between stimuli is proportional to the pedestal magnitude. Therefore, $k = \frac{\Delta I}{I_{Pedestal}}$, where k is a constant "Weber fraction".

A branch of these threshold-versus-contrast (TvC) functions often have a characteristic shape: the just-noticeable-difference (JND) initially decreases until the detection threshold (facilitation) and increases thereafter (masking), forming a "dipper" shape (Green 1960, Solomon 2009) where the masking region has a slope of about 1. The dip is generally explained as a product of inefficient processing of the human visual system, which could be due to an internal sensory threshold, intrinsic uncertainty, a non-linear transducer, or a combination thereof, while the masking region is assumed to be due to saturation in the transducer. There is no robust evidence of a dip in the motion coherence discrimination functions; since the dip likely reflects inefficiencies of the visual system such as an internal sensory threshold, this suggests that the processing of motion coherence does not suffer from such an inefficiency.

Experiment 1 shows radial motion discrimination to be fairly constant with increasing baseline (pedestal) coherence, and there is no masking region as has commonly been observed in studies of luminance (Bartlett 1942, Cornsweet & Pinsker 1965), orientation (Morgan, Chubb & Solomon 2008), and motion discrimination (Morgan, Chubb & Solomon 2006, 2011). Previous reports have found that contrast discrimination following adaptation to drifting Gabor patches behaves in a similar way - absolute detection sensitivity is reduced, while discrimination is unaffected (Morgan et al. 2006, 2011). This raises the possibility that related mechanisms underlie adaptation to contrast and motion coherence. Adaptation usually causes the dip in the TvC function of a test grating to be shifted upwards and to the right, but has no effect on the masking region at higher contrasts (Foley & Chen 1997, Ross, Speed & Morgan 1993), because masks can both shift the transducer function to the right and stimulate the detecting mechanism. This is predicted by a model that receives input from a linear receptive field as well as broadly tuned divisive inhibition (see Ross & Speed (1991) and Foley & Chen (1997)). Morgan et al. showed that the effects on contrast after adapting to a drifting Gabor could be accounted for by changes in divisive inhibition in the transducer function (a velocity-tuned mechanism is released from inhibition, producing an increased response in the direction opposite the adapter), beside a subtractive effect (recalibration of the zero-velocity point) (Morgan et al. 2011). These results suggest that adaptation-induced changes in divisive inhibition may explain why adaptation to radial motion increased thresholds at low, but not high, pedestals.

The finding that discrimination functions for radial motion coherence are quite flat and do not show a "dipper" shape suggests that the transducer does not saturate within the stimulus range, which would result in masking in the TvC function, and indicates that the neuronal response is linear with increasing dot coherence. In fact, Britten, Shadlen, Newsome & Movshon (1992*a*) recorded electrophysiological data from rhesus macaques as they were performing a psychophysical direction discrimination task using

partially-coherent random dot stimuli. Their results show that cell firing rates in MT account well for the psychophysical threshold and shape of the psychometric function for increasing translational motion coherence. Furthermore, Rees, Friston & Koch (2000) find that as humans observe patterns of increasing dot motion coherence, the BOLD response in V5 also increases linearly.

In this experiment, the total number of dots was constant and the proportion of coherent and incoherently moving dots was varied. Thus, at low coherences subjects could have estimated the numbers of coherently moving dots in each stimulus, while at high coherences they could have counted the incoherently moving dots. This suggests an alternative explanation - that the task may be mediated by a mechanism that is sensitive to the relative numbers of signal and noise elements, and that this number estimate is independent of pedestal coherence. While numerosity has been shown to obey Weber's law (Jevons 1871, Ross 2003), previous experiments have varied the total (rather than relative) number of elements. To test this hypothesis, an experiment was conducted in which discrimination functions were determined for orientation (see Experiment 2).

Another factor affecting the results is that in the present study the two test stimuli were presented on the left and right side of the screen at the same time. Previous studies have shown that spatial summation occurs over large receptive fields for optic flow (Burr, Morrone & Vaina 1998). It is therefore possible that global processing is interfering with the estimate of motion direction at the boundary between the two hemifields. To confirm that the high thresholds observed here are not due to interference between test stimuli, an additional study (see Experiment 3) was conducted with a temporal 2AFC procedure.

3.3 Experiment 2 - orientation discrimination in a spatial 2AFC task

3.3.1 Introduction

The results of Experiment 1 show that discrimination functions for radial motion are constant with increasing baseline coherence, suggesting that it does not follow Weber's law. It should be noted that the number of increment dots added was constant across pedestals. Therefore, the discrimination task might have been performed by making a number judgement on the dot directions (i.e. deciding how many dots were signal and how many were noise). In this case, we would expect the same pattern of results if we measure discrimination of orientation rather than motion. To clarify this possibility, the present study measures orientation discrimination functions using parameters as close as possible to those used in Experiment 1.

3.3.2 Methods

Equipment and stimuli

Stimuli were presented on a Sony Trinitron monitor with a refresh rate of 60 Hz and mean luminance of 22 cd/m^2. Subjects were positioned at a viewing distance of 70 cm from the screen using a chin rest. At this distance, the stimulus area subtended 8.2 by 16.7 degrees of visual angle. All observers used the same experimental set-up.

The stimuli consisted of two hemifields of 300 Gabor patches (see General Methods, Section 2.4.2), 0.25 degree in diameter each, presented within two rectangular apertures 8.2 degrees across, and were designed to be as similar as possible to the moving dot stimuli presented in Experiment 1. The Gabors had a limited lifetime of 0.6 seconds, and the phase of the sine wave component was jittered.

Procedures

Data was collected using a spatial two-alternative forced choice (s2AFC) procedure, as in Experiment 1. One hemifield contained the standard (baseline) stimulus, and the other contained the standard and an additional increment (signal).

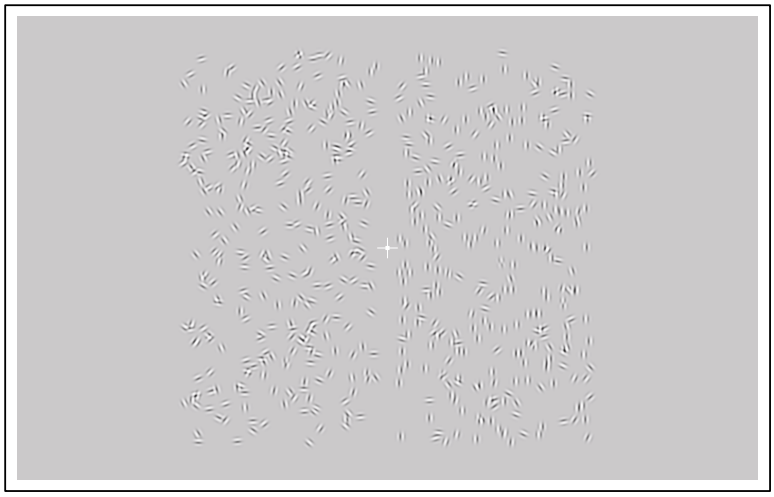

Figure 3.6: Orientation discrimination stimulus Stimuli for Experiment 2 consisted of two hemifields of 300 Gabor patches at varying orientation coherences.

For a measure of the absolute threshold, the signal side contained a varying percentage of coherently oriented Gabors (90° - vertical, or 0° - horizontal), and the standard contained either noise (evenly distributed on orientations of 0 - 180°) or a pedestal of coherently oriented elements (either horizontal or vertical, see Figure 3.6). The pedestal was varied in multiples of the observer's absolute threshold (0.5, 1, 2, 3 and 4). The test was presented for 0.5 seconds and the observer's task was to identify which hemifield contained more coherently oriented Gabor patches by pressing the left or right keyboard arrows for the left and right hemifields respectively. Feedback was provided in form of a colour change in the fixation point (green - correct, red - incorrect).

Coherence increments were determined by the method of constant stimuli, with a minimum increment of either 0 percent or the pedestal coherence, a maximum of 99 percent and 10 levels spaced equally in between. Each session contained ten repetitions at each increment, presented in a pseudo-random order. The pedestal conditions were

blocked, and each observer performed 3 to 5 sessions for each pedestal intensity in randomised order. Coherence detection thresholds were calculated for each session, allowing estimates of the mean and standard error across sessions. The data were collapsed across trials, and thresholds at the 75% correct point were estimated by a 2-parameter fit of a Cumulative Normal function as for Experiment 1.

Observers

Data was collected from five observers (JF, ME, MM, NN and SR). Of these, four were experienced in psychophysical tasks and all except MM and NN were naive as to the purpose of the experiment. Vision was corrected when necessary and all experiments were conducted binocularly with natural pupils.

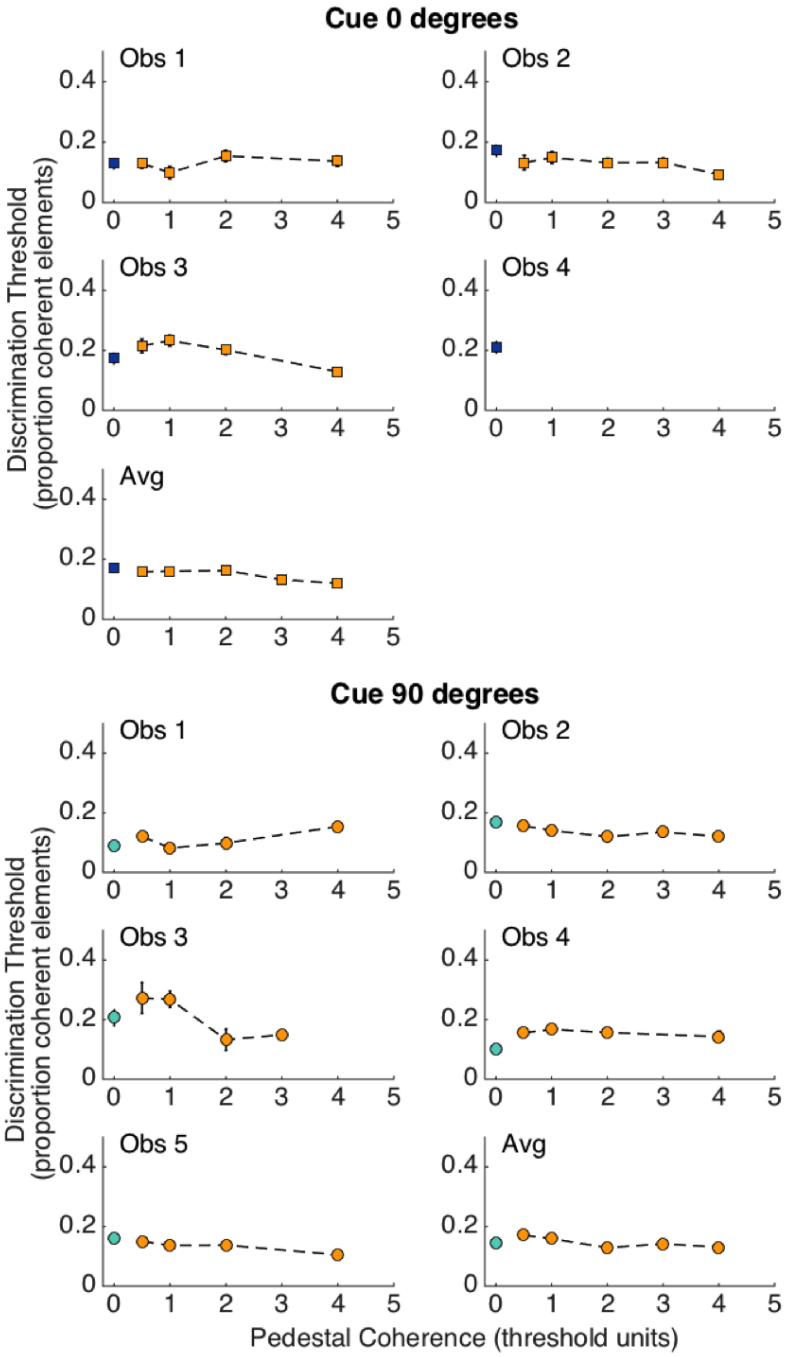

Figure 3.7: Orientation: t2AFC discrimination thresholds Orientation detection (blue/turquoise) and discrimination (yellow) thresholds for four/five observers are shown as a function of pedestal coherence in units of the detection threshold. Data points are based on at least 4 sessions of 100 trials each and error bars represent bootstrapped standard errors.

3.3.3 Results

Figure 3.7 shows the results of Experiment 2. The top panel shows discrimination for horizontal (0°) cues and the panel below for vertical (90°) cues. The detection thresholds for each observer are represented by blue/turquoise markers, and the discrimination thresholds by yellow markers. Detection thresholds varied from a proportion coherence of 0.09 to 0.21, and were therefore lower than those for radial motion by about a factor of two. A two-way repeated-measures ANOVA was carried out to determine the effect of pedestal on the discrimination thresholds. While they show minimal variations, there is no significant change in discrimination thresholds over pedestals for any of the five observers (2-factor repeated measures ANOVA).

3.3.4 Discussion

This experiment measured coherence sensitivity for oriented Gabor elements using a spatial 2AFC procedure. Observers were asked to indicate which of two stimuli contained 'more vertical' (or 'more horizontal') elements at a set pedestal value (0, 0.5, 1, 2, 3, and 4 times the absolute threshold). The discrimination functions are found to be unvarying over pedestal intensities, just as in Experiment 1.

It should be noted that the discrimination functions for motion and those for orientation remain comparably constant with increasing pedestal coherence. Assuming that observer responses are based on the perceived coherence, the shape of the discrimination function relates to the relationship between the mean perceived coherence and its variance. The constant discrimination functions for motion and orientation coherence indicate a common mechanism, and are most simply explained by linear transduction and a constant variance.

Our ability to estimate and compare quantities has been studied extensively in the past (see Anobile, Cicchini & Burr (2016) for a review), and some suggest the existence of visual mechanisms selective for numerosity (Burr & Ross 2008, Ross & Burr 2010). Cues for numerosity however, are often intertwined with cues for size and density; as

the number of elements is increased, size, density, or both will increase correspondingly. Observers have been shown to discriminate between size and density, indicating that there are distinct channels for these dimensions (Raphael & Morgan 2016). In the present experiment, the total number of elements was held constant, so that there were no associated size or density cues.

Number estimates are known to be most efficient for small quantities (in the subitizing range, < 5) which enable counting of all the elements in the set (Jevons 1871). In this experiment, each stimulus contained 300 elements, some with random orientations and others aligned to the vertical or horizontal. Except at the extreme ends of the stimulus range, there were therefore > 5 elements which were coherently (or incoherently) oriented. Based on this, the density of elements in the test stimuli fall within the *number estimation* range proposed by Anobile et al. (2016), within which errors typically follow Weber's law. Recent results however, show that observers can evaluate mean numerosity in regions of fixed size indicating that numerosity could be used as a summary statistic (Solomon & Morgan 2017). Estimates based on small subsets could then be extrapolated to stimuli containing a greater total number of elements. While counting in the subitizing range is highly efficient, observers do make occasional lapses where they effectively ignore all of the information available in the stimulus. A constant lapse rate combined with proportion estimates based on small subsets of elements could then account for the pattern of results observed in the present experiment.

Scaling the Gabors for eccentricity might enable observers to take more elements into account, thereby increasing their efficiency. In the experiment, observers were asked to fixate at the centre of the screen and the orientation judgements were most likely based on a few centrally located Gabor elements, whose orientation could clearly be identified. While subitizing has been shown to require attentional resources, a small number of items can be enumerated in presentation times as short as 50 ms (Egeth, Leonard & Palomares 2008), and 200 ms (Vetter, Butterworth & Bahrami 2008*b*).

Another point to consider is that detection for orientation coherence is found to be better than for radial motion. Since the experimental paradigm was chosen to be as close as possible between Experiments 1 and 2, it is unlikely that this is due to a procedural artefact. A more plausible account could lie in differential sensitivities of early orientation- and motion- selective mechanisms. Performance on proportion discrimination tasks has previously been shown to depend on the visual attribute distinguishing the two sets of elements. Discriminating relative numbers of dots moving in opposite directions is particularly poor (Raidvee et al. 2011), with decisions being based on as few at 0.5% of elements (Raidvee et al. 2012). Meanwhile, in a task of discriminating proportions of parallel and converging lines, observers performed as if considering about 2% of elements (Tokita & Ishiguchi 2009). This discrepancy between motion and orientation judgements, albeit small, could contribute to the difference between thresholds for motion and orientations observed in the present study. It appears likely then, that proportion discrimination includes processing stages which are discrete for different visual attributes, as well as later stages which compare relative numerosities.

An alternative account for the flat discrimination functions for orientation discrimination is through inefficient estimation of orientation variance. Morgan et al. (2008) measured the just-noticeable difference in orientation variance as a function of the pedestal variance using a roving pedestal which excluded counting and energy in any particular direction (e.g. vertical) as possible mechanisms. They found that the JND follows the characteristic 'dipper' function when plotted in terms of the standard deviation of the pedestal variance, which could be described by intrinsic noise in a mechanism specialised in computing variance, with a possible sensory threshold. Representing the Morgan et al. (2008) data in terms of orientation variance, an arguably more appropriate measure, Solomon (2009) showed that there was very slight, if any, facilitation. Decisions in the present experiment may then be similarly based on inefficient computation of orientation variance.

In summary, this experiment set out to test whether the flat discrimination functions observed in Experiment 1 could be explained by numerosity estimation mechanisms by measuring analogous discrimination functions for orientation. The results could be explained either by relative proportion estimates, possibly based on counting of subsets of elements within the subitizing range, or by inefficient estimates of orientation variance. Note that the experiment presented here does not confirm that relative numerosity judgements are underlying the results for motion coherence. Experiments that could provide further evidence to this idea could measure discrimination for elements of differing colours. When signal dots in an RDK have a different colour from noise dots, motion coherence thresholds are greatly improved (Croner & Albright 1997). Colour therefore provides a strong segmentation cue and motion integration would not be necessary in order to extract the signal. Further psychophysical studies of proportion discrimination could also help to uncover the relation between the mechanisms processing proportions and those for absolute numerosity.

3.4 Experiment 3 - effect of adaptation on motion discrimination in a temporal 2AFC task

3.4.1 Introduction

In Experiments 1 and 2, a *spatial* two-alternative forced choice procedure was used, in which the two test stimuli were presented simultaneously on the two sides of the screen. In this task, adapting to equal motion on both sides would affect both test stimuli equally. The procedure was chosen because when the stimuli are presented sequentially in time (temporal, t2AFC), the MAE would be expected to be stronger for the first stimulus than for the second, and the motion of the first stimulus would further influence the MAE perceived at the time of the second stimulus.

However, presentation of the two stimuli in adjacent hemifields may interfere with

global processing of motion. In fact, sensitivity for motion coherence has been shown to increase with stimulus area in a way that implies linear integration (Morrone, Burr & Vaina 1995). Burr et al. (1998) found summation over large receptive fields for optic flow, extending 30 - 70 degrees across the visual field. It is thus likely that spatial summation of the local motion signals can occur around the vertical boundary between the two hemifields, since some cells will have receptive fields that cover regions of both test stimuli and will integrate the two signals. In order to investigate this idea, this experiment tests discrimination following adaptation using a *temporal* sequence of the test alternatives.

As noted above, by presenting the two stimuli successively in time, the strength of adaptation will differ between the two test stimuli. If we assume the adaptation period ends at t_0, the first test stimulus is presented at t_1 (t_0 + 100 ms) and the second test stimulus at t_2 (t_0 + 400 ms). Since the velocity of the MAE declines exponentially (Taylor 1963), and its duration corresponds with the square root of the adaptation time (Hershenson 1989), the strength of adaptation would then be greater at t_1 than at t_2;

$$Duration = kI^x,$$

where k is a constant, I is the inspection duration and x is the exponent of the power function. This effect however, is balanced by using a true 2AFC procedure.

3.4.2 Methods

Equipment and stimuli

Stimuli were presented on a Sony Trinitron monitor with a refresh rate of 60 Hz and mean luminance of 22 cd/m^2. Subjects were positioned at a viewing distance of 70 cm using a chin rest. At this distance, stimuli subtended 16.7 degrees in diameter. All observers used the same experimental set-up.

The test stimuli were random dot fields with varying dot motion coherence levels. Two circular dot fields of 600 dots each were presented in sequence for 200 ms each, separated by a blank (mean luminance) screen containing only a fixation point for 100 ms. Each dot moved at a speed of 5.6 deg/s and had a limited lifetime of 0.6 seconds, after which it disappeared, was repositioned to a random position within the stimulus window and continued on its trajectory.

Procedures

A temporal 2AFC procedure was used for this experiment. The standard and signal stimuli were presented successively in time, separated by a blank screen containing only a fixation point on a mean-luminance background. Stimulus duration was 200 ms, and was kept shorter than for Experiments 1 and 2 in order to minimise temporal distortion of adaptation effects. The observer's task was to answer,"Does the first or second stimulus contain more coherent contracting/expanding motion?", using a button press.

In the adaptation conditions, a 20 second adaptation period preceded each session, and a 5 second top-up adaptation period preceded each successive trial. During the adaptation periods, all dots moved coherently in one radial direction (either contracting or expanding). Only one adaptation direction was tested on each day.

Data was collected for the two radial motion directions independently. Coherence increments were determined by the method of constant stimuli, with a minimum increment of either 0 percent or the coherence pedestal, a maximum of 99 percent and 10 levels spaced equally in between. Each session contained ten repetitions at each increment, presented in a pseudo-random order. The pedestal conditions were blocked, and each observer performed 3 to 5 sessions for each pedestal intensity in randomised order. The data were then collapsed across trials, and coherence detection thresholds were estimated at the 75% correct point as detailed for Experiment 1.

Observers

Four observers (AG, LS, MW and NN), three of which were naive, participated in this experiment. Vision was corrected when necessary and all experiments were conducted binocularly with natural pupils.

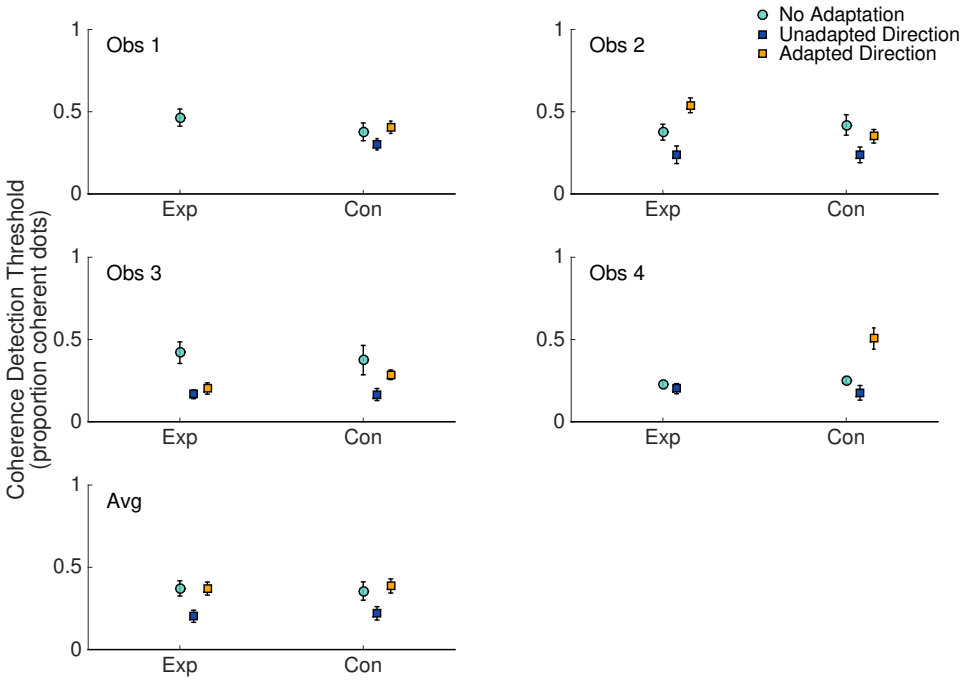

Figure 3.8: Motion: t2AFC detection thresholds for contraction and expansion Dot coherence detection thresholds for temporal 2AFC procedure for contraction and expansion for each observer individually, and averaged across observers. Data points are based on at least 3 sessions of 100 trials each (300 trials total) in each direction and error bars represent bootstrapped standard errors.

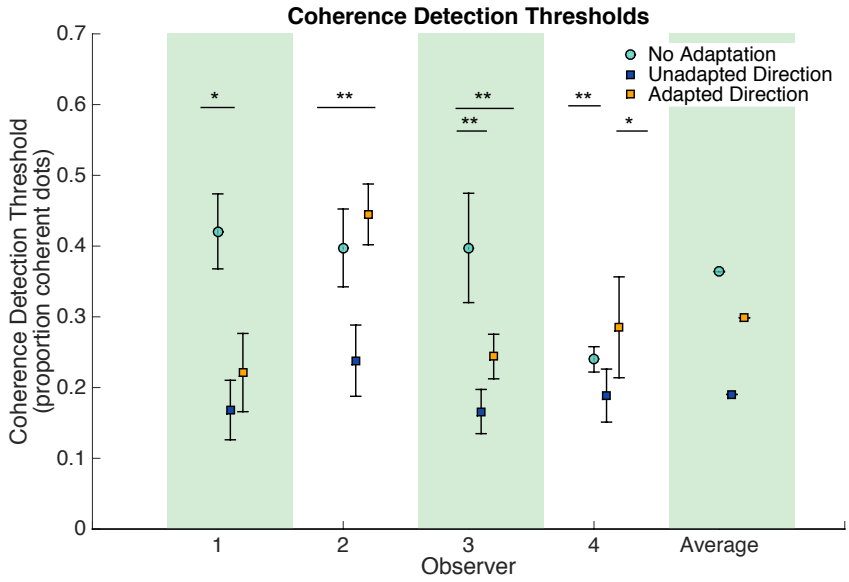

Figure 3.9: Motion: t2AFC detection thresholds Dot coherence detection thresholds for temporal 2AFC procedure pooled across direction (contraction and expansion) for each observer individually, and averaged across observers. Data points are based on at least 3 sessions of 100 trials each in each direction and error bars represent bootstrapped standard errors. Two-tailed t-test significance levels: * $p < 0.01$, ** $p < 0.005$. Upper stars show significance levels between No Adaptation and Adapted Direction conditions, and lower stars between No Adaptation and Unadapted Direction (left), and Unadapted and Adapted Direction conditions (right).

3.4.3 Results

Detection

The absolute threshold estimates for radial motion as measured by a temporal 2AFC procedure are shown in Figures 3.8 and 3.9. There was no consistent difference between contraction and expansion thresholds for any of the observers tested, as can be seen in Figure 3.8. In Figure 3.9, the results are collapsed across the two test directions (contraction and expansion) and are plotted for all three adaptation conditions (no adaptation, test in the adapted direction, test in the unadapted direction) for four observers and the average of those data. As in Experiment 1, both stimuli appeared to contain coherent motion due to adaptation, and the observer's task was to identify which of the two stimuli contained the greater signal. Thresholds in the adapted direction

are higher than those without adaptation and in the unadapted direction for two out of the four observers. There are however, large individual differences - adaptation has a facilitatory effect in the adapted direction for observers 1 and 3, and the detection thresholds vary between 0.25 and 0.42 (no adaptation) and between 0.23 and 0.43 proportion coherence (adapted direction).

Discrimination

Figure 3.10 shows TvC functions for expansion and contraction for stimuli presented in succession (temporal 2AFC). Data for four observers are plotted for the three adaptation conditions: no adaptation (turquoise circles), unadapted direction (blue squares) and adapted direction (yellow triangles). A three-way repeated-measure ANOVA was performed to examine the effect of adaptation direction, test direction and pedestal level on thresholds. A statistically significant interaction was found between the effects of adaptation direction and pedestal on thresholds, $F(2,4) = 37.75$, $p = 0.0025$. Discrimination thresholds in the adapted direction tend to decrease with increasing pedestals. Any adaptation effects on detection thresholds (zero-pedestal condition) appear to be erased by the addition of a pedestal coherence level. There is some variation between observers. Observer 4 shows a much stronger effect of adaptation on near-threshold discrimination sensitivity, where their discrimination thresholds are almost doubled.

3.4.4 Discussion

The purpose of this experiment was to test whether interference between the two test stimuli may be occurring due to spatial summation when using an s2AFC procedure, as in Experiments 1 and 2.

Detection thresholds without adaptation in the temporal 2AFC experiment presented here were slightly higher compared to those in spatial 2AFC, with an inter-subject

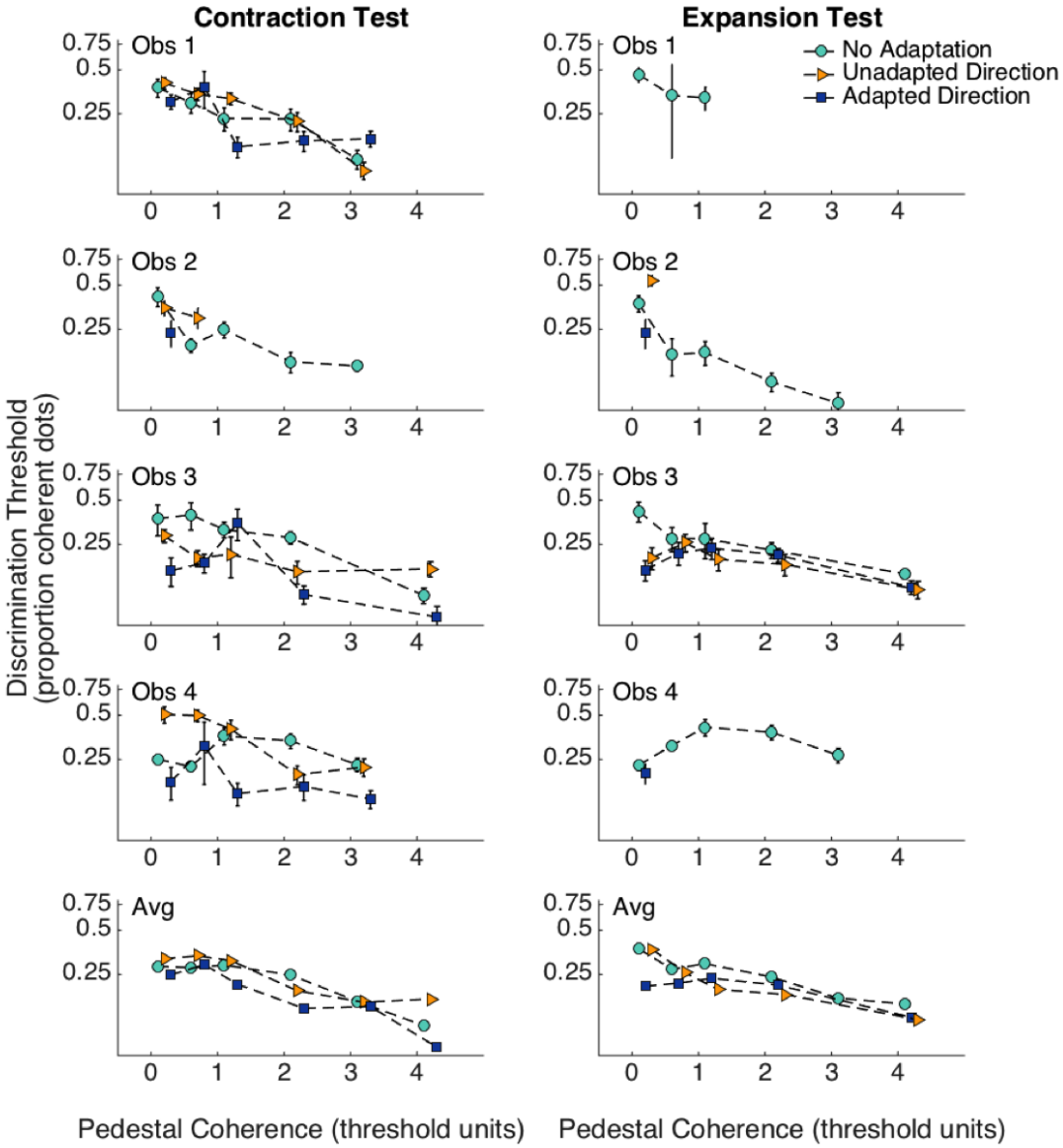

Figure 3.10: Motion: t2AFC discrimination thresholds Discrimination thresholds for contraction (left column) and expansion (right column) test directions, without adaptation (turquoise circles) and following adaptation in either the same direction (yellow triangles) or that opposite the test (blue squares) are shown as a function of pedestal coherence in units of detection threshold for all four observers. Data points are based on at least 3 sessions of 50 trials each and error bars represent bootstrapped standard errors. Note that markers are slightly offset for visibility.

mean of 0.36 and 0.31, respectively. The adapted and unadapted directions however, differed unexpectedly. While thresholds in the adapted direction were significantly higher than without adaptation or in the unadapted direction in the s2AFC experiment, in tAFC some subjects had reduced thresholds in the adapted and unadapted conditions, relative to thresholds without adaptation. In the s2AFC experiment, thresholds in the adapted direction averaged at 0.59 coherence over observers, whereas in the t2AFC experiment they averaged just 0.3. Adaptation therefore reduced sensitivity in the adapted direction in s2AFC by about a factor of 2 more than in the t2AFC paradigm. Note that the phenomenological effect of adaptation is to increase the apparent coherent motion in the direction opposite the adaptor. This is likely a product of a reduction in the perceived speed in the adapted direction, due to disinhibition of velocity-tuned mechanisms (Morgan et al. 2006). In the case of the zero pedestal level, both the signal and noise stimuli therefore appeared to contain coherent motion, effectively making it a discrimination task, which can be modelled as a rightward shift in the transducer function.

If differing motion signals in the two hemifields interfered with global motion processing, we would expect more uncertainty in the detection of both the signal and standard test stimuli, since motion around the inner vertical edge of one stimulus would be integrated with motion from the adjacent stimulus. For example, if the left hemifield contains the coherence signal and the right contains pure random dot motion, then integration of motion signals will cause the signal closest to the vertical meridian to look weaker on the left, and the noise to look more coherent on the right.

Discrimination thresholds in the temporal 2AFC task were not consistently higher than those for the spatial 2AFC task, indicating that summation over the two hemifields (Burr et al. 1998) did not interfere with task performance. Just as in Experiment 1, the addition of a pedestal did not increase the JND in motion coherence. Following adaptation to contracting or expanding motion, detection thresholds for the adapted

direction were either increased or decreased, but there was no effect of adaptation on discrimination of pedestal levels greater than the absolute threshold. These results further support the idea that the decision in this task is based on the relative numbers of coherent and randomly moving dots, as suggested and detailed in Experiments 1 and 2.

3.5 Experiment 4 - effect of directed attention on motion adaptation

3.5.1 Introduction

Numerous studies have attempted to understand the effect that attention has on motion processing, and on adaptation to motion in particular. In the very first of these in 1911, Wohlgemuth asked observers to perform mental arithmetic, reading and rapid serial visual presentation (RSVP) tasks while viewing a moving stimulus, and found that distracting attention had no effect on the duration of the motion aftereffect. Since then, results on the topic have been controversial. Eighty years later, Chaudhuri (1990*b*) measured the MAE duration after observers had concentrated on an RSVP task during adaptation. He found a reduction of about 50% in MAE durations compared to when there was no attentional distraction task. Other studies have subsequently also reported that distracting attention away from the adapting stimulus reduces the strength of adaptation (Rees et al. 1997, Rezec et al. 2004, Taya et al. 2009) possibly by interfering with motion processing.

However, most of these experiments have reported the duration measure of the aftereffect, which is known to be susceptible to experimenter and subject bias (Sinha 1952). Observers are asked to report when the apparent motion ceases, in a stimulus that they *know* is in fact stationary. In order to do the task, the observer needs to adopt a criterion, which can be easily shifted by manipulating the given instructions. Morgan (2011) used a 2AFC task to measure the loss in sensitivity following adaptation

in different conditions of attentional load, and found no effect of distracting attention on the contrast discrimination function.

Several studies have investigated the effects of 'tracking', or directing attention, to one component in transparent motion stimuli, and evidence suggests that this does produce a motion aftereffect in the direction opposite to the attended component (Alais & Blake 1999, Lankheet & Verstraten 1995, Raphael et al. 2010). Lankheet & Verstraten (1995) asked subjects to selectively attend to one component of a transparent random dot stimulus, in which the two components were moving in opposing directions, translating towards the left and right across the screen. They found that motion adaptation was increased for the attended component. However, they only tested two observers, and this effect of attentional tracking does not necessarily depend on the same underlying mechanism as the effect of distraction. In fact, Raphael et al. (2010) found an effect of attentional tracking on the MAE but none when attention was distracted away from the adapter. They varied the relative velocities of fields of transparently moving contracting and expanding dots in order to find the point at which the illusory motion of the MAE was cancelled. Furthermore, it has been suggested that the MAE measured with dynamic (flickering) test stimuli is more susceptible to attentional effects than when measured with static test stimuli (Culham et al. 2000).

This study aims to investigate whether attention directed to one component of a radial, transparently moving dot stimulus causes more adaptation to that component, using the same kind of stimuli as in Experiment 3 above.

3.5.2 Methods

Equipment and stimuli

Stimuli were presented on a Sony Trinitron monitor with a refresh rate of 60 Hz and mean luminance of 22 cd/m^2, and connected to an Apple MacBook Pro with OS X 10.8 "Mountain Lion" running Matlab 2013 and the PsychToolBox software (Brainard 1997,

Pelli 1997). Other variables were as detailed in Chapter 2. Subjects were positioned at a viewing distance of 70 cm from the screen using a chin rest. At this distance, stimuli subtended 16.7 degrees of visual angle. All observers used the same experimental set-up.

Stimuli consisted of partially-coherent moving random dots, just as in Experiments 1 and 3. Each dot had a limited lifetime of 0.6 seconds and moved at a speed of 5.6 deg/s. There were three classes of adaptation conditions. First, No adaptation, basically testing the absolute threshold as in Experiment 3. Second, Basic adaptation, where the initial adaptation period lasted 20 seconds, with an additional 5 second top-up before each trial. During adaptation, all 600 dots were black and moved coherently (either contracting or expanding), and observers had to perform an attentional task (see Procedures below). Lastly, in the Transparent adaptation condition, half the dots were black and moved in one radial direction (contracting or expanding) and the other half where white and moved in the opposing radial direction. Again, all dots moved coherently (i.e. there was no random dot motion), and observers performed an attentional task.

Procedures

A temporal 2AFC procedure was used for this experiment, as for Experiment 3. During the test period, the standard and signal stimuli were presented successively in time for 200 ms each, separated by a blank screen containing a fixation point on a mean-luminance background for 100 ms.

Data were collected for expansion and contraction independently. Coherence increments were determined by the method of constant stimuli, with a minimum increment of 0 percent, a maximum of 99 percent and 10 levels spaced equally in between. Each session contained ten repetitions at each increment, presented in a pseudo-random order. Each observer performed 3 to 5 sessions for each experimental condition in randomised order. The data were then collapsed across trials, and coherence detection thresholds at the 75% correct point were estimated by a 2-parameter fit of a Cumulative Normal

function as detailed for Experiment 1.

The Basic and Transparent adaptation conditions contained an attentional task. For this task, the adaptation period contained a few events, which consisted of brief periods (167 ms at 60 Hz) during which all dots in the motion component accelerated to 11.2 deg/s (2x base speed). The observer's task was to respond to events by pressing the space bar on a keyboard. Responses were considered correct if they occurred within 1 second of the start of the event. In the transparent adaptation condition, both of the components (black and white dot fields) contained events. Subjects were asked to respond to either one of them ("attend to contracting" and "attend to expanding" conditions) or to both ("attend to both"). If they were responding to both, subjects used the same button to indicate events in the two fields. There were two Transparent adaptation conditions for which attention to both components was required, one with the black dots contracting (white expanding), and another with the black dots expanding (and white contracting).

Observers

Five observers (AG, DPW, LR, NN and TP), four of which were naive, participated in this experiment. Vision was corrected when necessary and all experiments were conducted binocularly with natural pupils.

3.5.3 Results

In order to examine the effect of directing attention to a motion component, we used a test stimulus in which two components (contracting and expanding) contained equal motion energy and all that differed was *which component observers attended* while keeping their gaze on a central fixation point. The MAE following basic adaptation to only one radial direction of motion was also measured as a comparison. Figure 3.11 shows the results of Experiment 3, normalized to each observer's absolute detection

threshold. Plotted on the white background are the basic adaptation conditions (No Adaptation, Adapted Direction and Unadapted Direction), and on the green background are the transparent adaptor conditions (Attended Direction, Unattended Direction and Both Directions Attended). Yellow markers indicate the adapted (squares) and attended (stars) directions, and blue markers show the unadapted (squares) and unattended (stars) directions.

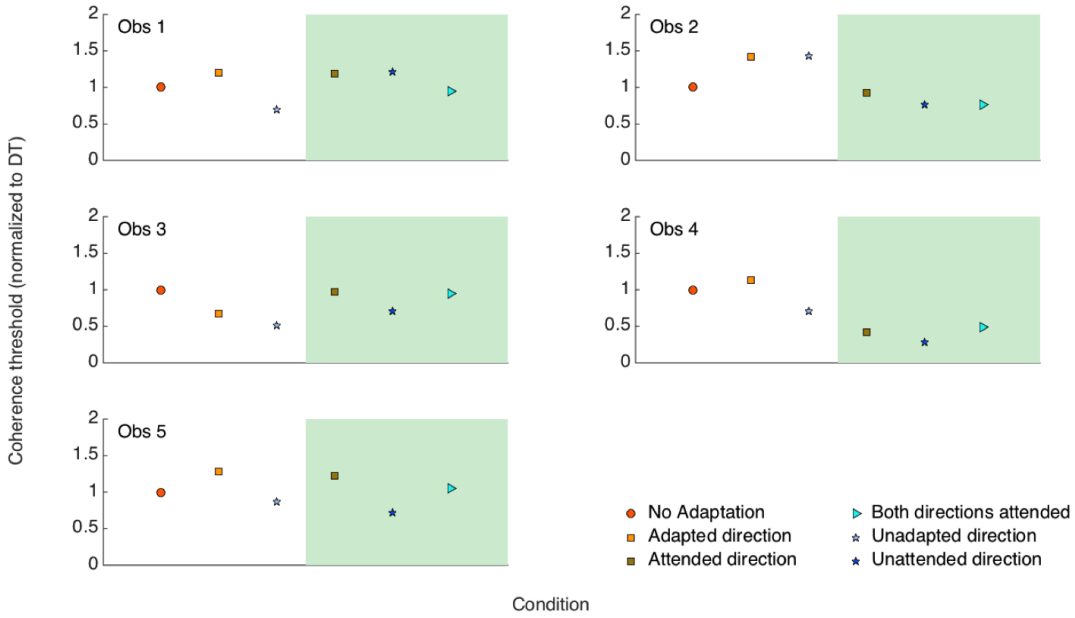

Figure 3.11: Manipulating attention during adaptation to radial motion Sensitivity following adaptation to radial motion, and under three attentional tracking conditions, shown for the five observers tested. Data were averaged over the two directions of radial motion (contraction and expansion). Standard adaptation conditions: No Adaptation (orange circles), Adapted Direction (light yellow squares), Unadapted Direction (light blue stars). Attentional tracking conditions (transparent adapter) are indicated on a green background: Attended Direction (dark yellow squares), Unattended Direction (dark blue stars), Both Directions Attended (turquoise triangles). Different conditions are shown on the abscissa, and the coherence threshold (normalized to the No Adaptation threshold of each observer) on the ordinal axis, data points are based on at least 3 sessions of 50 trials each.

Thresholds are significantly greater for the adapted direction than without adaptation for all but one of the five observers (observer 3, two-tailed, paired-sample t-tests, $p < 0.01$). Across all subjects, there was a significant difference between thresholds in the adapted and unadapted directions (two-tailed, paired-sample t-tests, $p < 0.05$). Directing attention to one component of the transparent motion stimulus resulted in higher thresholds for three observers (two-tailed, paired-sample t-tests, $p < 0.01$), but did not affect them for the other two. Attention directed to both components simultaneously does not affect the sensitivity for either direction. For three of the observers (1, 3 and 5), the thresholds for the attended direction do not differ significantly form those in the adapted direction. However, for observer 1 the thresholds in all transparent adaptor conditions are similarly high, indicating that they may have found the task more difficult in all attention conditions.

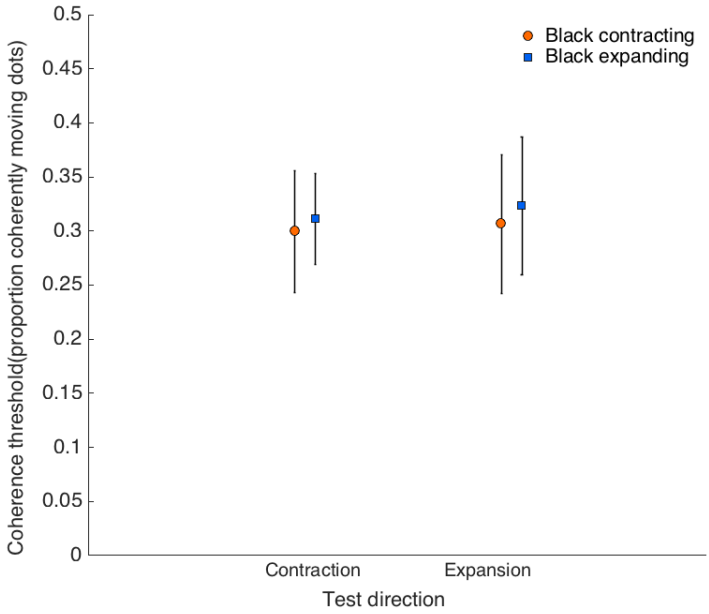

Figure 3.12: Attending to both directions Thresholds for contraction (left) and expansion (right) test directions following adaptation to transparent motion where both radial directions were attended. Data shown are inter-subject means, and represent trials on which the contraction component as black (and expansion white, orange circles), and those where the contraction component was white (and expansion black, blue squares).

Where only one component was attended, that component was black while the unattended component was white. When attention was to be directed to both motion components, black contracted for half of the sessions, and expanded for the other half. If adaptation were specific to the sign of contrast (i.e. to the white or black components), it should be apparent in the condition which requires attention to both motion components (turquoise triangles in Figure 3.11). If adaptation were selective to one sign of contrast, differing results would be expected for sessions in which the white dots were contracting and the sessions in which they were expanding. The detection thresholds were comparable across these two conditions (Figure 3.12), indicating that this is not the case.

It is clear from these results as well as those from the previous experiments (Sections 3.2 to 3.4), that while detection for radial motion is comparable across observers, there are large individual differences in the effect of adaptation thereon. The detection thresholds for Experiment 3 (t2AFC) are a good example of this; while thresholds were increased in the adapted direction for two observers, they were lower than without adaptation for the other two. Furthermore, for some subjects adaptation had different effects on the thresholds for contraction and expansion, increasing one but not the other, such as in the discrimination data for observer 1 in the s2AFC task (Section 3.2). Individual differences in the sensitivity to radial motion are also apparent in the present experiment, as both adaptation and directed attention had differing effects on the observers tested.

A possible reason why we do not find a more robust effect of the attentional manipulation is that the attentional task was not sampling an optimal point in the stimulus space. The task was to identify accelerations of 2x the base speed, but perhaps this was too easy for some observers, and too difficult for others. In order to equate the difficulty of the attentional task, an experiment could probe the psychometric function for detection of an acceleration as a function of speed.

3.5.4 Discussion

The results of this study show that directing attention to a single component in a transparently moving radial dot motion display can produce adaptation in the attended direction for some observers, but that there are inter-subject differences. Since the physical motion signal was equal in both directions in the stimulus, the aftereffect is a product only of observer's focus on a single component. This aftereffect is comparable in size to that seen following basic adaptation to only one direction of motion. These results support those of Culham et al. (2000), who first demonstrated an MAE of attention using flickering counterphase gratings.

Directing attention does not affect motion adaptation for two of the observers tested here. This could be due to the use of a single attentional task which was not calibrated in difficulty for each subject. Some observers may have found the task less demanding than others, and in turn attended less intently on the instructed component. This would lead to relatively low thresholds in all conditions involving a transparently moving stimulus, as is seen in the data for observers 2 and 4. This explanation is speculative, but it would be interesting to separately test performance at different speeds for the attentional task, in order to equate its difficulty across observers.

It is important to distinguish the effects of distracting attention (e.g. Rezec et al. (2004), Taya et al. (2009)) from attentional tracking (e.g. Alais & Blake (1999), Lankheet & Verstraten (1995), Raphael et al. (2010)). Attentional tracking results in an aftereffect with different properties from the traditional MAE - it is not retinotopic, and is independent from MAEs resulting from low-level motion (Culham et al. 2000). The results presented here are therefore independent of, and neither support nor undermine previous investigations that do not find an effect of attention on the MAE using distraction (Morgan 2011, Wohlgemuth 1911).

It is worthwhile to mention a few more things about the effect of distracting attention on the MAE. Most studies of this effect have used the aftereffect's duration as a measure, which is known to be susceptible to experimenter and observer bias (Sinha 1952). When

asked to report when a stimulus that they know is stationary has stopped 'moving', subjects are faced with a conflictive task. Where the criterion is set becomes a crucial factor, and one that can vary from subject to subject and from session to session, as suggested by Granit (1928). One study (Morgan et al. 2012) instructed observers to prefer one response over another in a method of single stimuli task. This caused a shift in their psychometric functions without a change in sensitivity, showing that response bias can easily masquerade as perceptual bias. Especially small effect sizes (for example, as in Taya et al. (2009)) are likely to be due to Type I (false positive) errors (see Section 1.2.2). Finally, it is possible that the relatively high proportion of studies that find an attentional effect on adaptation is a product of reporting bias in the published literature, and as Morgan et al. (2012) suggest, numerous results (especially those showing null effects) may be unreported.

3.6 Chapter summary

This chapter has described a series of psychophysical experiments designed to test whether directed attention can modulate the MAE to radial motion. While such effects have been demonstrated for translation, radial motion forms a more complex pattern and is therefore likely to be processed by higher cortical areas which are also more susceptible to the top-down modulatory effects of attention. In order to measure sensitivity, which - unlike bias - is free from expectation effects, observers adapted to contracting or expanding motion and then discriminated which of two partially-coherent dot stimuli appeared to move more coherently.

Adaptation is shown to reduce sensitivity to motion in the adapted direction at the detection threshold (zero pedestal), but not at higher coherence pedestals (Section 3.2). Since in this experiment the total number of dots was constant and the proportions of coherent and randomly moving dots were varied to achieve varying motion signals, it is possible that subjects used different strategies at low and high coherence levels,

effectively performing a proportion discrimination task. Observers could have estimated the number of coherent elements at low pedestal levels, and that of incoherent elements at high levels. It is suggested that this may be due to the probing of a mechanism sensitive to relative proportions rather than to motion energy, and this possibility is tested using orientation discrimination in Section 3.3. The results showed that the discrimination functions for orientation were unvarying across increasing pedestal values, suggesting that relative proportion judgements underlie observer performance on this task. Furthermore, a proportion discrimination account could explain how it is that adaptation affects threshold performance, but not sensitivity at higher pedestals. In order to investigate whether spatial summation of motion signals across the vertical boundary of the two stimulus alternatives may be interfering with motion processing, a temporal 2AFC experiment was performed (see Section 3.4). Neither detection nor discrimination thresholds in the t2AFC procedure were greater than in the s2AFC experiment, indicating that summation over the two stimulus alternatives did not affect this task, and adding further support for the idea that observers use relative numerosity cues. Finally, Experiment 4 (Section 3.5) shows that directing attention to one component of a radial transparent motion stimulus can result in selective adaptation to that direction of motion for some observers, but not for others, just as some, but not all, observers showed reduced sensitivity following adaptation to radial motion.

The result that absolute thresholds are increased by adaptation while JNDs at higher pedestals are unaffected is consistent with previous results on contrast discrimination (Foley & Chen 1997, Ross et al. 1993). Models that receive input from linear receptive fields as well as broadly-tuned divisive inhibition (Foley & Chen 1997) predict this pattern based on a rightward shift in a sigmoidal transducer function. Adaptation in this model increased the semi-saturation constant. Indeed, changes in divisive inhibition can account for the effect of adapting to a moving grating on the perceived contrast of the test grating (Morgan et al. 2006, 2011). This suggests that an analogous mechanism

may underlie adaptation to motion coherence; adapting to highly coherent contraction could inhibit mechanisms tuned to expansion which, when released from inhibition, produce an increased response resulting in an expanding aftereffect.

It is also useful to consider how a proportion discrimination account could explain the effect of adaptation in Experiments 1 to 3, namely reducing sensitivity at the detection level, but not at pedestals above the absolute threshold. Burr & Ross (2008) showed that adapting to displays containing large element sets led to subsequently viewed sets appearing less numerous. In the case of motion or orientation coherence, adaptation to a large proportion of coherent elements could then make a test stimulus appear to contain a smaller proportion of coherent elements. Observers would obviously need a greater coherence in order to generate the same internal response, which would decrease their sensitivity. Adaptation is then expected to have a similar effect on detection thresholds, whether the underlying process is sensitive to motion energy or number/proportions. One possibility for why adaptation does not affect discrimination once pedestal coherence is added, is that the number of random moving dot elements that observers take into account when estimating global motion direction increases at higher pedestal coherence levels. Raidvee et al. (2011) tested coherence thresholds in dot displays which contained only two opposing directions of motion (leftward and rightward) and analysed the performance using a classical Thurstone psychophysical discrimination model (Thurstone 1927) and a Bernoulli trial model in which the ideal observer selects a random sample of elements (left- or rightward moving dots) to base the decision upon. The Bernoulli trial model gives a simple relationship between the slope of a psychometric function and the size of the subset of randomly chosen elements. They showed that when a moving dot stimulus contained 800 dots (400 left- and 400 rightward moving), observer performance was determined on the basis about up to 10 randomly selected elements, while it was between 1 - 2 elements when the total number of dots was 12. Since Raidvee et al. purposefully designed their motion display to

eliminate the noise in all unnecessary directions, it is possible that what determines observer sensitivity is some number of the total signal dots while noise dots moving in random directions are ignored. As the signal/coherence increases at higher pedestals, the number of dots which contribute to the observer's decision would then also increase, and the total effect of adaptation (small reduction in the perceived number of coherent dots) would diminish. This is of course a speculative explanation, based on the assumption that adaptation affects proportions as Burr & Ross (2008) showed it to affect absolute numerosity. The fMRI findings that proportion and absolute number are processed in the same cortical areas (Jacob & Nieder 2009) suggest that they are mediated by similar processes, but future psychophysical studies are necessary in order to examine this idea.

A relative-numerosity account of motion coherence suggests that under certain conditions, coherence judgements may rely on numerosity judgements rather than on motion integration, even when counting is avoided by using limited lifetime dots. When a relatively small number of dots is used, such as the 600 dots in the experiments discussed here, individual dots can clearly be identified, and the coherent and incoherent dots can be segregated. At very high and low coherence levels, only a few dots are moving either coherently or incoherently and it may be that at these parts of the coherence range, numerosity estimates dominate. At medium coherence levels meanwhile, number estimates (and especially subitizing) become difficult, and performance may rely on motion integration instead. Care should therefore be taken when interpreting results from studies using sparse dot stimuli, when sensitivity is estimated at a single coherence level. This issue can be avoided by using dense dot stimuli in combination with carefully adjusted dot lifetimes.

While the aim of Experiments 1 and 3 was to measure how radial motion discrimination functions are affected by adaptation, some observers did not show the expected sensitivity reduction after adaptation, particularly in the t2AFC experiment. While the MAE has been documented extensively using different stimuli (including spirals,

stripes, drifting sine gratings and random dot kinematograms), measures (duration, verbal reports, contrast sensitivity, coherence thresholds, etc.) and procedures (method of adjustment, 2AFC tasks, etc.) (Mather et al. 1998, Wade 1994), large inter-subject differences in the MAE have been observed in a visual search task (Morgan, Hauperich & Solomon 2017), as well as by others (Granit 1928, Sinha 1952). Nevertheless, Experiment 2 showed that performance on the discrimination tasks used here may be mediated by a mechanism selective for proportions, rather than for motion energy. In order to probe the later, stimuli could be composed of a greater number of much smaller dots which would not allow counting, similar to Lankheet & Verstraten (1995) who used single-pixel dots. Further evidence for this idea could be provided by experiments measuring discrimination of elements of different colours. When signal dots in an RDK have a different colour from the noise dots, motion coherence thresholds improve significantly (Croner & Albright 1997), showing that colour provides a strong segmentation cue and motion integration would not be necessary in order to extract the signal. Further psychophysical studies of proportion discrimination could also help to uncover the relation between the mechanisms processing proportions and those for absolute numerosity.

It should also be noted that any observed effect of attentional modulations on the MAE would be more convincing if a clear trend is evident over different observers. Additional experiments using stimuli which reliably elicit motion adaptation, as well as involving more observers, are necessary in order to confirm the influence of directed attention on the MAE to radial motion.

In the following Chapter, the reference frame of the radial MAE will be examined in order to estimate at what level of visual processing adaptation to radial motion occurs.

Chapter 4

Reference Frame of the Motion Aftereffect

4.1 Motivation

The neural responses in most early visual areas are encoded in a retinotopic reference frame, meaning that cells respond to stimuli in particular locations on the retina. Despite this, we perceive the world as stable and can integrate visual information with input from other senses which are not retinotopically organised. The frame of reference of a cortical area therefore gives an indication to its function. In order to estimate at what level of visual processing adaptation to radial motion occurs, we can investigate whether this MAE is retinotopic, or whether it also has spatiotopic properties. In the present study, this question is evaluated using relative velocity adjustments of contracting and expanding motion components to null the MAE at different retinal locations. The results suggest that adaptation to radial motion is mainly retinotopic.

4.2 Introduction

How does the visual system maintain a stable image of the world despite saccadic eye movements occurring multiple times a second, and constant head- and body-movements? One favoured possibility is that the brain creates a spatiotopic representation of the external world, in which spatial location is encoded independently from where the eyes are looking. A construction of such maps requires integration of retinotopic information with position signals from the eyes and body in the form of corollary discharge. While electrophysiological studies have not found spatiotopic maps of external space (Wurtz 2008), activity within retinotopic receptive fields of posterior parietal neurons has been shown to be modified by gaze-direction (Andersen et al. 1985), and some neurons in the ventral intraparietal area (VIP) represent information in a head-centred reference frame (Duhamel et al. 1997). Meanwhile, functional imaging and psychophysical studies have shown mixed results.

A retinotopic aftereffect is fixed to its retinal location and moves with the eye, while a spatiotopic aftereffect remains in the same location in space even when eye movements or changes in gaze direction have occurred between the adaptation and test times. Several psychophysical studies have shown MAEs in un-adapted retinal locations, such as Snowden and Milne's 'phantom aftereffect' of rotational motion (1997), and von Grünau and Dubé's 'remote aftereffect' observed with flickering gratings (2002). Whether there is also a spatiotopic component to the MAE is less clear. Some evidence for encoding in spatiotopic coordinates was observed using translating dots (Ezzati, Golzar & Afraz 2008). Mapping the topography of the MAE, Ezzati et al. observed that following a saccade, the map splits into a retinotopic region and a spatiotopic region. Furthermore, Nishida, Motoyoshi, Andersen & Shimojo (2003) found that the MAE is affected by changes in gaze direction, and is stronger in adapted gaze directions. Knapen et al. (2009) meanwhile, using translating random dot stimuli to null the MAE, suggested that the reference frame of the MAE is purely retinotopic and that any

spatiotopic effects could be explained by spreading of motion adaptation across the visual field.

Previous studies have shown that adaptation causes a decrease in the perceived speed of a test stimulus moving in the adapted direction (Smith & Hammond 1985, Thompson 1981). Adaptation to one direction of motion would thus bias a transparent stimulus with half of the dots moving in the adapted direction and half in the unadapted direction to appear to move more slowly in the adapted direction. It is possible then, to perceptually null the MAE by making adjustments in the relative velocities of the two components. This experiment uses a novel test stimulus first suggested by Raphael et al. (2010) to examine whether the MAE is encoded in retinotopic or spatiotopic coordinates using a method of relative velocity adjustment of the contracting and expanding components of a transparently moving dot stimulus. Following adaptation to radial motion (either contracting or expanding), the strength of the resulting MAE was determined by finding the point of subjective equality between contracting and expanding dot fields. The results indicate that the MAE is mainly retinotopic, and that a modest level of adaptation at spatiotopic locations may be attributable to spreading of adaptation.

4.3 Methods

4.3.1 Equipment and stimuli

Stimuli were presented on a Sony Trinitron monitor with a refresh rate of 60 Hz and mean luminance of 22 cd/m^2. Subjects were positioned at a viewing distance of 70 cm from the screen using a chin rest. At this distance, the stimuli subtended 8 degrees in diameter. All observers used the same experimental set-up. For a follow-up experiment (Section 4.4.2), an EyeLink 1000 desktop eye tracker was additionally used to record eye movements and ensure that observers were following the stimulus with their gaze (see General Methods, Section 2.7 for details).

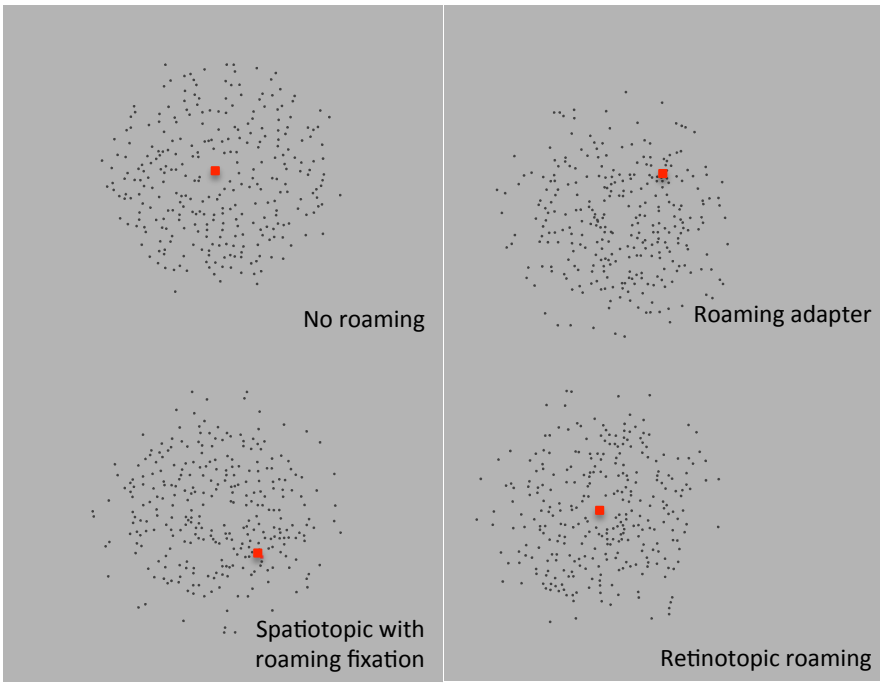

Figure 4.1: Stimulus representation - reference frame of the MAE No roaming, both adapter and test centred on the screen with central fixation; Spatiotopic roaming, adapter and test centred on the screen, fixation roamed during adaptation period; Roaming adapter, adaptation stimulus roamed the screen, while fixation and test stimulus were presented in the centre; Retinotopic roaming, both the fixation point and the adapter roamed the screen during adaptation, and the test stimulus was presented in the centre.

Adaptation stimuli were fields of 300 black dots presented within a circular window 8 degrees in diameter, all of which were moving coherently and at a constant speed of 3.8 deg/s in the adapting direction (contraction or expansion). The test stimuli were also comprised of 300 black dots, half of which (150 dots) were always expanding and the other half contracting. During adaptation, subjects were asked to keep their gaze on a large fixation point which changed colour at a rate of 2.5 Hz, and to press a button to identify when it displayed a specified colour.

4.3.2 Procedures

The initial adaptation period at the start of each session lasted 20 seconds, and an additional top-up adaptation period of 5 seconds was presented before every test stimulus, which lasted for 350 msec. There were four main adaptation conditions (see Figure 4.1), and one supplementary control condition (Blank roaming):

- No roaming: Both adapter and test stimuli were centred on the screen. The adapter did not shift in position and no eye movements were required.

- Spatiotopic with roaming fixation: Both the adapter and test were always centred on the screen. The fixation point location jumped to random positions along 4 degree circumference from the centre of the screen with a frequency of 1 Hz.

- Roaming adapter: The centre of motion jumped to random positions along 4 degree circumference from the centre of the screen at a rate of 1 Hz. The fixation point and test stimulus stayed centred on the screen, and thus no eye movements were required. This condition is neither retinotopic nor spatiotopic.

- Retinotopic roaming: Both the centre of motion and the fixation point jumped to random positions along the 4 degree circumference of the centre of the screen at a frequency of 1 Hz.

- Blank roaming: As in the No roaming condition, both adapter and the test were centred on the screen. Here however, the adapter was interrupted by a blank (mean background) period for 100 ms at a rate of 1 Hz, in order to mimic loss of motion information due to saccadic suppression in conditions in which eye movements were required.

Data were collected using the method of single stimuli (MSS), in which only one test stimulus is shown per trial and the observer makes a decision between two response alternatives based on the information contained in this stimulus. The test stimulus was always presented at the centre of the screen. The observer's task was to indicate, with a button press, if the test appeared to contain more expanding or more contracting motion. No feedback was given. The velocity of one motion component (contraction or expansion) was held constant, while the velocity of the second component was varied using an adaptive procedure (APE, see General Methods, Section 2.5.3 for details) in order to estimate the point of subjective equality.

4.3.3 Observers

Six observers (CC, NN, MM, SA, SR and ZS), three experienced (MM, NN and SR) and three naive participated in this experiment. The observers were between the ages of 24 and 70 when the data was collected. Vision was corrected to normal when necessary and all experiments were conducted binocularly with natural pupils.

4.4 Results

4.4.1 Psychophysics

This experiment examined the reference frame of the motion aftereffect by measuring the relative velocities of components in a transparently moving dot stimulus necessary to null the apparent motion. It is helpful to note that it is the difference between the velocities for the contracting and expanding components that indicates the effect of adaptation.

Figure 4.2 shows the differences in the velocities between the two components for each observer, along with the group average. Here, positive ordinate values indicate the velocity of the expanding component, and negative values that of the contracting component. After adapting to contraction observers needed faster contracting motion in order to null the perceived expanding MAE. The difference between the velocity balance points for contraction and expansion were tested for statistical significance using two tailed t-tests. In the No Roaming condition, the balance points for contraction and expansion were significantly different for four subjects ($p < 0.0023$). In the Spatiotopic with Roaming Fixation condition, subjective balance points for contraction and expansion were significantly different for one observer and in the Retinotopic Roaming condition for two observers. Three subjects completed an additional Blank roaming condition, which was equivalent to No Roaming with the exception that the adapter was replaced with a blank screen for the last 100 ms of every second in order

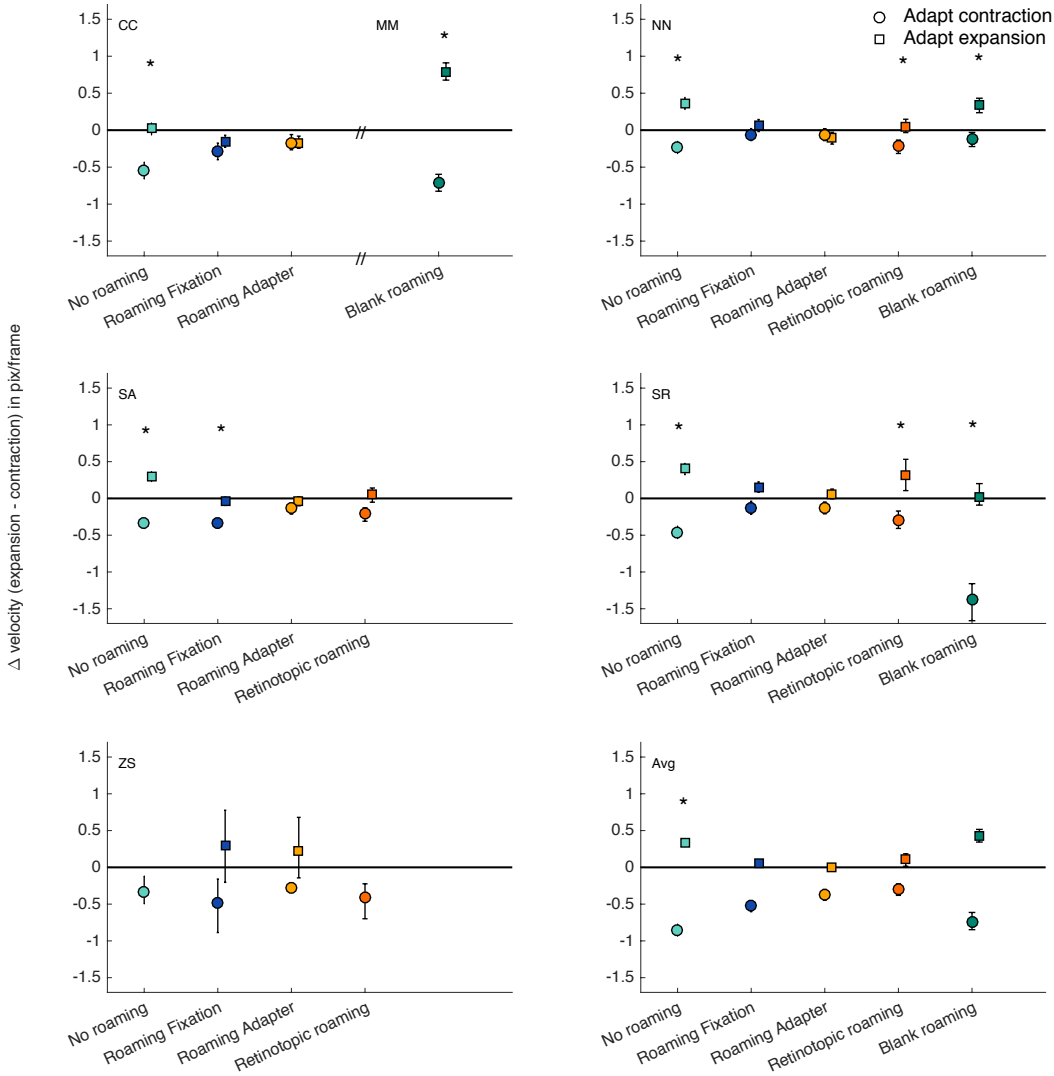

Figure 4.2: Effect of adapting condition on perceived direction of motion Data for adaptation to Expansion (circles) and Contraction (squares) are shown for the four roaming conditions, and 'blank roaming' control condition (abscissa). The ordinate indicates velocity of the contraction (positive) and expansion (negative) components. Each set of two data points represents the point of subjective equality based on 7 sessions each with two interleaved staircases. Note that the test stimulus contained both contracting and expanding motion components, and the point of perceptual equality between the two were therefore determined at the same time. Error bars represent ± standard error. Asterisks indicate significant difference from zero (one-tailed t-test, Bonferroni corrected, * $p < 0.0023$).

to mimic loss of information during saccadic eye movements. The balance points for the contracting and expanding components in this condition were significant for all observers. Finally, a further control experiment comparing data with and without the fixation task confirmed that the task did not significantly affect the strength of adaptation. Averaged over observers, only the No Roaming condition resulted in a significant adaptation effect.

The method of velocity adjustment for measuring the MAE reveals a clear effect of adaptation in the No roaming condition, when the adapter and test occurred in the same location both on the retina and on the screen. Although a slight effect was observed in the Spatiotopic with Roaming Fixation condition, this was not statistically significant over all subjects. Since the effect size observed in the Spatiotopic condition was comparable in size to that in the Roaming Adapter condition, but smaller than in the No Roaming (retinotopic, no eye movements necessary) condition, a spatiotopic aftereffect is excluded. The Roaming adapter condition is neither spatiotopic nor retinotopic, and can thus reflect spreading of motion adaptation to nearby cortical locations. Four observers show retinotopic adaptation when no eye movements are required, suggesting that eye movements can interfere with adaptation. These results indicate that the reference frame for the MAE to radial motion is basically retinotopic, and that adaptation is reduced following eye movements.

4.4.2 Eye movements

Two of the conditions in this study (Spatiotopic with Roaming Fixation and Retinotopic Roaming) required the observer to make eye movements to follow a roaming fixation point. It is known that information takes around 80 ms to travel from the retina to the visual cortex (Bair 1999), and that saccade durations last several milliseconds. Because of this, saccades cannot be modified in flight by visual information. It is therefore likely that saccades overlapped temporally with the adaptor duration; this would decrease the effective adaptation time for conditions involving eye movements. In this experiment, eye movements were recorded so that saccade latency and durations, as well as fixation times and accuracy, could be determined.

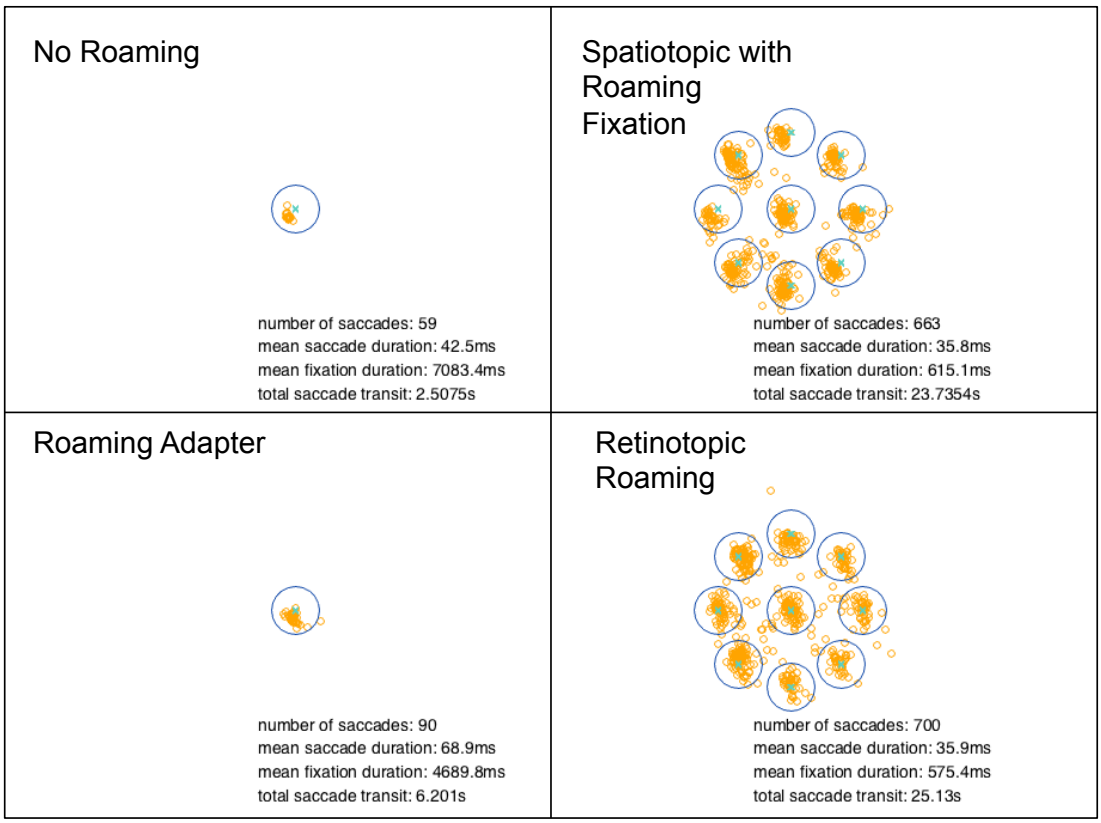

Figure 4.3: Spatiotopic roaming fixations Locations of fixations lasting longer than 40 ms (blue circles) are plotted in relation to the position of the fixation point locations (orange crosses) for the four adaptation conditions tested: No Roaming, Roaming Adapter, Spatiotopic with Roaming Fixation, and Retinotopic Roaming. The data presented are from one representative session, performed by observer 1. Also presented are the mean saccade and fixation durations for all observers.

Figure 4.3 shows the coordinates of all fixations (blue circles) lasting longer than 40 ms relative to the locations of the fixation point (orange crosses) for the four adaptation conditions for one representative session performed by observer 1. The large orange circles represent the 1.3 degree circumference of each fixation point location, and are presented for reference along with the number of saccades/session for each condition, the mean fixation and saccade durations, and the total saccade transit time. When recoding eye positions, eye tracking systems are known to make systematic errors (drift) in gaze locations over the course of an experiment (Hornof & Halverson 2002). Several sessions show such drift, as can be seen in the lower panels of Figure 4.3. While drifts can be removed manually by identifying and correcting for patterns emerging from

superposition of fixations and visual stimuli, the drifts observed here were relatively small, and drift correction was not performed.

The majority of fixations landed within the 1.3 degree circumference from target fixation points, indicating that subjects could indeed follow the fixation point as it roamed the screen. Saccades were fewer and fixation durations longer in the conditions that did not explicitly require the observer to make eye movements than in the roaming conditions. Where no eye movements were required during adaptation, fixations routinely exceeded several seconds. While in conditions requiring eye movements the mean fixation durations are considerably less than 1 second (the maximum expected due to the 1 Hz roaming rate of the fixation point), observers often made several short adjustment fixations in these conditions, as can be seen in Figure 4.3. Because of this, the total adaptation time at each location of the fixation point did approach a full second. In conditions requiring eye movements, the saccade transit times averaged at less than 30 sec per session, while each session contained a total of 180 sec of adaptation time. Even in the extreme assumption that all saccades occurred only during adaptation periods, only 17% of adaptation time should be lost. Along with the results presented above for the Blank Roaming condition, these data suggest that the net adaptation time was not considerably reduced in the conditions requiring eye movements, and that this cannot account for the lack of adaptation observed in the psychophysical data.

4.5 Discussion

Using a method of relative velocity adjustments of transparently moving dot fields, the reference frame for the motion aftereffect for radial motion was examined. Adaptation was found to be represented mainly in retinotopic coordinates. While a small spatiotopic effect was observed, it could be accounted for by spreading of motion adaptation, as suggested by Knapen et al. (2009). The results of a Blank Roaming control condition in which the stationary adapter was interrupted by a 100 ms blank at the end of every

second suggest that saccadic suppression during adaptation in conditions requiring eye movements did not significantly affect the effective adaptation time. However, saccadic suppression begins at early stages of visual analysis (Burr, Morgan & Morrone 1999) and Berman, Cavanaugh, Mcalonan & Wurtz (2017) recently showed that saccadic suppression can begin 100 ms before the saccade is initiated. The suppression of motion information may therefore extend over longer durations than anticipated. Eye movements were analysed during the experiment in order to examine whether the net adaptation time in the conditions requiring eye movements was reduced compared to the conditions in which no eye movements were necessary. The total fixation durations at each location where a fixation point was presented approach one second, indicating that the effective adaptation time was not significantly reduced. The data support previous psychophysical results from Knapen et al., and functional imaging investigations of Gardner, Merriam, Movshon & Heeger (2008).

The large, radially moving stimuli and dynamic test used in this study were chosen because they involve higher level motion processes than translating motion, which are more likely to have spatiotopic properties. Despite this, we do not find evidence of a spatiotopic aftereffect for radial motion. The measure used here is the relative difference in velocities of transparently moving contracting and expanding dot fields. The results support those of Knapen et al. (2009) who measured a shift in the mean velocity distribution and reported that a velocity of 1 degree/sec was necessary to null the MAE. The magnitude of the effects is comparable, as the 1 pixels/frame observed here (the difference between the velocities of the two components) translate to about 0.7 degree/sec. Ezzati et al. (2008) reported a spatiotopic MAE following a saccade, however the effect is approximate to that observed in non-retinotopic *non-spatiotopic* conditions in this study and in Knapen et al. While Ezzati et al. did not measure the spread of the MAE to a non-retinotopic and non-spatiotopic location, their results are comparable to those of Knapen et al. and this study for the spatiotopic condition. It is

thus likely that their procedure would produce a similar effect size for a non-retinotopic, non-spatiotopic location, as detailed by Knapen et al., indicating that the 'spatiotopic' effect is due to the same mechanism (e.g. spatial spreading of adaptation across the visual field).

The data from this study suggest an effect of gaze modulation, as the magnitude of the MAE is reduced when the adaptor and test were presented in different gaze directions even when they stimulated the same retinal location. This was previously observed by Nishida et al. (2003), but was not shown by Knapen et al.. The later study suggests that the difference might be due to the size of saccade between adapter and test and to the type of stimulus used. Interestingly, both of these factors in this study are closer to those used by Knapen et al. (gaze modulation of 4 - 8 degrees, global motion and dynamic test stimuli), and yet here an effect of gaze modulation is observed. Only one saccade was necessary on each trial in this experiment, while in both of the other studies two saccades were required. The only relevant procedural differences between the present study and that of Knapen et al. are our use of radial motion (translating motion in Knapen et al.), and that unlike theirs, the stimuli used here did not have Gaussian edges. One possible explanation is that motion-defined boundaries were present around the circumference of the radial stimuli in this study, resulting in a more retinotopic effect, as suggested by Ezzati et al..

By measuring BOLD activation in fMRI, D'Avossa et al. (2007) demonstrated that MT responses are modulated by gaze direction, suggesting that it represents stimuli based on screen coordinates whereas in earlier visual areas they are rendered in retinotopic coordinates. In contrast, Gardner et al. (2008) reported that area MT, along with eleven other occipital visual areas, responds in a retinotopic reference frame. While D'Avossa et al. used functional localisers to define visual areas, Gardner et al. additionally used visuotopic (a.k.a. retinotopic) mapping, and considered robustness of the visual responses. It is not clear however, if these methodological differences entirely

account for the opposing results. Subsequent studies have continued to debate the reference frame in which information is processed in area MT. Golomb & Kanwisher (2012) reported retinotopic representation of object location while Crespi et al. argued for spatiotopic coding (2011). A possible reconciliation was proposed by Turi & Burr (2012), who showed that the *positional* motion aftereffect (the change in perceived position following adaptation to motion) is spatiotopic, while the classical motion aftereffect (illusory motion after prolonged viewing of a moving stimulus) is represented in retinotopic coordinates. The psychophysical results of the present study indicate that the MAE for radial motion is processed in a retinotopic frame of reference, and therefore support the claims of Gardner et al. (2008), Golomb & Kanwisher (2012) and Turi & Burr (2012).

Another issue is that of whether a spatiotopic reference frame is even necessary for an eye-movement invariant representation of the visual field. Nishimoto et al. (2017) recorded fMRI responses to natural films during stable fixation and free viewing in order to map eye-movement invariant cortical areas, and found MT along with other ventral temporal visual areas to be largely unaffected by eye movements. They suggested that a local receptive-field organisation and a spatiotopic (or world-centred) reference frame are not strictly necessary for an eye-movement invariant representation, and that the previous studies had defined the problem too narrowly.

This experiment extends on that of Knapen et al. (2009) by examining the reference frame of the MAE to radial motion. Complex motions such as contraction and expansion are expected to be mediated by higher cortical sites than translation, and are thus more likely to be represented in a non-retinotopic reference frame. The results of this study show that the radial MAE is mainly retinotopic and is diminished by gaze modulations.

It is important to note the difference between retinotopic mapping using functional imaging (Gardner et al. 2008) (the eye position is fixed in order to measure the relationship of cortical representation to retinal position, neighbourhood relationships

are preserved in visiotopically organised areas) and retinotopic representation (the cortical representation is encoded in retina-based coordinates). In the following chapter, retinotopic mapping is performed in order to delineate the borders of early visual areas, and these are not to be confused with areas representing information in a retina-centred reference frame.

Chapter 5

BOLD Signal Responses to Contraction and Expansion in Human MT Complex

5.1 Motivation

This chapter describes a study investigating the neural basis of the perception of radial motion using functional magnetic resonance imaging (fMRI). While the macaque MST contains neurons selective for different types of optic flow, there are few demonstrations of similar selectivity in human cortical areas. In this Chapter, experiments using moving random dot stimuli to examine cortical selectivity to radial motion give evidence suggesting the existence of distinct neural populations within area MST which are selective for contraction and expansion, supporting results from neurophysiology.

5.2 Introduction

In order to coordinate movement and to guide behaviour as we move through the environment, the visual system relies on patterns of image motion formed on the retina

- so-called optic flow patterns (radial motion, rotation and spiral motion). The ability to detect and process optic flow is crucial for the guidance of self-motion and object avoidance. Analysis of global radial motion provides visual cues that can be used to subtract and parse flow motion, information that is necessary for object tracking during self movement (Warren et al. 2009).

The areas of the cerebral cortex which mediate these percepts are well-understood in monkeys, but remain unclear in humans. The monkey area MT (also called V5) is known to respond selectively to motion (Albright 1984, Allman & Kaas 1971, Desimone & Ungerleider 1986, Dubner & Zeki 1971, Saito et al. 1986, Zeki 1974), as well as the neighbouring middle superior-temporal gyrus (MST), which has larger receptive fields and additionally responds to ipsilateral activation (Duffy & Wurtz 1991*a*,*b*, Orban et al. 1992). The dorsal portion of MST (MSTd) contains neurons which are selectively activated by complex motions such as expansion and rotation (Duffy & Wurtz 1991*a*, Tanaka & Saito 1989).

It is crucial to understand to what degree neurophysiological (often single-cell recording) experiments on monkeys relate to fMRI findings in humans. Rees, Friston & Koch (2000) investigated this relationship by measuring the human BOLD response to moving dot fields of varying coherence and found that the responses in V5 were linearly dependent on motion coherence, and that a simple mathematical expression relates them to data from single-unit recordings in monkeys. They suggested that the BOLD response is directly proportional to the neuronal firing rate (see also Heeger et al. (1999)). Meanwhile, Braddick et al. (2001) have shown that coherent motion produces greater activation in areas V5 and V3A, compared to dynamic visual noise. Psychophysical studies show that the human visual system is sensitive to patterns of global motion (Bex, Metha & Makous 1998, Freeman & Harris 1992, Snowden & Milne 1997, Warren & Hannon 1988), and functional imaging has identified area MT+/hV5 as the homologue of MT/V5 in monkeys, based on its location, anatomical structure (Dumoulin et al. 2000,

Tootell & Taylor 1995) and its selective responses to different kinds of moving stimuli (Braddick et al. 2001, Chawla et al. 1998, Culham et al. 2001, Smith et al. 1998, Tootell, Reppas, Kwong, Malach, Born, Brady, Rosen & Belliveau 1995, Watson et al. 1993). As in other primates, MT+ in humans is likely to be composed of several interconnecting motion-selective regions. It has tentatively been proposed that these subregions perform similar functions as areas MT and MST in monkeys (Amano et al. 2009). This idea was first explored by Dukelow et al. (2001), who used ipsilateral stimulation to identify an area in the anterior portion of MT+ as the homologue of monkey MST. This region appears to be more specialised for the processing of optic flow patterns than MT (Smith et al. 2006). Huk et al. (2002) thereafter showed that MT, which does not respond to ipsilateral stimulation, exhibits retinotopic organisation, while MST does not. Wall et al. (2008) used fMRI adaptation to observe selective responses to different kinds of optic flow motion (i.e. expansion and rotation) in MST, and to a lesser degree in MT. A recent study used transcranial magnetic stimulation (TMS) to disrupt cortical activity in MST, and reported an associated disruption in radial direction discrimination (Strong et al. 2017). Taken together, these data suggest that MST is involved in the processing of large, complex movement and raise the possibility that the human MT+ complex, and especially area MST, contains distinct neural populations selective for different kinds of optic flow motion.

Neurophysiological studies suggest that contraction and expansion are processed asymmetrically; there are cells in macaque MST that respond selectively to *either* contraction or expansion (Saito et al. 1986, Tanaka & Saito 1989). Shirai, Birtles, Wattam-Bell, Yamaguchi, Kanazawa, Atkinson & Braddick (2009) examined the first harmonic (F1) in steady-state visually evoked potentials (VEP) in response to contracting and expanding dot stimuli, and found asymmetrical F1 amplitudes for contraction and expansion. It is possible then, that distinct neural populations mediate the processing of contracting and expanding motion in humans. The present study sets out to probe whether fMRI can reveal selective responses to the two directions of radial motion.

5.3 Methods

5.3.1 Equipment and stimuli

Distinct stimuli were used for retinotopic mapping, for localisation of regions of interest, and for the measurement of responses to radial motion. The radial motion stimuli which consisted of random-dot kinematograms were matched between the psychophysical studies described in Chapter 3 and these functional imaging experiments.

Retinotopic mapping

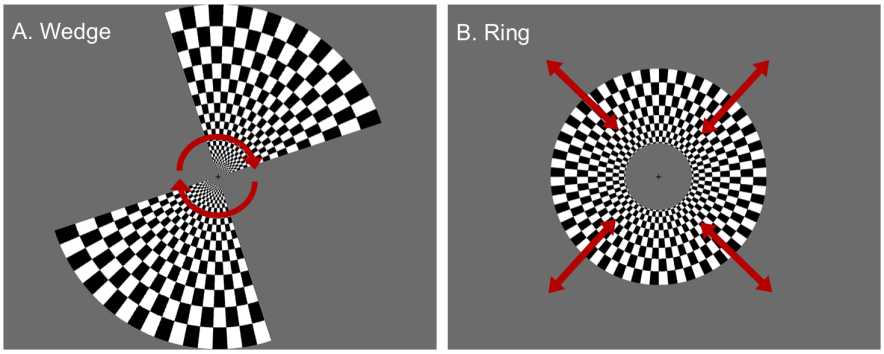

Figure 5.1: Retinotopic mapping stimuli The stimuli presented for retinotopic mapping. A. Polar wedge B. Eccentricity ring

The stimuli used for retinotopic mapping were rotating double-wedge shaped checker-boards and expanding/contracting concentric rings which were presented on a uniform grey background (see Figure 5.1). The checker-board itself flickered at a rate of 8 Hz, meaning that the white checks became black and vice-versa. The polar wedges were of 90° arc extending from fixation to 4 degrees of visual angle, contained 21 checks along the radius and 18 checks along the arc, and rotated about fixation at a speed of 6 deg/s, taking 60 seconds to complete one cycle. The thickness of the eccentricity ring stimuli was scaled by the cortical magnification factor, so that thickness increased as rings expanded towards the periphery. The maximum radius reached by the eccentricity ring stimulus was 4 degrees. They moved at 6 deg/s, and needed 23 seconds to complete one cycle. Each session consisted of 4 cycles for the wedge stimuli, and 8 cycles for the ring stimuli and lasted 4 min and 8 min respectively.

MT-MST localiser

The contracting and expanding stimuli used for the MT localiser consisted of 600 white dots (see below for details) positioned randomly in a circular field centred on the fixation cross. To locate MST, the focus of radial motion was shifted by 10 degrees to either side of fixation, in order to allow for mapping of cortical regions responding to ipsilateral stimulation. The dots moved at a constant velocity of 5.6 deg/s, either all towards the outer rim or all towards the centre, and the direction of motion switched at a rate of 1 Hz. Reaching the borders of the circular aperture, a dot would disappear, reappear at a random location and proceed on its destined course.

Selectivity for radial motion

To measure responses to contraction and expansion, stimuli were very similar to those for the MT-MST localiser. Purely contracting or expanding stimuli were composed of 600 black dots positioned within a circular aperture and moving at a constant velocity of 5.6 deg/s. The transparent motion stimuli were composed of two fields of 300 dots each, one moving towards the outer rim of the circle and the other moving towards the fixation point. The dots in one field were black and in the other white, and the direction of motion of the two components was balanced across sessions. An on-off block design was used, with each motion block lasting 18 seconds and alternating with 18 second periods containing stationary dots. This allowed for the haemodynamic response underlying one stimulus to be compared to baseline signals, and to those from other stimuli.

All dots were black or white and had a diameter of about 0.1 degrees at a viewing distance of 202 cm. They were shown on a grey background field of 22 cd/m^2 within a circular field with a diameter of 8.5 degrees for the MST localiser stimuli, and 11.2 degrees for all other stimuli. The whole screen subtended 11.5 by 15.2 degrees of visual angle (see Figure 5.2).

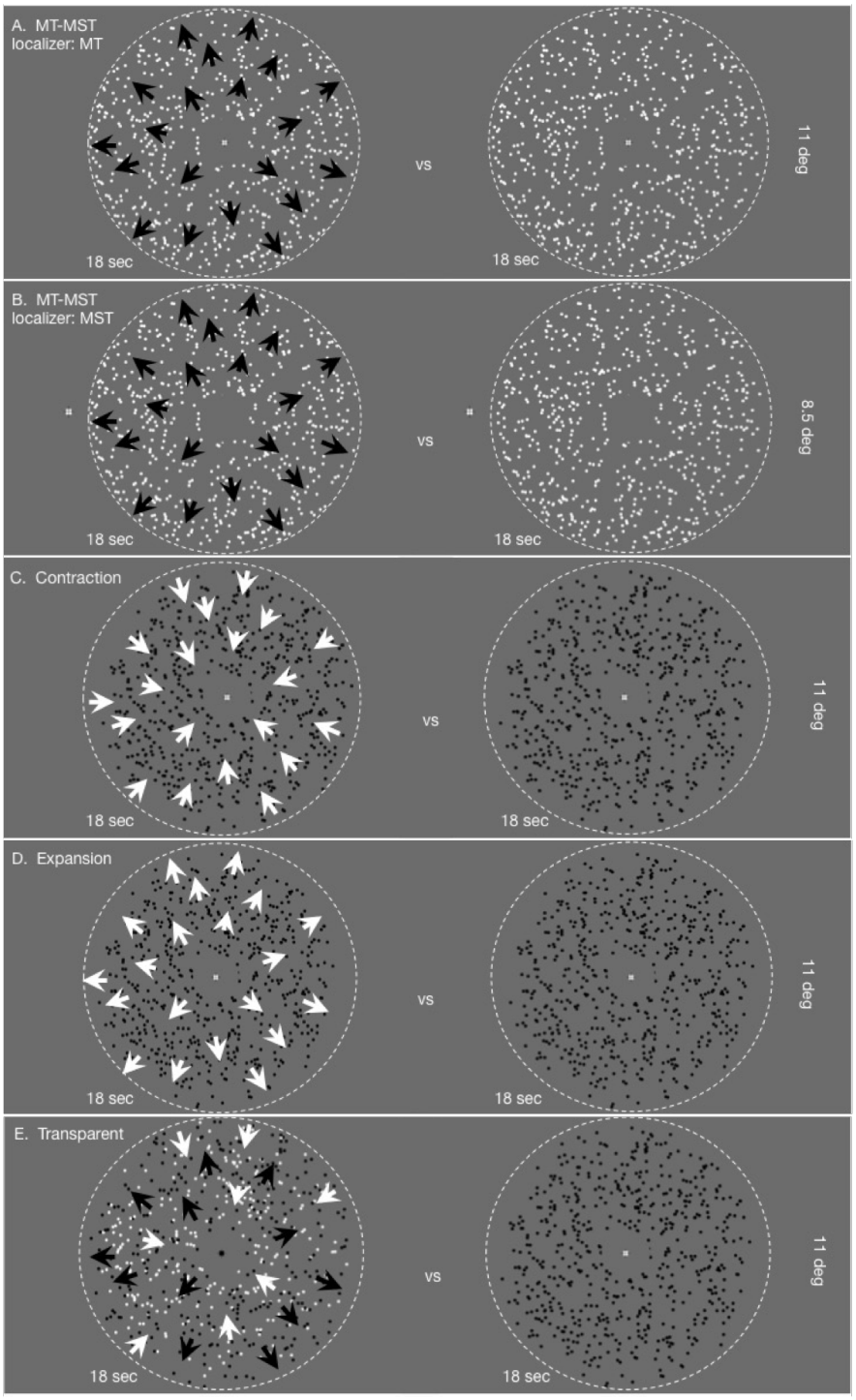

Figure 5.2: Moving dot stimuli A, Moving versus stationary dots, to identify MT+. B, Ipsilateral stimulation, used to locate MST. C, Contraction versus stationary. D, Expansion versus stationary. E, Transparent motion, used to identify cells responsive to both contraction and expansion.

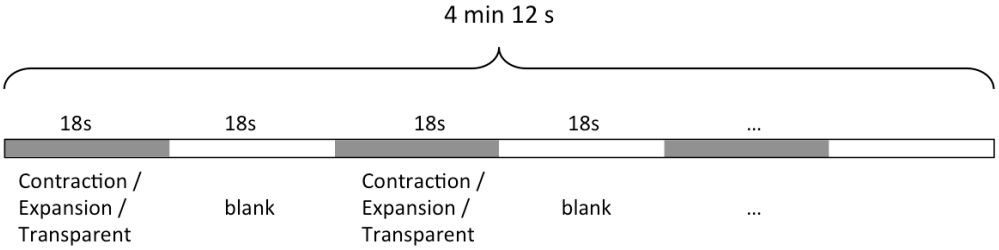

Figure 5.3: Blocked design Contraction, expansion and transparent motion stimuli were presented for 18 seconds, followed by an 18 second stationary period, in an on-off block design. Throughout the viewing of motion stimuli, subjects were asked to perform an attentional task - a brief 'jerk' (velocity increase) of the motion components. On average, these attentional effects occurred once every 100 seconds or 10 -11 times per block.

In order to control for attention, participants had to perform a task during the experiment; the dot field components sometimes 'jerked' (advanced at an increased speed) for 200 ms, and subjects had to respond to these jerk events by pressing a button with the right hand. The probability of an event occurring at each second was 0.01, meaning that on average, there was one jerk event every 100 seconds. On transparent motion sessions, the jerk events were applied to the expanding and contracting components in a pseudo-random manner.

The fMRI data acquisition parameters and analysis procedures are described in more detail in the General Methods, Section 2.8.

5.3.2 Observers

Five right-handed observers (AG, LR, MM, NN and TP, aged 27 to 74) participated in the study. All participants were experienced with psychophysical experiments and maintaining fixation. Vision was corrected when necessary and all experiments were conducted binocularly with natural pupils. Optical correction was either in the form of contact lenses or prescription goggles designed to be worn in the scanner. Written consent was obtained and the experiments were conducted in accordance with the Declaration of Helsinki, and were approved by ethics committee of the Faculty of Medicine at the University of Cologne (Study-nb: 10-236). Standard screening procedures for MRI were

followed and the participants who were not employed at the Max Planck Institute were paid for their participation. Before scanning, the participants were instructed on the experimental procedure and performed enough test runs to ensure they understood the instructions correctly and felt comfortable with the task.

5.4 Results

5.4.1 Retinotopic mapping

Light entering the eye is refracted through the cornea so that an inverted image is projected onto the retina. The topographical representation of this information is preserved as it is relayed through the layers of the lateral geniculate nucleus (LGN) of the Thalamus, the primary visual cortex, and subsequent cortical areas. We can map the representation of the retina in the early visual cortex by using a Phase Encoding technique developed by Sereno et al. (1995). This classic method has been used widely since its introduction, not only for delineating retinotopic areas, but also for mapping other stimulus attributes, such as V1 orientation columns. The approach is based on the following assumption: when a stimulus changes cyclically along a dimension, we can expect that the signal (e.g. the BOLD response) of the neuronal population selective for the stimulus dimension will be modulated cyclically as well (see Figure 2.2 in the General Methods, Chapter 2). This is well illustrated in the example of polar angle retinotopic mapping. Consider a checkerboard wedge stimulus that rotates around a fixation point in the centre for a set number of cycles. Knowing that the early visual areas are retinotopically organised, we can assume that the response of cells (and therefore voxels) whose receptive fields are in a particular location in space will respond when the stimulus passes through that location, and the response will fade away as the stimulus moves out of the receptive field. The time-series of such a voxel ends up following a sinusoid pattern, so we can find the preferred retinal location of the voxel by calculating the correlation coefficient between any possible sine wave and the observed BOLD response.

An alternative analysis method, and the one used here, is to calculate the fast Fourier transform of the observed signal in order to determine where in the visual field the response is the highest. The entire frequency spectrum is analysed, not only the fundamental frequency of the stimulus cycle. The output of the transform is a vector of complex numbers for the entire spectrum, where the real and imaginary components are equivalent to the correlation coefficients in the general linear model and can be used to determine the preferred phase angles.

In order to account for the lag in the haemodynamic response function, we can run two experiments in opposing directions along the stimulus dimension (e.g. one wedge rotating clockwise, and the other anti-clockwise). The components of the two experiments are then averaged, and the result is used for calculating the phase maps. The haemodynamic lag of the two directions cancels out, and gives a more accurate estimate of the true phase.

The borders between the early visual areas coincide with the horizontal and vertical meridians of the visual field. Neighbouring locations in the visual field are represented in mirror-revered maps in neighbouring cortical areas, so the meridians can usually be seen as mirror-reversals in the *polar angle map*. Standard retinotopic mapping methods were applied in this study, using these mirror-reversals to define the boundaries between visual areas on flattened representations of the cortical surface (Deyoe et al. 1996, Engel et al. 1997, Larsson & Heeger 2006).

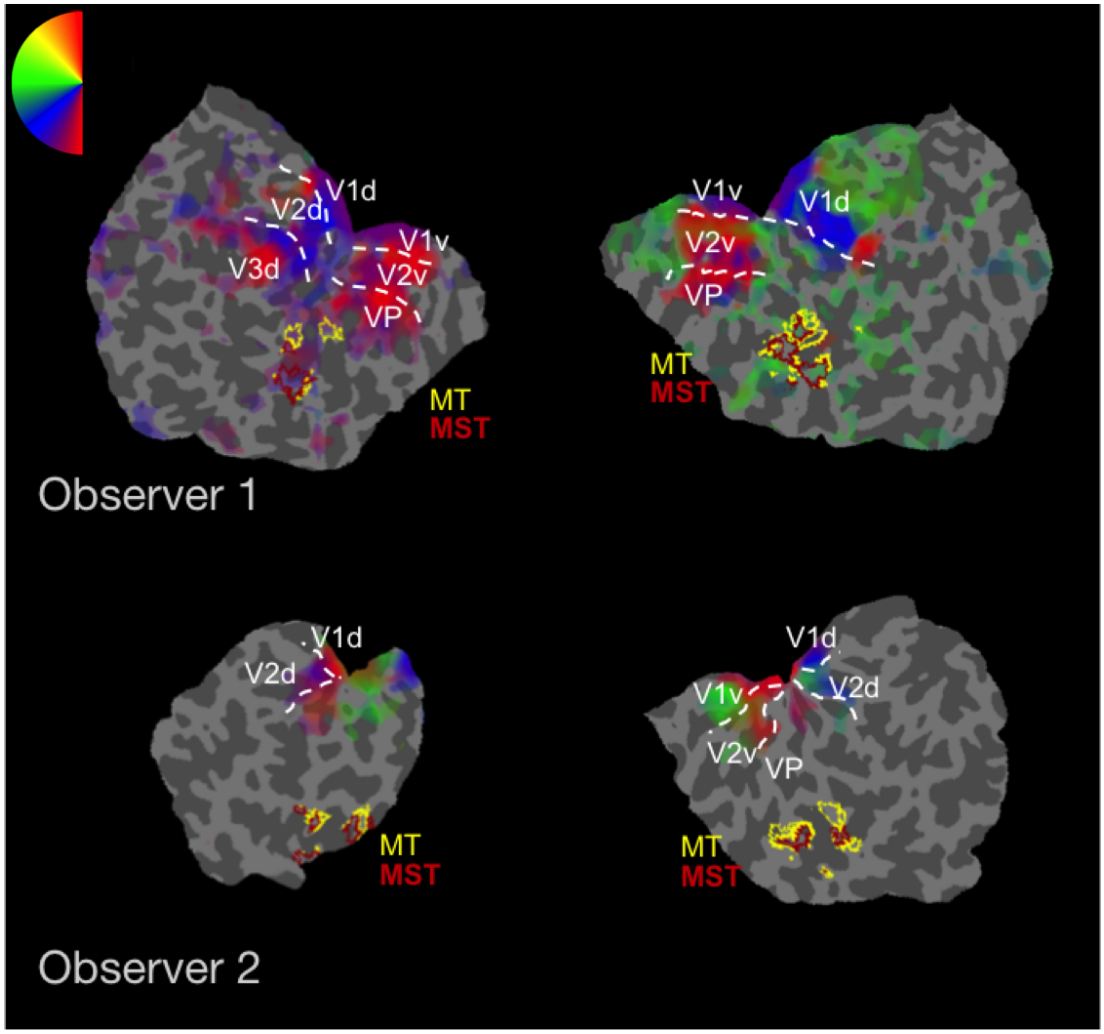

Figure 5.4: Polar angle retinotopic maps A Cortical representations of the polar angle (wedge) stimulus for all five observers, displayed on computationally unfolded and flattened patches of the occipital lobe. The two columns show the left and right occipital lobes. Colour indicates polar angle (red - vertical meridian, green - horizontal meridian), and approximate visual area boundaries are delineated by the white lines. The locations of ROIs for MT and MST are shown in yellow and red outlines.

Figures 5.4, 5.5, 5.6 and 5.7 show the BOLD responses to retinotopic mapping stimuli, the rotating wedge (polar) and expanding/contracting ring (eccentricity). Where possible, retinotopic areas V1, V2 and V3 were identified on the flattened occipital lobe. Figures 5.4 and 5.5 show the polar angle phase maps projected onto the left and right hemispheres of the five subjects who participated in the functional imaging experiments.

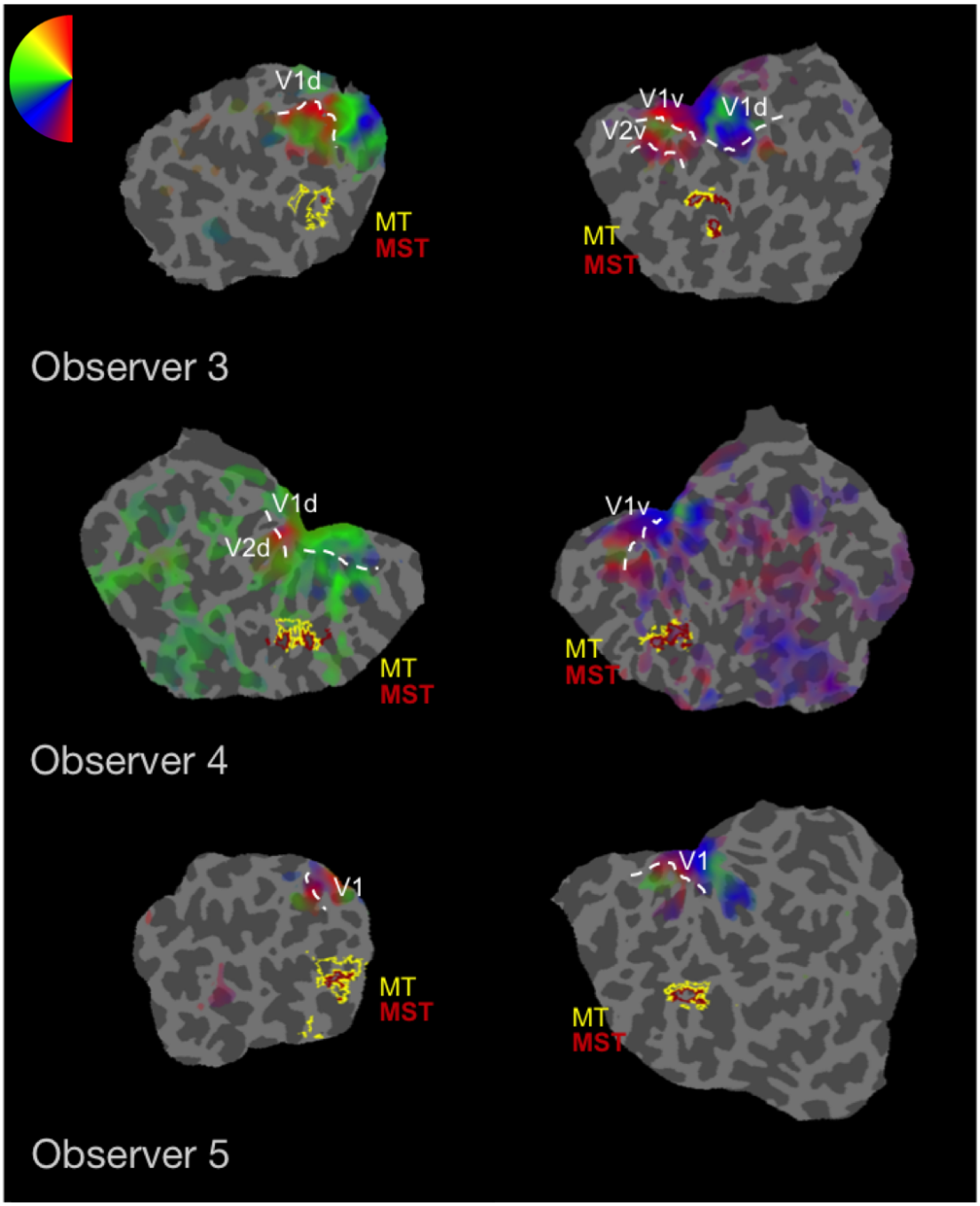

Figure 5.5: Polar angle retinotopic maps B

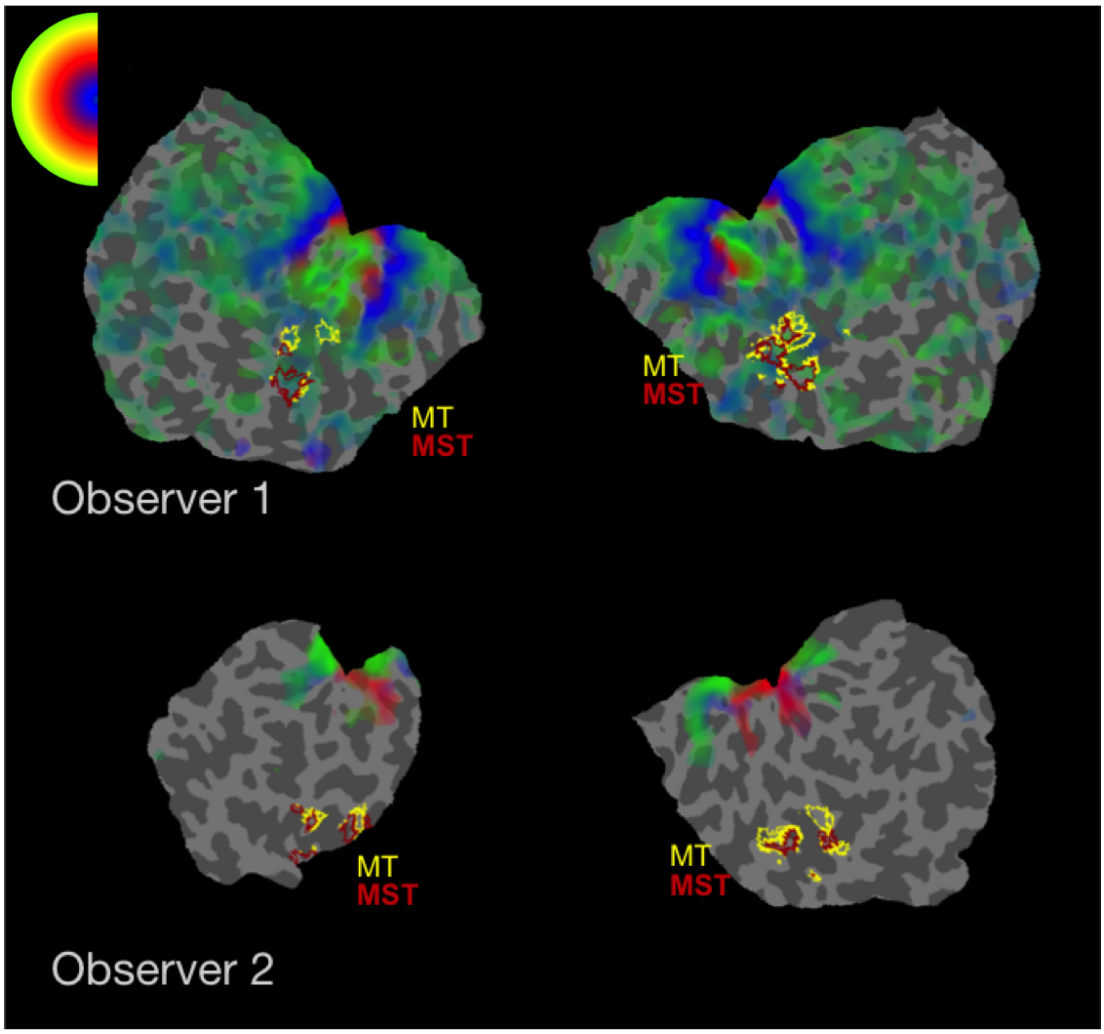

Figure 5.6: Eccentricity retinotopic maps A Cortical representations of the eccentricity (ring stimulus) for all five observers, displayed on computationally unfolded and flattened patches of the occipital lobe. The two columns show the left and right occipital lobes. Colour indicates eccentricity from 0 to 4 degrees of visual angle (blue - fovea, red - parafovea, yellow/green - periphery). The locations of ROIs for MT and MST are shown in yellow and red outlines.

The colours correspond to angular and eccentricity positions in the visual field according to the colour wheel on the top left, for responses above the correlation threshold ($r > 0.5$). The results shown are averaged over two to four runs of each stimulus (clockwise and anti-clockwise rotation), and the yellow and red outlines indicate the locations of areas MT and MST respectively, as defined by a separate functional localisation experiment (see Section 5.4.2 below).

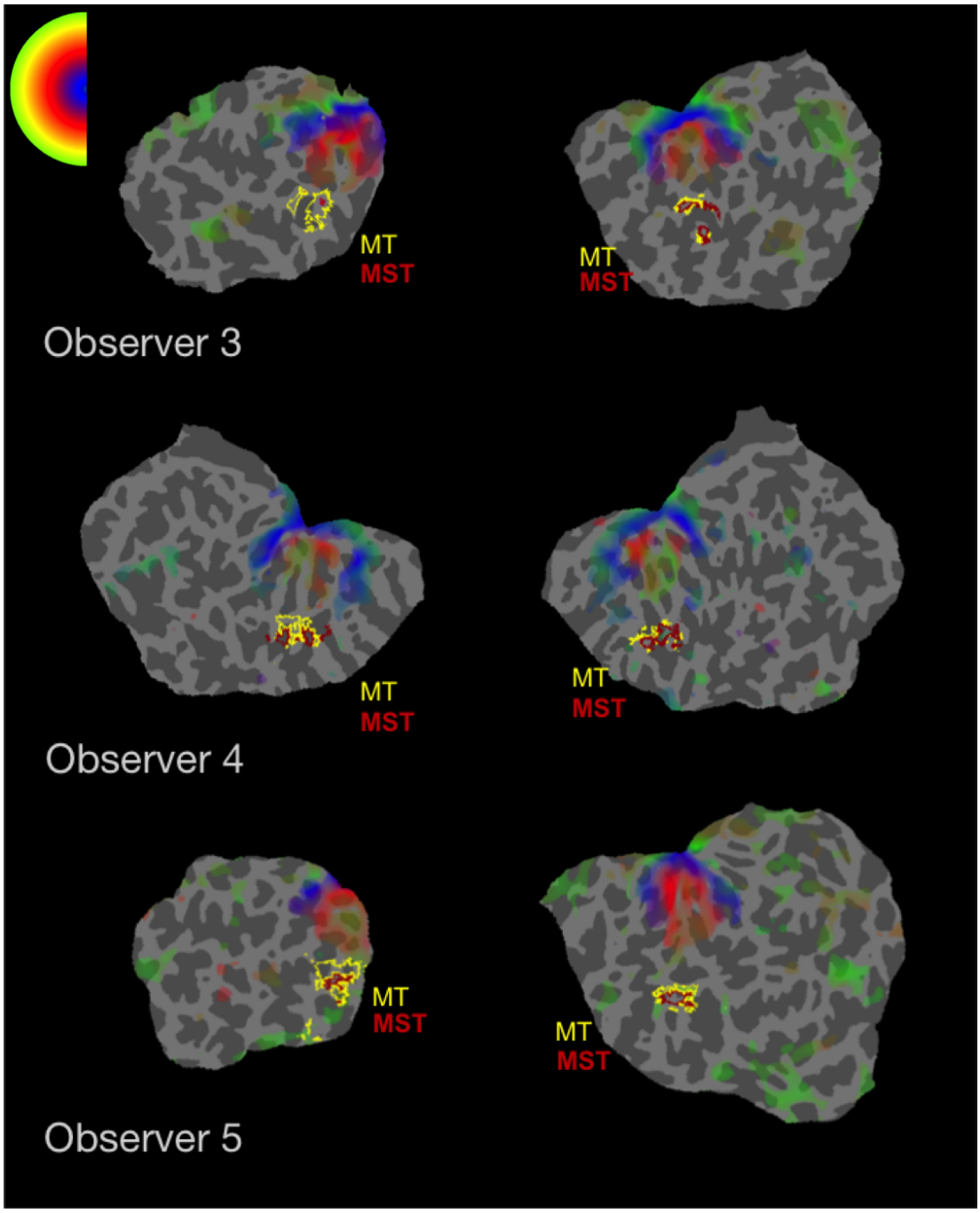

Figure 5.7: Eccentricity retinotopic maps B

As it can be seen from the colour wheel, red indicates the vertical meridian, so the red strips neighbouring blue and green areas were designated as borders between retinotopically-organised visual areas. While in four hemispheres these phase reversals were relatively clear, the distinctions were less straight forward in the remaining hemispheres. Since the colour represents retinotopic specificity, low activations can be due either to a lack of response, or to equal responses to all different retinotopic locations. While it has been shown that several representations of the visual field can be mapped onto the surface of the occipital pole (at least V1, V2 and V3), not all are always clearly identifiable. This is not unusual, as it is known that there are large individual differences in the organisation of the visual cortex (Van Essen et al. 2001), and other studies report that mapping of particular areas was possible in some but not all imaged hemispheres (for example, see D'Avossa et al. (2007) and Huk et al. (2002)).

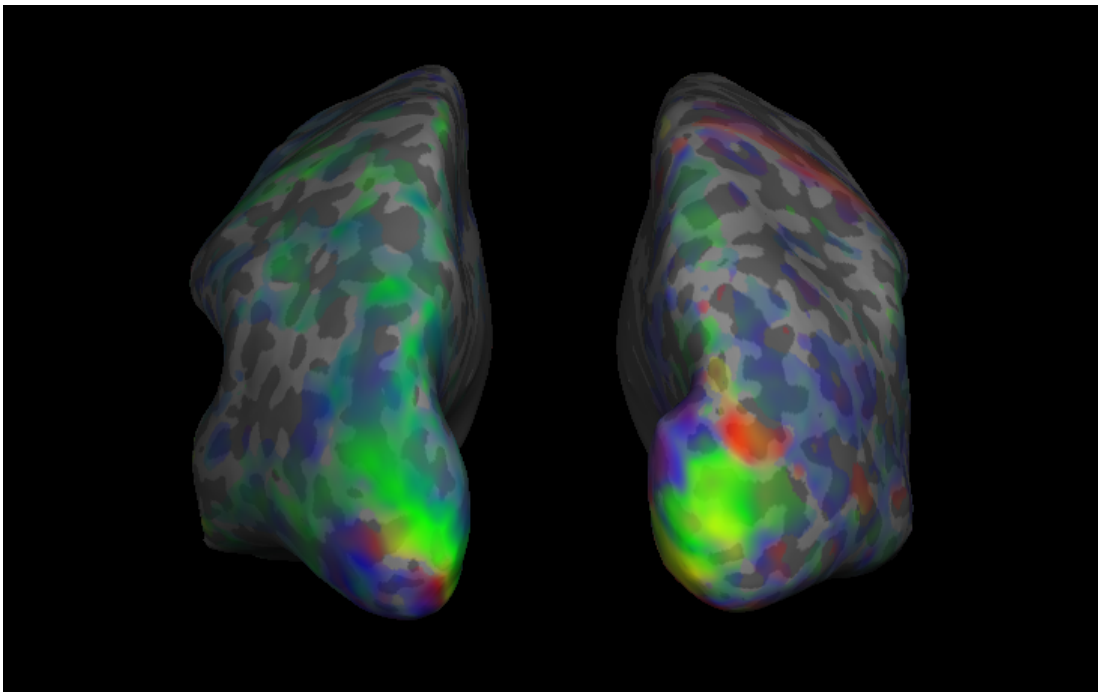

Figure 5.8: Inflated hemispheres with projected eccentricity maps Cortical representations of the eccentricity (ring stimulus) for one participant, displayed on the inflated hemispheres. Colour indicates eccentricity from 0 to 4° of visual angle.

Figures 5.6 and 5.7 show the eccentricity maps, with colours corresponding to eccentricity positions in the visual field (blue centre to green periphery), for responses above the correlation threshold ($r > 0.5$). As above, the data presented are averages over two to fours runs per stimulus, and the yellow and red outlines indicate the locations of areas MT and MST. As in previous studies (Sereno et al. 1995), the representation of eccentricity increases systematically along the medial wall of the occipital cortex, as seen on the patches here. The same response is show again, on the inflated surface of both hemispheres for one participant (observer 1) in Figure 5.8, where a progression of visual field eccentricity is clearly visible.

5.4.2 MT and MST localiser

This experiment aims to map and disassociate between retinotopic areas (i.e. V1, V2, V4 and V5/MT) responding exclusively to stimulation in the ipsilateral visual field, and non-retinotopic MST which responds to ipsi- as well as contralateral stimuli, in order to identify regions of interest for areas MT and MST. The time-courses from these ROIs will be extracted and analysed for selective responses to contraction and expansion in the next section.

The left panel of Figures 5.9 and 5.10 show the activation in response to an alternating contracting and expanding dot stimulus viewed on either the left or right side of the visual field. A large area of activation can be seen in the contralateral hemisphere, mainly in the occipital cortex and MT+. A smaller patch is observed in the ipsilateral hemisphere, corresponding to MST. In the right panel are shown the resulting ROIs for each subject, drawn based on the voxels in which the response is grater than a set threshold ($F > 3.2$). Yellow denotes MT+, and red denotes MST. Two things are important to note; first, by subtracting the MST ROI from MT+, we can identify a region which corresponds to MT, and second, that the MST ROIs are generally located in the anterior portion of the MT+ complex (except for one of the ten hemispheres analysed), as seen in previous studies (Huk et al. 2002).

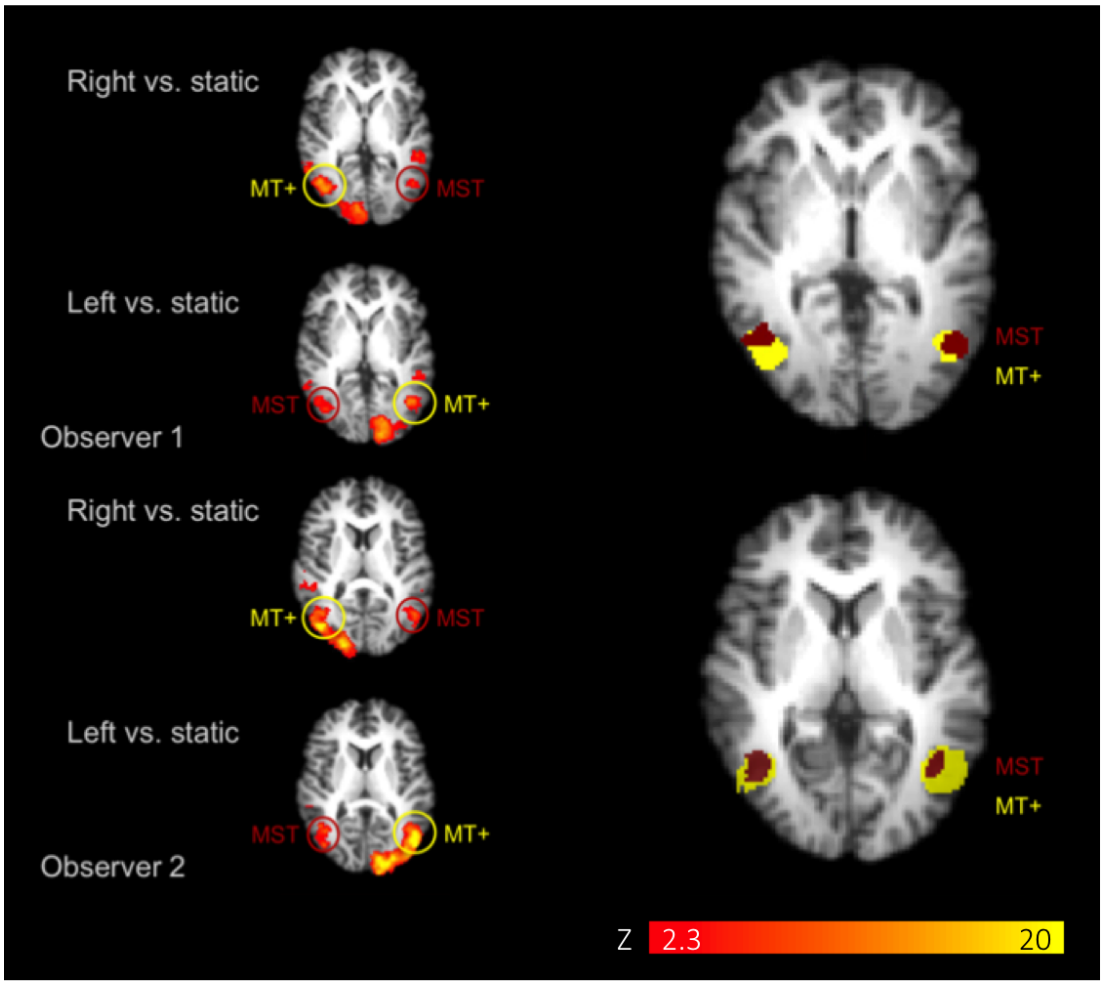

Figure 5.9: MT and MST regions of interest (ROIs) A MT+ activity and subdivision in all five observers. Left side: axial slice showing the activation clusters for the stimulus located either in the right (top) or left (bottom) visual field. Right side: the resulting ROIs (yellow MT+, red MST). MST is defined by the motion-selective voxels responding to ipsilateral stimulation, while MT+ is defined as all motion selective voxels. The left hemisphere is on the left in the images.

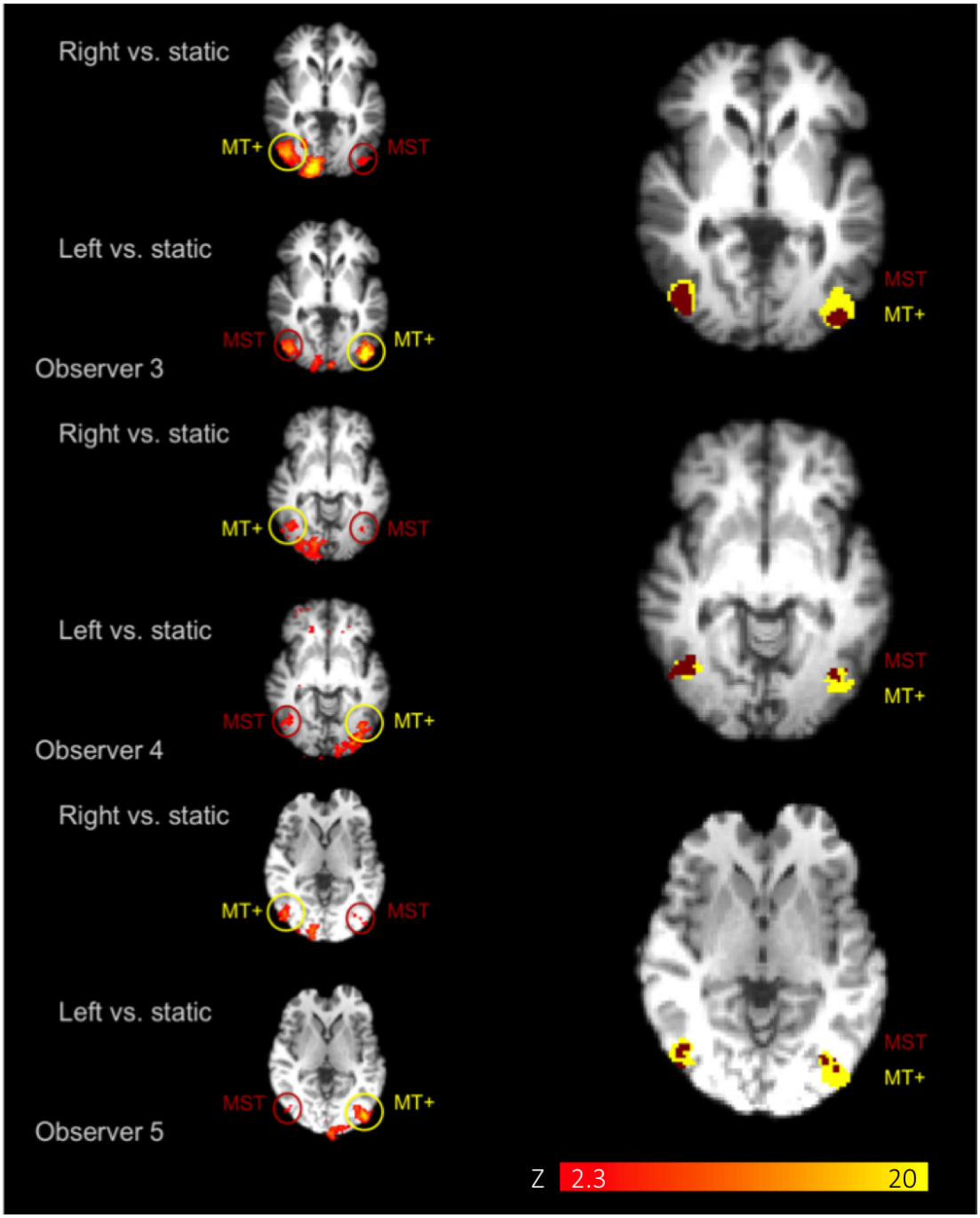

Figure 5.10: MT and MST regions of interest (ROIs) B

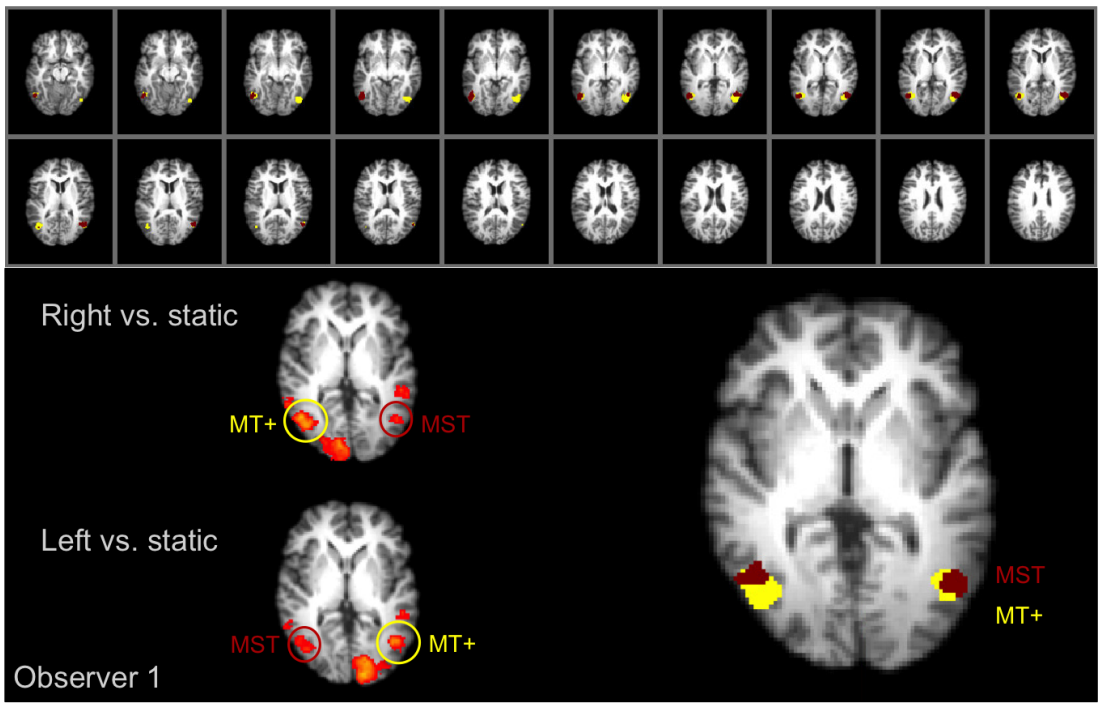

Figure 5.11: MT and MST regions of interest (ROIs), detailed view Top panel: representation of MT and MST ROIs for Observer 1, across all axial slices that cover the ROIs. Bottom panel: as in Figure 5.9

Table 5.1: Voxel coordinates of centroids for MT and MST regions of interest

	Left hemisphere						Right hemisphere					
	MT			MST			MT			MST		
Observer	x	y	z	x	y	z	x	y	z	x	y	z
1	69	30	38	45	54	45	19	29	35	45	54	45
2	67	31	38	45	54	45	22	32	37	45	54	45
3	67	20	35	45	54	45	22	26	36	45	54	45
4	64	27	35	45	54	45	21	29	33	45	54	45
5	66	23	37	45	54	45	21	28	32	45	54	45

All axial slices covering the ROIs for MT and MST are shown Figure 5.11, for observer 1, as well as a magnification of the activations. The pattern of activation and ROI sizes are representative of all observers.

Table 5.2: Number of voxels in visual ROIs

	Left hemisphere			Right hemisphere		
Observer	V1	MT	MST	V1	MT	MST
1	1177	361	255	1272	231	312
2	625	339	285	540	539	116
3	1079	473	91	1046	237	326
4	945	212	88	804	96	155
5	1391	483	111	1093	189	103
Mean	1043	373	166	951	258	202
S.D.	285	111	96	284	167	108

The voxel coordinates of the centroids for MT and MST in each hemisphere for each participant are detailed in Table 5.1, and the number of voxels defined for each ROI, along with the group mean and standard deviation are shown in Table 5.2. These ROI sizes are comparable to those of about 400 (1 x 1 x 1 mm^3) voxels as previously shown for hMT+ by Weigelt, Singer & Kohler (2012).

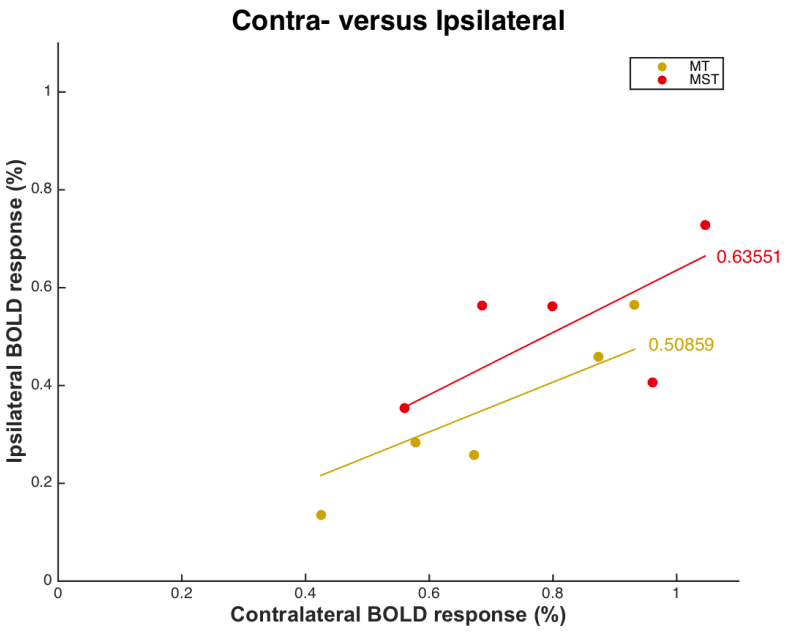

Figure 5.12: BOLD responses to contra- and ipsilateral stimuli in MT and MST Each point represents the average BOLD response of the ROIs in both hemispheres for each of the five observers. Yellow points indicate area MT and red points indicate area MST. There was a greater response to ipsilateral stimulation in area MST, compared with area MT. The solid yellow and red lines show linear regressions, whose slopes are indicated on the right and signify the average ratio of ipsilateral to contralateral response. The regression slopes and 95% confidence intervals were 0.508 ± 0.098, and 0.635 ± 0.918, for MT and MST respectively.

Figure 5.12 shows the average percent signal change observed for contra- and ipsilateral stimuli in the MT and MST ROIs, for each of the five observers. Each point shows the average BOLD response in an ROI over the two hemispheres of one observer. The yellow points indicate area MT, and the red points show area MST. Responses to ipsilateral stimuli were greater in MST than in MT. The solid yellow and red lines show linear regressions to the data, and give the average ratio of ipsilateral to contralateral responses. For area MT this ratio was 0.508 ± 0.098, and for MST, 0.635 ± 0.918. Note that the percent signal change is greater for contralateral than ipsilateral stimulation in both MT and MST but that the difference between the two is smaller in MST. There is a considerable overlap between the 95% confidence intervals, which could be due to the ipsilateral stimulus being presented relatively close to fixation. As Huk et al. propose,

the receptive fields of monkey MT neurons that represent the fovea extend over several degrees, and many cross into the ipsilateral visual field. For this reason they exclude the central 10 degrees of visual field from stimulation. The ipsilateral stimuli presented in this study only excluded 1.5 degrees around the fixation point, and may thus have activated both MT and MST.

5.4.3 Selectivity for radial motion

To test whether spatially distinct populations of neurons respond to the two directions of radial motion, the BOLD response to contraction, expansion and transparently moving dots was measured. The conditions were presented in blocks over separate scans, and subjects performed a task to control for attention. To evaluate the responses to these stimuli, standard retinotopic mapping procedures (Engel et al. (1994), Larsson & Heeger (2006), Sereno et al. (1995), Wandell, Dumoulin & Brewer (2007)) were applied to place the visual areas (see Section 5.4.1), and a functional localiser was used to ensure MT and MST were well defined according to published criteria (Huk & Heeger 2002, Tootell, Reppas, Kwong, Malach, Born, Brady, Rosen & Belliveau 1995) (Section 5.4.2).

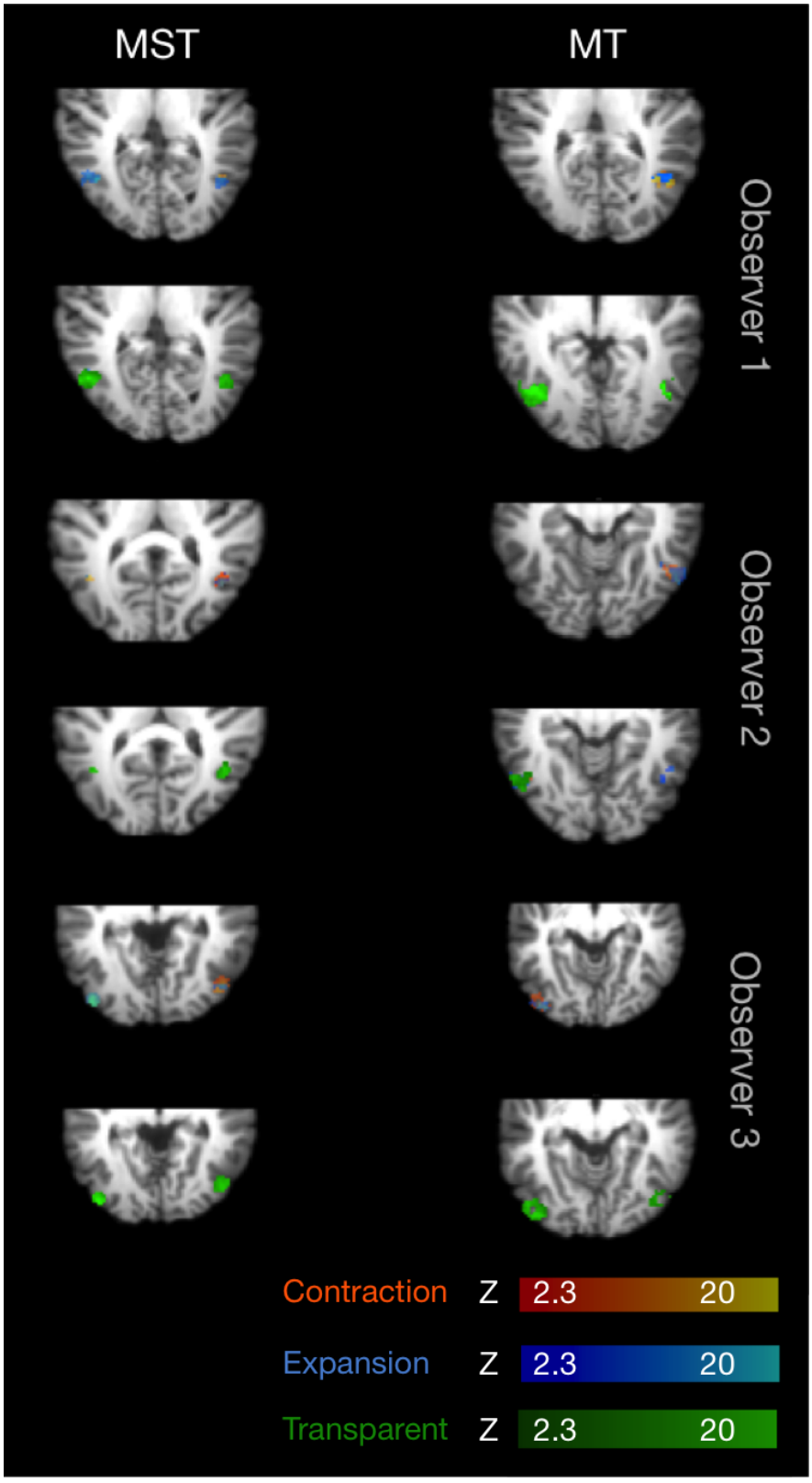

Figure 5.13: Activation in response to radial motion A

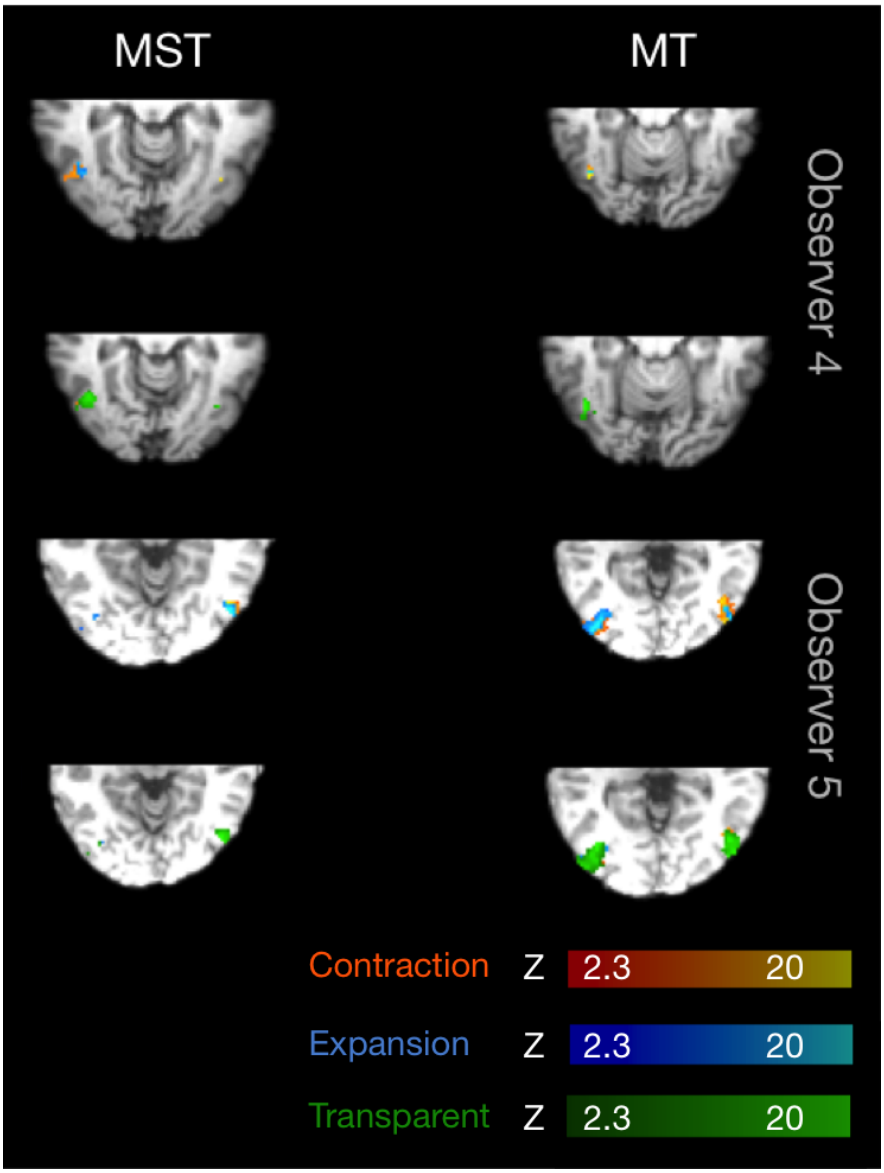

Figure 5.14: Activation in response to radial motion B Axial slices showing the activation clusters for contraction (orange), expansion (blue) and transparent motion (green), for observers 4 and 5. Top panels for each observer show activations to contraction and expansion, and bottom panels show the response to transparent motion.

The responses to different directions of radial motion were mapped and compared to stationary dot patterns for areas MT and MST. Figures 5.13 and 5.14 show voxels within the MT and MST ROIs which respond more to contraction (yellow - red) or expansion (light blue - dark blue), and voxels that respond to the transparent motion stimulus (light green - dark green) in each subject. Voxel clusters which respond to contraction and expansion overlap only partially, while the response to transparent motion appears to extend over all of MT and MST. Note that distinct voxel clusters appear to respond selectively for contraction or expansion. Examination of the raw voxel time courses confirms these findings.

Figure 5.15 shows the BOLD response (percent signal change) for radial motion versus static dots for all of the five observers who participated in the study, along with the group mean. Averaged over observers, BOLD responses to transparent motion are significantly greater than those to either contraction (two-tailed t-test, d.f. = 8, p = 0.247) or expansion (d.f. = 8, p = 0.0002), as well as for contraction over expansion (d.f. = 8, p = 0.0112) in area MT in the right hemisphere. Furthermore, the response to transparent motion is greater than to expansion in right MST (d.f. = 8, p = 0.0450).

The fact the transparent motion stimuli contained both black and white dots while the purely contracting and expanding stimuli only contained motion, raises the possibility that the higher luminance could account for the greater activation to transparent motion. We would expect increased response in V1 due to the higher-luminance stimuli, which could be inherited in downstream motion-selective areas. This increased response to transparent motion does not appear to be inherited from activity in V1 due to the contrast of the white dots in the transparent motion stimulus, since responses in V1 do not differ significantly for transparent motion and contraction or expansion (two-tailed t-test, d.f. = 8, p = 0.8053, and p = 0.7673 for contraction and expansion respectively). Transparent motion is a composite of both contraction and expansion, and may instead be stimulating neuronal populations within MT+ that are selective for either or both directions of movement.

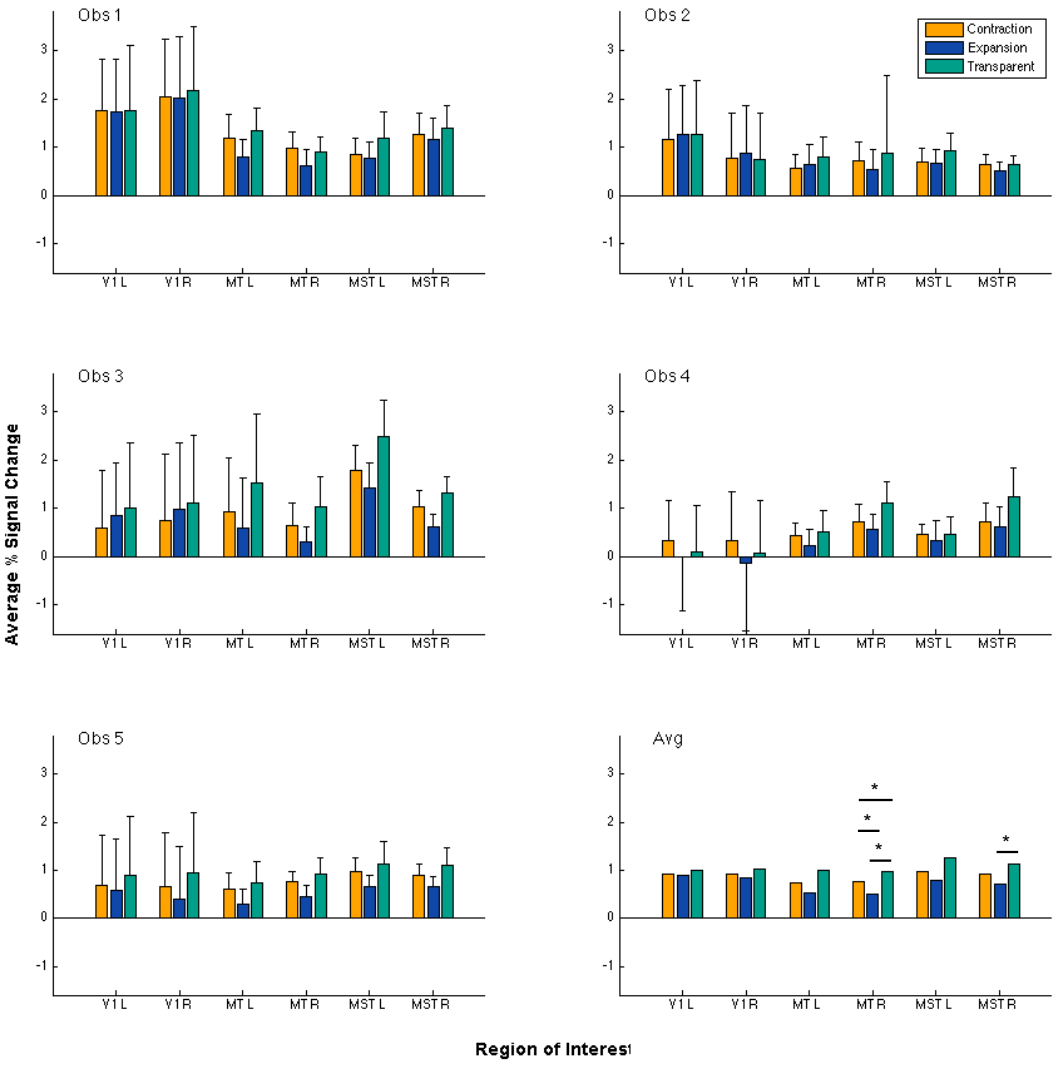

Figure 5.15: Selective responses to contraction and expansion Average percent signal change for contraction, expansion, and transparent motion versus static dots in V1, MT and MST are plotted for each observer and the group average (bottom right). Error bars show one standard deviation. Asterisks indicate significance (two-tailed paired-sample t-test, * $p < 0.05$)

Note that all ROIs examined show increased response to moving over stationary dots in all but one observer; although the effect is very small, V1 in observer 4 responds less to expanding motion than to stationary dots. This may be an effect of age, since this observer is the only one above 40 years old, although admittedly it is not clear how this might affect the observed result.

It is interesting to note that the responses for the two directions of motion are unbalanced, with all subjects showing greater activation for contraction than for expansion. In order to compare if this physiological asymmetry corresponds with the psychophysical data, the BOLD data are represented alongside each subject's psychophysical detection thresholds for contraction and expansion (Figure 5.16). Plotted are the ratios of contraction/expansion - percent signal change for the BOLD response, and proportion coherently moving dots at 75% correct point for psychophysical thresholds. Here, the data for all subjects are represented together for each region of interest. For four out of five subjects, the BOLD activity and threshold ratios are greater than 1, meaning that they are both greater for contraction than for expansion. There is however, no clear correlation between thresholds and BOLD response.

5.5 Discussion

This experiment has explored the physiological underpinnings of the perception of radial motion, suggesting that spatially distinct neural populations within area MST respond selectively to contracting and expanding motion. In order to delineate the early retinotopically organised visual areas, retinotopic mapping was performed using a Fourier-based phase-encoding method (Sereno et al. 1995), and the maps were projected onto the inflated and flattened brain surface. Moving dot stimuli designed to show differences in receptive field size were used to localise motion-selective areas MT and MST, and functional ROI maps of the two areas were drawn based on the resulting activations.

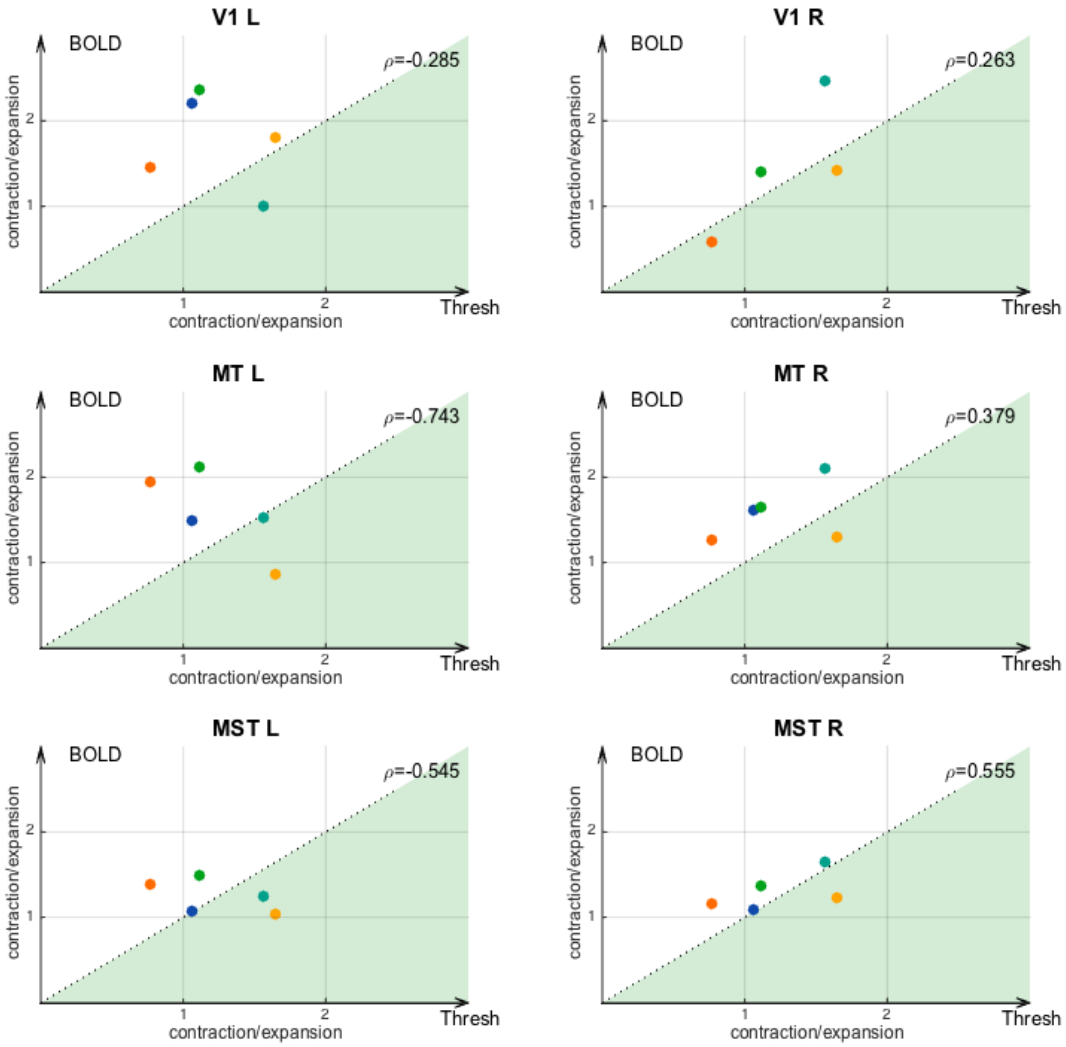

Figure 5.16: Relationship between BOLD activity and psychophysical thresholds Ratios of contraction/expansion are plotted for BOLD activation (abscissa) and psychophysical thresholds (ordinate), in the ROIs for V1, MT and MST. Correlation coefficients are shown in the top right. The different colours of dots represent different subjects, the diagonal represents equal contraction/expansion ratios for BOLD and thresholds.

The locations of visual areas in the occipital cortex vary greatly between individuals (Amunts et al. 2000, Andrews et al. 1997), making anatomical reference points poor for visual areas (Saxe, Brett & Kanwisher 2006). Functional localisation is therefore necessary to study response patterns in the visual cortex. Retinotopic mapping reliably revealed the early visual areas V1 and V2. While the isoeccentricity curves can be seen clearly, they extend over several areas, and the polar angle maps sometimes showed only a narrow vertical meridian band at the border of an area. Nevertheless, borders between V1 and V2 could be drawn for all subjects, and V3 and VP were identifiable for observers 1 and 2.

The human MT+ complex can be subdivided into two functional areas, tentatively identified as the homologues of monkey MT and MST, as first shown by Huk et al. (2002). Area MT responds primarily to stimuli in the contralateral visual field, while area MST has a greater response to ipsilateral stimulation. Huk et al. also demonstrated that MT has a retinotopic organisation and MST does not. The response to retinotopic mapping stimuli in this study is weaker and less extensive than reported by Huk et al., and a retinotopic organisation is not seen in area MT. Huk et al. used a motion-defined wedge composed of white dots in a black background rather than a checkerboard to map the polar angle component of the retinotopic map of MT. Responses in MT are likely greater for RDK stimuli than for a rotating checkerboard pattern, and this could account for the retinotopic organisation observed by Huk et al.. The locations and sizes of MT and MST observed here are comparable to those previously documented (Dukelow et al. (2001), Strong et al. (2017), Weigelt et al. (2012), Kolster, Peeters & Orban (2010)), and the region MST produces a greater response to ipsilateral stimuli than MT, confirming that the locations of the ROIs are well-founded.

Radial motion is produced on the retina as we move through the environment - forward movement produces expansion, and backward movement produces contraction. Analysis of the resulting optic flow patterns can yield information which can help us to

navigate in space (Gibson 1950). Previous neurophysiological studies have shown the existence of cells responding preferentially to contraction or expansion in the macaque (Saito et al. 1986, Tanaka & Saito 1989). Saito et al. found that these cells make up 15.7% of cells in MST (others respond preferentially to translating motion - 51.4% and rotation - 13.7%), and do not alter their response under varying brightness levels. Tanaka & Saito further showed that large stimuli extending over a wide area of the visual field elicit greater responses than smaller stimuli, and that the responses are shape and contrast invariant but that contraction/expansion cells are selective for velocity. This study suggests that cells selective for contraction and expansion exist in humans as well, and that they are spatially segregated (but see also Future Work, Section 6.2).

In contrast with true optic flow stimuli which typically extend over a large portion of the visual field, use a velocity gradient so that peripheral areas of the stimulus move faster than central areas, and produce a sense of vection (feeling of self-motion), the stimuli presented here were relatively small (due to the limitation on stimulus size imposed by viewing of the presentation screen through a mirror attached to the head coil in the scanner) and used a constant velocity. Despite this, the simple radial motion stimuli elicited a differential response to contraction and expansion.

The data presented here are based on a univariate analysis and suggest the possibility of distinct cell populations mediating the percepts of contraction and expansion, and reflects differences in activation amplitudes. It would be very interesting to combine this with a multivariate analysis (multi-voxel pattern analysis, MVPA), which is sensitive to voxel-level variability between conditions. By detailing how much of the activity in a voxel is explained by each stimulus, MVPA can provide further evidence as to what information is represented within a cortical area.

The BOLD response to contracting radial motion is greater than for expansion in 18 out of the 20 ROIs tested (MT and MST, in the left and right hemispheres of 5 observers), indicating a clear asymmetry in the processing of the two directions.

intriguingly, this is associated with higher psychophysical sensitivity to expansion than contraction as measured by coherence detection thresholds. Anisotropies between contraction and expansion could be due to cognitive expectations, prior experiences favouring one direction of motion, or because of adaptational benefits. It is possible that multiple functional systems processing contracting and expanding motion have evolved for different purposes in vision. Detecting mechanisms for expansion can aid in estimating the speed and direction of self-motion in the environment. Mechanisms biased for contraction meanwhile, may be involved in reaching actions, estimating the velocity of the receding hand in approach to an object (Edwards & Badcock 1993), or in helping to prevent dangerous backward falls (Edwards & Ibbotson 2007). Since expansion is the dominant direction of optic flow as we move forward through the environment, it may be affected by long-term adaptation, and therefore generate a reduced cortical response.

Several previous studies have shown greater cortical responses for contraction over expansion. Giaschi, Zwicker, Young & Bjornson (2007) found greater BOLD response for contracting dot motion in MT+, though this was associated with lower coherence thresholds for contraction. Shirai, Birtles, Wattam-Bell, Yamaguchi, Kanazawa, Atkinson & Braddick (2009) observed greater F1 (first harmonic) activity in steady-state VEP responses for contraction in infants over 4 months of age and in adults. While there are a couple reports of greater activity for expansion over contraction (Ptito et al. 2001, Wunderlich et al. 2002), these have been in V2, V3 and other areas in the lateral occipital cortex, and not in MT+. It therefore appears that cortical responses tend to be greater for contraction than expansion. The psychophysical result in this study suggest that sensitivity is greater for expansion. Other behavioural studies have shown an advantage for expansion over contraction using visual search tasks (Shirai & Yamaguchi 2004, Takeuchi 1997) and ambiguous 3D stimuli (Lewis & McBeath 2004), and objects (Perrone 1986), in human (Shirai et al. 2006) and in monkey infants (Shirai,

Imura, Hattori, Adachi, Ichihara, Kanazawa, Yamaguchi, Tomonaga, Tomoko, Hattori, Ikuma, Ichihara, So, Yamaguchi & Tomonaga 2009). Meanwhile, two reports have found an advantage for contraction (Edwards & Badcock 1993, Edwards & Ibbotson 2007). The differing results may result from differences in experimental design and stimuli. While studies showing an expansion bias used discrimination between radial and coherent translating (unidirectional) motion (Lewis & McBeath 2004, Perrone 1986, Shirai et al. 2006, Shirai & Yamaguchi 2004, Takeuchi 1997), those which report a bias for contraction (Edwards & Badcock 1993, Edwards & Ibbotson 2007) used a discrimination task between radial and random (incoherent) motion. It is then possible that experimental designs requiring a comparison of radial and translating motion preferentially involve mechanisms biased for expansion, while those comparing radial and random motion involve mechanisms more sensitive to contraction.

A greater cortical response and lower sensitivity for contraction appears counter-intuitive, as greater cortical activation could be expected to lead to improved performance. This issue is interesting to consider in light of a study using an apparent motion paradigm to look at the BOLD response to expected and unexpected stimulus configurations. Alink et al. (2010) showed that when a stimulus was shown along the expected motion path, it produced lesser BOLD activity in V1 and MT+ than when it was presented in a spatiotemporal position incongruent with the apparent motion. Their results are explained within a predictive coding framework; the increase in BOLD activity is interpreted as an error response due to a mismatch between the incoming signal and predictive feedback connections. If more predictable stimuli indeed cause lesser BOLD responses than more unexpected stimuli, then this could offer a reconciliation between the psychophysical and fMRI results reported here. If we tend to experience expanding optic flow patterns and are predisposed to expect them, we may be more sensitive to expansion and contracting patterns could be expected generate a greater BOLD response.

Chapter 6

Discussion

The work presented in the preceding chapters of this thesis characterises the visual processing of radial motion, including changes in discrimination sensitivity after adaptation and effects of directed attention on the motion aftereffect. The reference frame of motion adaptation is investigated, and the cortical substrates of contracting and expanding motion are studied using fMRI. In this chapter I summarise the main findings and describe future experiments which would expand on this work.

6.1 Summary of findings

Previous research on the motion aftereffect has most often focused on translating movement, and has reported the duration of the aftereffect - a measure that is susceptible to biases and expectations. Two of the studies presented in Chapter 3 investigated the effect of adaptation on discrimination functions for radial motion using different two-alternative forced choice paradigms. The results replicated (Edwards & Ibbotson 2007) and extended (Hirahara 2006) those from previous reports. Discrimination functions for radial motion were found to be mostly flat over increasing pedestal dot coherence levels. Adaptation increased absolute thresholds but had no effect at higher pedestals in the discrimination function, analogous to previous results (Morgan et al. 2006, 2011).

An orientation discrimination experiment was performed to evaluate whether the flat discrimination functions found for radial motion could be explained by a mechanism that compares relative proportions. Similarly flat discrimination functions were obtained for orientation, indicating that this may be the case. In contrast discrimination, adaptation also has the effect of increasing detection, but not discrimination thresholds at higher pedestals. It is possible that an analogous divisive-inhibition mechanism underlies coherence discrimination.

Neither detection nor discrimination thresholds differed greatly between the spatial and temporal 2AFC procedures, indicating that there was no significant interference in global motion processing due to spatial summation over large receptive fields as suggested by Burr & Ross (2008) and Ross & Burr (2010).

Several studies have reported an MAE following attentional tracking (e.g. Alais & Blake (1999), Culham et al. (2000), Lankheet & Verstraten (1995), Raphael et al. (2010)) which has different properties from the classical MAE. Experiment 4 was carried out to investigate the effect of attentional tracking in the context of radial motion. Attention was directed to components of a transparently moving dot display in which one component was contracting and the other expanding. Observers performed a speed-increment detection task in order to control for attention. The results show that directed attention can produce an MAE for radial motion, consistent with previous psychophysical findings of Culham et al. (2000), and supporting those of Alais & Blake (1999), Lankheet & Verstraten (1995) and Raphael et al. (2010). These results are independent of the reported effect of distracting attention on the MAE (Chaudhuri (1990*b*), Rezec et al. (2004), Taya et al. (2009), but see also Morgan (2011), Wohlgemuth (1911)). Inter-subject variability was observed in the effects of both adaptation and attention on motion sensitivity, as seen in other investigations (Granit 1928, Morgan et al. 2017, Sinha 1952).

The results of Experiment 4 in Chapter 3 suggest that the detection of radial motion

is dependent on mechanisms that can be modulated by attention. Some high-level visual processes have been shown to be affected by attention, and to occur in a reference frame that is not purely retinotopic (Boi, Vergeer, Ogmen & Herzog (2011), Noory, Herzog & Ogmen (2015), but see also Golomb, Chun & Mazer (2008)). These findings stimulated the question of whether radial coherent dot motion is represented in a retinotopic or rather spatiotopic reference frame, which was addressed in Chapter 4. A novel method of relative velocity adjustment on a transparently moving (contracting and expanding) dot stimulus was used to null the MAE in purely retinotopic, purely spatiotopic and non-retinotopic non-spatiotopic locations. The aftereffect was shown to be mostly retinotopic and modulated by eye movements, supporting previous functional imaging reports (Gardner et al. 2008, Knapen et al. 2009).

In light of findings from physiological studies in the macaque (Saito et al. 1986, Tanaka & Saito 1989) and human (Shirai, Birtles, Wattam-Bell, Yamaguchi, Kanazawa, Atkinson & Braddick 2009), a functional imaging experiment was designed to look into whether contraction and expansion might be processed in distinct cortical regions. The results presented in Chapter 5 show the presence of voxel clusters in MT+ responding preferentially for either of the two directions of radial motion. The BOLD response to contracting motion was greater than for expanding, supporting the EEG findings of Shirai, Birtles, Wattam-Bell, Yamaguchi, Kanazawa, Atkinson & Braddick (2009) and psychophysical observations of Edwards & Ibbotson (2007) and Edwards & Badcock (1993). Since the results of other studies show an opposite effect (Lewis & McBeath 2004, Perrone 1986, Ptito et al. 2001, Takeuchi 1997), an interesting question remains as to which stimuli preferentially involve processes favouring one direction of motion over the other.

6.2 Future directions

6.2.1 Motion adaptation

The experiments described in this thesis have employed a constrained set of parameters for the moving dot fields. The dot density and velocity were chosen to match the response properties of cells in the MT complex (Britten et al. 1992*a*, Maunsell & Van Essen 1983*b*). Further experiments are needed to examine how discrimination functions vary with the size and number of dots used, since the use of many more, smaller dots (similar to white noise) would make a numerosity judgement difficult, allowing the measure of thresholds based on motion energy in the discrimination task.

While the results presented here are consistent with discrimination of motion coherence in terms of relative numerosity judgements, additional experiments could provide further evidence for this account. For example, adding a strong segmentation cue such as colour (Croner & Albright 1997) to differentiate signal from noise dots would allow the measurement of proportion discrimination functions.

The results from some of the experiments described here (e.g. Sections 3.4 and 3.5) show large individual differences in the effect of adaptation on motion sensitivity. Similarly large inter-subject variability has been observed for the MAE using a visual search task by Morgan et al. (2017). Further studies with more observers are necessary in order to be able to make definite conclusions about the general population.

6.2.2 Reference frame of the MAE

In Chapter 4, adaptation to radial motion was shown to be weak in non-retinotopic conditions and to be affected by gaze modulation. Inevitably, there are multiple differences between the conditions tested - where eye movements are required, adaptation was 'broken up' by saccades, and the net adaptation time was slightly reduced compared to where no eye movements were made. Eye-movements could additionally act to reset adaptation. Paradiso, Meshi, Pisarcik & Levine (2012) show that saccades reset

orientation discrimination; although stimulus orientation on each fixation transiently influences the orientation perceived on the next fixation, this influence is greatly reduced when a sacked is made in between. Another study found that saccades shorten the duration of percepts in bistable stimuli (the Necker cube), which suggests that visual input from the preceding fixation may be erased during the saccade (Ross & Ma-Wyatt 2004).

Ezzati et al. (2008) suggested that the presence of motion-defined boundaries produce more retinotopic adaptation than when stimuli are presented within a Gaussian envelope (see Knapen et al. (2009)), which blurs the motion-defined edges. It would then be interesting to examine the reference frame of the MAE using radial motion shown within a Gaussian window.

6.2.3 Multivariate analysis of fMRI response to radial motion

Chapter 5 describes an activation-based (i.e. univariate) analysis of the fMRI signal in response to contracting, expanding and transparent radial stimulation. While the results suggest that the patterns of voxels responding to contraction and expansion differ, they should not be taken as conclusive evidence of distinct neural populations for the two directions of radial motion. Functional imaging data are noisy, and the parameters used in the analysis (such as spatial averaging and ROI definitions) can significantly alter the results. It could be complementary to additionally perform multi-variate pattern analysis (MVPA) on the acquired data. MVPA methods analyse neural responses as patterns of activity, and benefit from increased sensitivity relative to traditional univariate approaches (Norman, Polyn, Detre & Haxby 2006). Rather than performing spatial pooling to reduce noise MVPA uses pattern classification techniques to identify signals in the patterns of response across multiple voxels which, alone, may not show significant responses to the experimental variables. Due to this, MVPA methods are often assumed to indicate what information is represented in a cortical region. However,

care is needed when interpreting MVPA results, as they are especially sensitive to voxel-level variability in the parameters (Davis et al. 2014), which is a fundamental assumption in neuroimaging.

6.2.4 fMRI adaptation to probe for motion opponency in MST

The data presented in Chapter 5 suggest that the neural populations responding to contracting and expanding dot motion may be spatially distinct, within cortical area MT and MST. Due to the limited spatial resolution of the functional scans in this study, further investigations are required to verify this issue. One possibility is to use an fMRI adaptation paradigm to attempt to distinguish sub-voxel activations.

The technique of fMRI adaptation has been used to map functional properties of neurons within single voxels. The reasoning is the following: prolonged viewing of a stimulus S1 causes a decrease in the BOLD response of neuronal populations responsive to that stimulus (Grill-Spector et al. 2006, Krekelberg et al. 2006, Wall et al. 2008), and this adaptation (i.e. reduced response) will transfer to any stimuli for which the adapted mechanism is selective, but not to other stimuli S2. If a given voxel contains populations of cells selective for both S1 and S2, then its response will be reduced by adaptation, but will rebound when S2 is presented since the cells selective for S2 have not been adapted.

Motion selective cells in the monkey visual cortex show motion opponency, meaning that their response is suppressed by motion opposite to their preferred direction. Heeger et al. (1999) observed such motion-opponent mechanisms in human area MT using fMRI. A stimulating question remains as to whether expanding and contracting motion are mediated by opposing mechanisms, similar to unidirectional motion. The phenomenological observation that separate MAEs can be observed with contracting and expanding radial motion suggests that this is likely the case. A technique such as fMRI adaptation could be used to test whether the perception of contraction and

expansion are mediated by directionally selective channels and an opponent mechanism, probably within area MST. Further studies have confirmed an opponent mechanism for translational motion (Heeger et al. 1999, Singh et al. 2000, Thompson et al. 2016).

It should be noted that there are numerous difficulties in the interpretation of fMRI adaptation data (Bartels et al. (2008), see also Grill-Spector & Malach (2001) and Krekelberg et al. (2006) for reviews). As demonstrated by Boynton et al. (2003), adaptation in early visual areas is inherited downstream. The mechanisms underlying adaptation in V1 and MT differ, and therefore differentially affect the BOLD signal. The firing rate of V1 neurons reduces due to intra-neuronal mechanisms, while in MT it is due to suppressed synaptic input. Since the BOLD signal likely reflects peri-synaptic activity and not neuronal spiking, not only could any adaptation observed in MT be inherited from earlier visual areas (such as V1), but the actual site of adaptation may not produce BOLD activation at all. The specificity of fMRI adaptation in localising neuronal populations is therefore contentious.

6.2.5 Effect of attention on motion adaptation in the visual cortex

If distinct populations for contraction and expansion can be identified reliably, it would be possible to test if directed attention to one component of a transparent motion stimulus affects the neural response to the attended direction differently than to the unattended direction.

Several studies have suggesed that directed attention increases the selectivity of fMRI adaptation (e.g. Beauchamp et al. (1997), Huk & Heeger (2000), O'Craven et al. (1997)). However, the effects of attentional manipulation on motion adaptation are disputable, and it is unclear how the fMRI response is related to behavioural measures. Studies have shown that the percept of apparent motion, due to adaptation to motion (the MAE) for example, causes neural activity in MT+ despite the absence of physical motion energy, and that directing attention leads to increased BOLD activity even without any visual

stimulation (Kastner et al. 1999). Huk et al. (2001) argue that the increased neural activation during a motion aftereffect percept can be accounted for entirely by increased attention during apparent motion. In their 2001 article, Huk et al. show that the BOLD signal increase during the motion aftereffect can be attributed to attention; a test that appears to move because of the MAE commands more attention than a purely stationary one. Once attention was equalled across conditions (with a threshold-level speed task performed on the test stimulus), the BOLD increase was abolished. It follows that attention directed to one component in a transparent motion stimulus could unbalance an opponent mechanism; the response to the attended direction would be adapted and thus decrease. If attention is then switched to the other motion component, a release from adaptation is expected, along with a resulting increase in BOLD response.

6.3 Conclusion

The findings reported in this thesis add to the body of research on how and where radial motion is processed in the human brain. Several ideas have been re-evaluated in light of the results presented here, and new contributions have been made. Notably, directing attention can affect adaptation to radial motion, the reference frame of the motion aftereffect for radial motion is revealed to be mostly retinotopic, and contracting and expanding motion are shown to be processed in spatially distinct cortical areas within area MST. Much of the work discussed here has already been published in abstract format (Nikolova & Morgan 2013*a*,*b*,*c*, Nikolova & Raphael 2012), and has been presented at national and international conferences. It is hoped that these findings will stimulate future research on visual motion perception.

Bibliography

Adelson, E. H. & Bergen, J. R. (1985), 'Spatiotemporal energy models for the perception of motion', *Journal of the Optical Society of America A* **2**(2), 284–299. 12, 14, 15

Adelson, E. H. & Movshon, J. A. (1982), 'Phenomenal coherence of moving visual patterns', *Nature* **300**(9 December 1982), 523–525. 16

Alais, D. & Blake, R. (1999), 'Neural strength of visual attention gauged by motion adaptation.', *Nature neuroscience* **2**(11), 1015–1018. 76, 82, 136

Albright, T. D. (1984), 'Direction and orientation selectivity of neurons in visual area MT of the macaque.', *Journal of neurophysiology* **52**(6), 1106–30. 104

Alink, A., Schwiedrzik, C. M., Kohler, A., Singer, W. & Muckli, L. (2010), 'Stimulus Predictability Reduces Responses in Primary Visual Cortex', *Journal of Neuroscience* **30**(8), 2960–2966. 134

Allman, J. M. & Kaas, J. H. (1971), 'A representation of the visual field in the caudal third of the middle temporal gyrus of the owl monkey (Aotus trivirgatus)', *Brain Research* **31**(1), 85–105. 104

Amano, K., Wandell, B. A., Dumoulin, S. O., Takeda, T., Haji, T., Terao, M., Maruya, K., Matsumoto, K., Murakami, I. & Nishida, S. (2009), 'Human neural responses involved in spatial pooling of locally ambiguous motion signals.', *Journal of neurophysiology* **102**(5), 2704–2718. 105

Amunts, K., Malikovic, A., Mohlberg, H., Schormann, T. & Zilles, K. (2000), 'Brodmann's Areas 17 and 18 Brought into Stereotaxic Space - Where and How Variable?', *NeuroImage* **11**(1), 66–84. 131

Andersen, R. A., Essick, G. K. & Siegel, R. M. (1985), 'Encoding of spatial location by posterior parietal neurons', *Science* **230**(4724), 456–458. 89

Andersen, R. A., Snowden, R. J., Treue, S. & Graziano, M. (1990), 'Hierarchical processing of motion in the visual cortex of monkey.', *Cold Spring Harbor symposia on quantitative biology* **55**, 741–8. 16

Andrews, T. J., Halpern, S. D. & Purves, D. (1997), 'Correlated Size Variations in Human Visual Cortex, Lateral Geniculate Nucleus, and Optic Tract', *Journal of Neuroscience* **17**(8). 131

Anobile, G., Cicchini, G. M. & Burr, D. C. (2016), 'Number As a Primary Perceptual Attribute: A Review', *Perception* **45**(1-2), 5–31. 25, 64, 65

Anstis, S., Verstraten, F. A. & Mather, G. (1998), 'The motion aftereffect', *Trends Cogn Sci* **2**(3), 111–117. 22

Atchley, P. & Andersen, G. J. (1998), 'The effect of age, retinal eccentricity, and speed on the detection of optic flow components.', *Psychology and aging* **13**(2), 297–308. 17

Attwell, D. & Iadecola, C. (2002), 'The neural basis of functional brain imaging signals', *Trends in Neurosciences* **25**(12), 621–625. 28

BIBLIOGRAPHY

Bair, W. (1999), 'Spike Timing in the Mammalian Visual System.', *Current Opinion in Neurobiology* **9**, 447. 96

Bakan, P. & Mizusawa, K. (1963), 'Effect of inspection time and direction of rotation on a generalized form of the spiral aftereffect', *Journal of Experimental Psychology* **65**(6), 583–586. 51, 57

Baker, C. L. & Braddick, O. J. (1985), 'Eccentricity-dependent scaling of the limits for short-range apparent motion perception.', *Vision research* **25**(6), 803–12. 16

Bandettini, P. a. & Ungerleider, L. G. (2001), 'From neuron to BOLD: new connections.', *Nature neuroscience* **4**(9), 864–866. 26, 27

Bandettini, P. A., Wong, E. C., Hinks, R. S., Tikofsky, R. S. & Hyde, J. S. (1992), 'Time course EPI of human brain function during task activation', *Magnetic Resonance in Medicine* **25**(2), 390–397. 26

Barbur, J. L. (1985), 'Speed discrimination and its relation to involuntary eye movements in human vision', *Neuroscience Letters* **54**(1), 7–12. 16

Barlow, H. B. & Hill, R. M. (1963*a*), 'Selective sensitivity to direction of movement in ganglion cells of the rabbit retina', *Science* **139**(3553), 412–414. 20

Barlow, H. B. & Levick, W. R. (1965), 'The mechanism of directionally selective units in rabbit's retina.', *The Journal of Physiology* **178**(3), 477–504. 3

Barlow, H. & Hill, R. M. (1963*b*), 'Evidence for a Physiological Explanation of the Waterfall Phenomenon and Figural after-Effects', *Nature* **200**(4913), 1345–1347. 22

Bartels, A., Logothetis, N. K. & Moutoussis, K. (2008), 'fMRI and its interpretations: an illustration on directional selectivity in area V5/MT.', *Trends in neurosciences* **31**(9), 444–53. 141

Bartlett, N. R. (1942), 'The discrimination of two simultaneously presented brightnesses.', *Journal of Experimental Psychology* **31**(5), 380–392. 58

Beauchamp, M. S., Cox, R. W. & DeYoe, E. A. (1997), 'Graded effects of spatial and featural attention on human area MT and associated motion processing areas.', *Journal of neurophysiology* **78**(1), 516–20. 29, 141

Beck, D. M., Rees, G., Frith, C. D. & Lavie, N. (2001), 'Neural correlates of change detection and change blindness', *Nature Neuroscience* **4**(6), 645–650. 24

Beissner, F., Deichmann, R. & Baudrexel, S. (2011), 'fMRI of the brainstem using dual-echo {EPI}', *NeuroImage* **55**(4), 1593–1599. 40

Belliveau, J., Kennedy, D., McKinstry, R., Buchbinder, B., Weisskoff, R., Cohen, M., Vevea, J., Brady, T. & Rosen, B. (1991), 'Functional mapping of the human visual cortex by magnetic resonance imaging', *Science* **254**(5032), 716–719. 26

Berman, R. A., Cavanaugh, J., Mcalonan, K. & Wurtz, R. H. (2017), 'A circuit for saccadic suppression in the primate brain', *Journal of Neurophysiology* **117**, 1720–1735. 99

Bex, P. J., Metha, A. B. & Makous, W. (1998), 'Psychophysical evidence for a functional hierarchy of motion processing mechanisms.', *Journal of the Optical Society of America.* **15**(4), 769–776. 104

Bex, P. J., Verstraten, F. a. & Mareschal, I. (1996), 'Temporal and spatial frequency tuning of the flicker motion aftereffect.', *Vision research* **36**(17), 2721–7. 20

Blake, R. & Hiris, E. (1993), 'Another means for measuring the motion aftereffect', *Vision Res* **33**(11), 1589–1592. 34, 47, 56

Boi, M., Vergeer, M., Ogmen, H. & Herzog, M. H. (2011), 'Nonretinotopic Exogenous Attention', *Current Biology* **21**(20), 1732–1737. 137

Borst, A., Euler, T., Zhou, Z. J., Tachibana, M., Pastan, I., Nakanishi, S., Usui, S., Noda, M. & Bamberg, E. (2011), 'Seeing things in motion: models, circuits, and mechanisms.', *Neuron* **71**(6), 974–994. 3

Bower, J. D., Bian, Z. & Andersen, G. J. (2012), 'Effects of retinal eccentricity and acuity on global-motion processing.', *Attention, perception & psychophysics* **74**(5), 942–9. 17

Boynton, G. M., Kohn, A. & Movshon, J. A. (2003), 'Neuronal adaptation to visual motion in area MT of the macaque', *Neuron* **39**(4), 681–691. 20, 22, 141

Braddick, O. J., O'Brien, J. M. D., Wattam-Bell, J., Atkinson, J., Hartley, T. & Turner, R. (2001), 'Brain areas sensitive to coherent visual motion', *Perception* **30**, 61–72. 104, 105

Braddick, O. J., O'Brien, J., Wattam-Bell, J., Atkinson, J. & Turner, R. (2000), 'Form and motion coherence activate independent, but not dorsal/ventral segregated, networks in the human brain', *Current Biology* **10**(12), 731–734. 6

Braddick, O. J., Wishart, K. A. & Curran, W. (2002), 'Directional performance in motion transparency', *Vision Research* **42**(10), 1237–1248. 23

Brainard, D. H. (1997), 'The Psychophysics Toolbox'. 34, 48, 76

Brainard, D. H., Pelli, D. G. & Robson, T. (2002), 'Display characterization', *In J. Hornak (Ed.), Encyclopedia of Imaging Science and Technology* pp. 172—-188. 34

Brewer, A. A., Press, W. A., Logothetis, N. K. & Wandell, B. A. (2002), 'Visual areas in macaque cortex measured using functional magnetic resonance imaging', *The Journal of neuroscience* **22**(23), 10416–10426. 29

Britten, K. H., Shadlen, M. N., Newsome, W. T. & Movshon, J. A. (1992*a*), 'Responses of neurons in macaque MT to stochastic motion signals.', *Journal of Neuroscience* **12**(12), 4745–65. 58, 138

Britten, K. H., Shadlen, M. N., Newsome, W. T. & Movshon, J. A. (1992*b*), 'The analysis of visual motion: a comparison of neuronal and psychophysical performance', *The Journal of neuroscience* **12**(12), 4745–65. 35

Burr, D. C., Morgan, M. J. & Morrone, M. (1999), 'Saccadic suppression precedes visual motion analysis', *Current Biology* **9**(20), 1207–1209. 99

Burr, D. C., Morrone, M. C. & Vaina, L. M. (1998), 'Large receptive fields for optic flow detection in humans', *Vision Research* **38**(12), 1731–1743. 59, 68, 74

Burr, D. C., Turi, M. & Anobile, G. (2010), 'Subitizing but not estimation of numerosity requires attentional resources', *Journal of Vision* **10**(6), 20–20. 25

Burr, D. & Ross, J. (1983), *Visual analysis during motion.*, MIT Press. 14

Burr, D. & Ross, J. (2008), 'A Visual Sense of Number', *Current Biology* **18**(6), 425–428. 24, 64, 85, 86, 136

Burton, G. J. & Moorhead, I. R. (1987), 'Color and spatial structure in natural scenes.', *Applied optics* **26**(1), 157–70. 33

Cavanagh, P. (1991), 'Short-range vs Long-range motion: Not a valid distinction', *Spatial Vision* **5**(4), 303–309. 45

Cavanagh, P. & Eizner Favreau, O. (1985), 'Color and luminance share a common motion pathway', *Vision Research* **25**(11), 1595–1601. 17

Cavanagh, P. & Mather, G. (1989), 'Motion: the long and short of it.', *Spatial Vision* **4**(2), 103–29. 45

Chaudhuri, A. (1990*a*), 'A motion illusion generated by after nystagmus suppression', *Neurosci. Lett.* **118**, 91–95. 24

Chaudhuri, A. (1990*b*), 'Modulation of the motion aftereffect by selective attention.', *Nature* **344**(6261), 60–62. 24, 75, 136

Chawla, D., Phillips, J., Buechel, C., Edwards, R. & Friston, K. J. (1998), 'Speed-Dependent Motion-Sensitive Responses in V5: An fMRI Study', *NeuroImage* **7**(2), 86–96. 105

Chun, M. M. & Marois, R. (2002), 'The dark side of visual attention', *Current Opinion in Neurobiology* **12**(2), 184–189. 29

Collins, T., Semroud, A., Orriols, E. & Doré-Mazars, K. (2008), 'Saccade Dynamics before, during, and after Saccadic Adaptation in Humans', *Investigative Opthalmology & Visual Science* **49**(2), 604–612. 39

Cornsweet, T. N. & Pinsker, H. M. (1965), 'Luminance discrimination of brief flashes under various conditions of adaptation', *J. Physiol* **176**, 294–310. 58

Courtney, S. M. & Ungerleider, L. G. (1997), 'What fMRI has taught us about human vision', *Current opinion in neurobiology* **7**(4), 554–561. 29

Cox, R. W. (1996), 'AFNI: Software for Analysis and Visualization of Functional Magnetic Resonance Neuroimages', *Computers and Biomedical Research* **29**(3), 162–173. 40, 44

Crespi, S., Biagi, L., D'Avossa, G., Burr, D. C., Tosetti, M. & Morrone, M. C. (2011), 'Spatiotopic coding of BOLD signal in human visual cortex depends on spatial attention.', *PloS one* **6**(7), e21661. 101

Croner, L. J. & Albright, T. D. (1997), 'Image Segmentation Enhances Discrimination of Motion in Visual Noise', *Vision Research* **37**(11), 1415–1427. 67, 87, 138

Culham, J. C., Dukelow, S. P., Vilis, T., Hassard, F. A., Gati, J. S., Menon, R. S., Goodale, M. A., Shepherd, A. J. & Siniatchkin, M. (1999), 'Recovery of fMRI Activation in Motion Area MT Following Storage of the Motion Aftereffect', *Journal of Neurophysiology* **81**, 388–393. 20, 30

Culham, J. C., Verstraten, F. A., Ashida, H. & Cavanagh, P. (2000), 'Independent aftereffects of attention and motion', *Neuron* **28**(2), 607–615. 20, 45, 76, 82, 136

Culham, J., He, S., Dukelow, S. & Verstraten, F. A. J. (2001), 'Visual motion and the human brain : what has neuroimaging told us ?', *Acta Psychologica* **107**, 69–94. 29, 105

Dakin, S. C., Mareschal, I. & Bex, P. J. (2005), 'Local and global limitations on direction integration assessed using equivalent noise analysis', *Vision Research* **45**, 3027–3049. 35

Dakin, S. C., Tibber, M. S., Greenwood, J. A., Kingdom, F. A. A. & Morgan, M. J. (2011), 'A common visual metric for approximate number and density', *Proceedings of the National Academy of Sciences* **108**(49), 19552–19557. 24

Dale, A. M., Fischl, B. & Sereno, M. I. (1999), 'Cortical Surface-Based Analysis: I. Segmentation and Surface Reconstruction', *NeuroImage* **9**(2), 179–194. 40, 44

Davis, T., LaRocque, K. F., Mumford, J. A., Norman, K. A., Wagner, A. D. & Poldrack, R. A. (2014), 'What do differences between multi-voxel and univariate analysis mean? How subject-, voxel-, and trial-level variance impact fMRI analysis', *NeuroImage* **97**, 271–283. 140

D'Avossa, G., Tosetti, M., Crespi, S., Biagi, L., Burr, D. C. & Morrone, M. C. (2007), 'Spatiotopic selectivity of BOLD responses to visual motion in human area MT.', *Nature neuroscience* **10**(2), 249–55. 100, 116

de Valois R. L. & de Valois K. K. (1988), *Spatial Vision*, Vol. 31, Oxford University Press, New York. 5, 33

De Valois R. L. & De Valois, K. K. (1991), 'Vernier acuity with stationary moving Gabors', *Vision Research* **31**(9), 1619–1626. 21

Dehaene, S. & Changeux, J.-P. (1993), 'Development of Elementary Numerical Abilities: A Neuronal Model', *Journal of Cognitive Neuroscience* **5**(4), 390–407. 24

Desimone, R. & Duncan, J. (1995), 'Neural mechanisms of selective visual attention.', *Annu. Rev. Neurosci.* **18**, 193–222. 24

Desimone, R. & Ungerleider, L. G. (1986), 'Multiple Visual Areas in the Caudal Superior Temporal Sulcus of the Macaque', *The Journal of comparative neurology* **248**, 164–189. 104

Deyoe, E. A., Carmant, G. J., Bandettinit, P., Glickman, S., Wieser, J., Cox, R., Miller, D. & Neitz, J. (1996), 'Mapping striate and extrastriate visual areas in human cerebral cortex', *Neurobiology* **93**, 2382–2386. 111

Douglas, R. J. & Martin, K. A. C. (2004), 'Neuronal circuits of the neocortex.', *Annu. Rev. Neurosci* **27**, 419–51. 28

Dubner, R. & Zeki, S. M. (1971), 'Response properties and, receptive fields of cells in an anatomically defined region of the superior temporal sulcus in the monkey', *Brain Research* **35**, 528–532. 104

Duffy, C. J. & Wurtz, R. H. (1991*a*), 'Sensitivity of MST neurons to optic flow stimuli. I. A continuum of response selectivity to large-field stimuli', *J Neurophysiol* **65**(6), 1329–1345. 8, 104

Duffy, C. J. & Wurtz, R. H. (1991*b*), 'Sensitivity of MST neurons to optic flow stimuli. II. Mechanisms of response selectivity revealed by small-field stimuli', *Journal of Neurophysiology* **65**(6), 1346–1359. 8, 104

Duhamel, J.-R., Bremmer, F., BenHamed, S. & Graf, W. (1997), 'Spatial invariance of visual receptive fields in parietal cortex neurons', *Naure* **108389**(6653), 845–848. 89

Dukelow, S. P., DeSouza, J. F. X., Culham, J. C., van den Berg, A. V., Menon, R. S. & Vilis, T. (2001), 'Distinguishing subregions of the human MT+ complex using visual fields and pursuit eye movements', *J Neurophysiol* **86**(4), 1991–2000. 29, 43, 105, 131

Dumoulin, S. O., Bittar, R. G., Kabani, N. J., Baker, C. L., Le Goualher, G., Bruce Pike, G. & Evans, A. C. (2000), 'A new anatomical landmark for reliable identification of human area V5/MT: a quantitative analysis of sulcal patterning.', *Cerebral cortex* **10**(5), 454–63. 43, 104

Durgin, F. H. (1995), 'Texture Density Adaptation and the Perceived Numerosity and Distribution of Texture', *Journal of Experimental Psychology: Human Perception and Performance* **21**(1), 149–169. 25

Edwards, M. & Badcock, D. R. (1993), 'Asymmetries in the Sensitivity to Motion in Depth: A Centripetal Bias', *Perception* **22**(9), 1013–1023. 133, 134, 137

Edwards, M. & Ibbotson, M. R. (2007), 'Relative sensitivities to large-field optic-flow patterns varying in direction and speed', *Perception* **36**(1), 113–124. 47, 57, 133, 134, 135, 137

Egeth, H. E., Leonard, C. J. & Palomares, M. (2008), 'The role of attention in subitizing: Is the magical number 1?', *Visual Cognition* **16**(4), 463–473. 65

Emerson, R. C., Bergen, J. R. & Adelson, E. H. (1992), 'Directionally Selective Complex Cells and the Computation of Motion Energy in Cat Visual Cortex', *Vision Research* **32**(2), 203–218. 15

Engel, S. A., Glover, G. H. & Wandell, B. A. (1997), 'Retinotopic organization in human visual cortex and the spatial precision of functional MRI.', *Cerebral cortex* **7**(2), 181–92. 29, 44, 111

Engel, S. A., Rumelhart, D. E., Wandell, B. A., Lee, A. T., Glover, G. H., Chichilnisky, E.-J. & Shadlen, M. N. (1994), 'fMRI of human visual cortex', *Nature* **369**(6481), 525–525. 123

Exner, S. (1887), '"Einige Beobachtungen uber Bewegungsnachbilder"', *Zentralblatt fur Physiologie* **1**, 135–140. 19

Exner, S. (1888), '"Uber optische Bewegungsempfindungen"', *Biologisches Zentralblatt* **8**, 437–448. 19

Ezzati, A., Golzar, A. & Afraz, A. S. R. (2008), 'Topography of the motion aftereffect with and without eye movements.', *Journal of vision* **8**(14), 23.1–16. 89, 99, 100, 139

Favreau, O. E., Emerson, V. F. & Corballis, M. C. (1972), 'Motion perception: a color-contingent aftereffect.', *Science* **176**(4030), 78–9. 17

Fennema, C. L. & Thompson, W. B. (1979), 'Velocity determination in scenes containing several moving objects', *Computer Graphics and Image Processing* **9**, 301–315. 12, 14

Field, D. J. (1987), 'Relations between the statistics of natural images and the response properties of cortical cells.', *Journal of the Optical Society of America. A, Optics and image science* **4**(12), 2379–94. 33

Field, D. J. (1994), 'What Is the Goal of Sensory Coding?', *Neural Computation* **6**(4), 559–601. 33

Fischer, E., Büthoff, H. H., Logothetis, N. K., Bartels, A., Buïthoff, H. H., Logothetis, N. K. & Bartels, A. (2012), 'Visual Motion Responses in the Posterior Cingulate Sulcus: A Comparison to V5/MT and MST', *Cerebral Cortex April* **22**, 865–876. 43

Foley, J. M. & Chen, C.-C. (1997), 'Analysis of the effect of pattern adaptation on pattern pedestal effects: A two-process model', *Vision Research* **37**(19), 2779–2788. 58, 84

Freeman, T. C. & Harris, M. G. (1992), 'Human sensitivity to expanding and rotating motion: effects of complementary masking and directional structure.', *Vision research* **32**(1), 81–7. 104

Fried, S. I., Münch, T. A. & Werblin, F. S. (2002), 'Mechanisms and circuitry underlying directional selectivity in the retina', *Nature* **420**(6914), 411–414. 20

Gandhi, S. P., Heeger, D. J. & Boynton, G. M. (1999), 'Spatial attention affects brain activity in human primary visual cortex', *Proc Natl Acad Sci U S A* **96**(6), 3314–3319. 23, 24

Gardner, J. L., Merriam, E. P., Movshon, J. A. & Heeger, D. J. (2008), 'Maps of visual space in human occipital cortex are retinotopic, not spatiotopic.', *The Journal of Neuroscience* **28**(15), 3988–99. 99, 100, 101, 137

Georgeson, M. A. (1994), 'From filters to features: location, orientation, contrast and blur.', *Ciba Foundation symposium* **184**, 147–65; discussion 165–9, 269–71. 9

Giaschi, D., Douglas, R., Marlin, S. & Cynader, M. (1993), 'The time course of direction-selective adaptation in simple and complex cells in cat striate cortex', *J Neurophysiol* **70**(5), 2024–2034. 20

Giaschi, D., Zwicker, A., Young, S. A. & Bjornson, B. (2007), 'The role of cortical area V5/MT+ in speed-tuned directional anisotropies in global motion perception', *Vision Research* **47**(7), 887–898. 133

Gibson, J. J. (1950), 'The perception of the visual world.', *Psychological Bulletin* **48**(4), 1–259. 8, 47, 132

Golomb, J. D., Chun, M. M. & Mazer, J. A. (2008), 'The native coordinate system of spatial attention is retinotopic.', *The Journal of neuroscience* **28**(42), 10654–62. 137

Golomb, J. D. & Kanwisher, N. (2012), 'Higher level visual cortex represents retinotopic, not spatiotopic, object location.', *Cerebral cortex* **22**(12), 2794–810. 101

Goodale, M. A. & Milner, A. D. (1992), 'Separate visual pathways for perception and action', *Trends Neurosci.* **15**(1), 20–50. 6

Gordon, G. R. J., Choi, H. B., Rungta, R. L., Ellis-Davies, G. C. R. & MacVicar, B. A. (2008), 'Brain metabolism dictates the polarity of astrocyte control over arterioles', *Nature* **456**(7223), 745–749. 28

Granit, R. (1928), 'On inhibition in the after-effect of seen movement', *British Journal of Psychology* **19**(2), 147–157. 83, 87, 136

Graziano, M. S. A., Andersen, R. A. & Snowden, R. J. (1994), 'Tuning of MST Neurons to Spiral Motions', *The Journal of Neuroscience* **14**(l), 54–67. 8

Green, D. M. (1960), 'Psychoacoustics and Detection Theory', *The Journal of the Acoustical Society of America* **32**(10), 1189–1203. 57

Green, D. M. & Swets, J. A. (1966), *Signal detection theory and psychophysics*, 1st edn, John Wiley & Sons, New York, NY. 9

Grill-Spector, K., Henson, R. & Martin, A. (2006), 'Repetition and the brain: neural models of stimulus-specific effects', *Trends in cognitive sciences* **10**(1), 14–23. 140

Grill-Spector, K. & Malach, R. (2001), 'fMR-adaptation: a tool for studying the functional properties of human cortical neurons', *Acta Psychol (Amst)* **107**(1-3), 293–321. 141

Guilford, J. P. (1954), *Psychometric methods*, McGraw-Hill series in psychology, McGraw-Hill. 36

Haag, J., Denk, W. & Borst, A. (2004), 'Fly motion vision is based on Reichardt detectors regardless of the signal-to-noise ratio', *Proceedings of the National Academy of Sciences of the United States of America* **101**(46), 16333–16338. 12

Hammond, P. & Mouat, G. S. (1988), 'Neural correlates of motion after-effects in cat striate cortical neurones: interocular transfer', *Exp Brain Res* **72**(1), 21–28. 20

Hassenstein, B. & Reichardt, W. (1959), 'Systemtheoretische analyse der zeit-, reihenfolgen-und vorzeichenauswertung bei der bewegungsperzeption des rüsselkäfers chlorophanus.', *Zeitschrift für Naturforschung* **11b**, 513–524. 12

Hautzel, H., Taylor, J. G., Krause, B. J., Schmitz, N., Tellmann, L., Ziemons, K., Shah, N. J., Herzog, H. & Mueller Gaertner, H. W. (2001), 'The motion aftereffect: More than area V5/MT? Evidence from 15O-butanol PET studies', *Brain Research* **892**(2), 281–292. 20

He, S., Cohen, E. R. & Hu, X. (1998), 'Close correlation between activity in brain area MT/V5 and the perception of a visual motion aftereffect', *Curr Biol* **8**(22), 1215–1218. 30

Heeger, D. J., Boynton, G. M., Demb, J. B., Seidemann, E. & Newsome, W. T. (1999), 'Motion opponency in visual cortex', *J Neurosci* **19**(16), 7162–7174. 29, 104, 140, 141

Heeger, D. J., Huk, A. C., Geisler, W. S. & Albrecht, D. G. (2000), 'Spikes versus BOLD: what does neuroimaging tell us about neuronal activity?', *Nature Neuroscience* **3**(7), 631–633. 28

Heeger, D. J. & Ress, D. (2002), 'What does fMRI tell us about neuronal activity?', *Nature Reviews Neuroscience* **3**(February), 142–151. 26, 27

Hershenson, M. (1989), 'Duration, time constant, and decay of the linear motion aftereffect as a function of inspection duration', *Perception & Psychophysics* **45**(3), 251–257. 68

Hirahara, M. (2006), 'Reduction in the motion coherence threshold for the same direction as that perceived during adaptation.', *Vision research* **46**(28), 4623–33. 57, 135

Hiris, E. & Blake, R. (1992), 'Another perspective on the visual motion aftereffect.', *Proceedings of the National Academy of Sciences of the United States of America* **89**(19), 9025–9028. 20, 35, 47, 54

Hornof, A. J. & Halverson, T. (2002), 'Cleaning up systematic error in eye-tracking data by using required fixation locations', *Behavior Research Methods, Instruments, & Computers* **34**(4), 592–604. 97

How, M. J. & Zanker, J. M. (2014), 'Motion camouflage induced by zebra stripes', *Zoology* **117**(3), 163–170. 12

Huebel, D. H. & Wiesel, T. N. (1959), 'Receptive fields of single neurones in the cat's striate cortex', *Journal of Physiology* **148**(1), 574–591. 5

Huebel, D. H. & Wiesel, T. N. (1962), 'Binocular Interaction and Functional Architecture in the Cat's Visual Cortex', *Journal of Physiology* **160**(1), 106–154. 5

Huk, A. C., Dougherty, R. F. & Heeger, D. J. (2002), 'Retinotopy and Functional Subdivision of Human Areas MT and MST', *J. Neurosci.* **22**(16), 7195–7205. 29, 43, 105, 116, 117, 122, 131

Huk, A. C. & Heeger, D. J. (2000), 'Task-related modulation of visual cortex.', *Journal of neurophysiology* **83**(6), 3525–36. 141

Huk, A. C. & Heeger, D. J. (2002), 'Pattern-motion responses in human visual cortex.', *Nature neuroscience* **5**(1), 72–5. 123

Huk, A. C., Ress, D. & Heeger, D. J. (2001), 'Neuronal basis of the motion aftereffect reconsidered', *Neuron* **32**(1), 161–172. 21, 30, 142

Jackman, S. L., Babai, N., Chambers, J. J., Thoreson, W. B. & Kramer, R. H. (2011), 'A Positive Feedback Synapse from Retinal Horizontal Cells to Cone Photoreceptors', *PLoS Biology* **9**(5), e1001057. 4

Jacob, S. N. & Nieder, A. (2009), 'Tuning to non-symbolic proportions in the human frontoparietal cortex', *European Journal of Neuroscience* **30**(7), 1432–1442. 25, 86

Jacob, S. N., Vallentin, D. & Nieder, A. (2012), 'Relating magnitudes: the brain's code for proportions', *Trends in cognitive sciences* **16**(3), 157–166. 25

Jevons, S. W. (1871), 'The power of numerical discrimination', *Nature* **3**, 363–372. 24, 59, 65

Johnson, C. A. & Scobey, R. P. (1980), 'Foveal and peripheral displacement thresholds as a function of stimulus luminance, line length and duration of movement.', *Vision research* **20**(8), 709–15. 16

Johnston, A., Mcowan, P. W. & Buxton, H. (1992), 'A Computational Model of the Analysis of Some First-Order and Second-Order Motion Patterns by Simple and Complex Cells', *Proceedings of the Royal Society of London B: Biological Sciences* **250**(1329), 297–306. 14

Julesz, B. (1971), *Foundations of cyclopean perception.*, U. Chicago Press, Oxford, England. 34

Kastner, S., Pinsk, M. A., De Weerd, P., Desimone, R. & Ungerleider, L. G. (1999), 'Increased activity in human visual cortex during directed attention in the absence of visual stimulation.', *Neuron* **22**(4), 751–61. 142

Kim, S.-G. & Ogawa, S. (2012), 'Biophysical and physiological origins of blood oxygenation level-dependent fMRI signals.', *Journal of cerebral blood flow and metabolism* pp. 1–19. 26

Kingdom, F. A. A. & Prins, N. (2010), *Psychophysics: A Practical Introduction*, Academic Press: An imprint of Elsevier. 38

Knapen, T., Rolfs, M. & Cavanagh, P. (2009), 'The reference frame of the motion aftereffect is retinotopic.', *Journal of vision* **9**(5), 16.1–7. 89, 98, 99, 100, 101, 137, 139

Kolster, H., Peeters, R. & Orban, G. a. (2010), 'The Retinotopic Organization of the Human Middle Temporal Area MT/V5 and Its Cortical Neighbors.', *The Journal of neuroscience* **30**(29), 9801–20. 131

Krekelberg, B., Boynton, G. M. & van Wezel, R. J. (2006), 'Adaptation: from single cells to BOLD signals', *Trends Neurosci* **29**(5), 250–256. 140, 141

Kwong, K. K. (1995), 'Functional magnetic resonance imaging with echo planar imaging.', *Magnetic resonance quarterly* **11**(1), 1–20. 26

Kwong, K. K., Belliveau, J. W., Chesler, D. A., Goldberg, I. E., Weisskoff, R. M., Poncelet, B. P., Kennedy, D. N., Hoppel, B. E., Cohen, M. S. & Turner, R. (1992), 'Dynamic magnetic resonance imaging of human brain activity during primary sensory stimulation.', *Proceedings of the National Academy of Sciences of the United States of America* **89**(12), 5675–5679. 26

Lankheet, M. J. & Verstraten, F. A. (1995), 'Attentional modulation of adaptation to two-component transparent motion.', *Vision research* **35**(10), 1401–12. 76, 82, 87, 136

Larsson, J. & Heeger, D. J. (2006), 'Two Retinotopic Visual Areas in Human Lateral Occipital Cortex', *Journal of Neuroscience* **26**(51). 111, 123

Lauritzen, M. (2005), 'Reading vascular changes in brain imaging: is dendritic calcium the key?', *Nature reviews. Neuroscience* **6**(1), 77–85. 28

Lavie, N. (1995), 'Perceptual load as a necessary condition for selective attention', *J Exp Psychol Hum Percept Perform* **21**(3), 451–468. 24

Levick, W. R., Oyster, C. W. & Takahashi, E. (1969), 'Rabbit lateral geniulate nucelus: sharpener of irectional information', *Science* **165**, 712–714. 12

Levinson, E. & Sekuler, R. (1976), 'Adaptation alters perceived direction of motion.', *Vision research* **16**(7), 779–81. 54

Lewis, C. F. & McBeath, M. K. (2004), 'Bias to Experience Approaching Motion in a Three-Dimensional Virtual Environment', *Perception* **33**(3), 259–276. 133, 134, 137

Livingstone, M. & Hubel, D. (1988), 'Segregation of Form, Color, Movement, and Depth: Anatomy, Physiology, and Perception', *Science* **240**(4853), 740–749. 6

Logothetis, N. K. (2003), 'The Underpinnings of the BOLD Functional Magnetic Resonance Imaging Signal', *The Journal of Neuroscience* **23**(10), 3963–3971. 28

Logothetis, N. K., Pauls, J., Augath, M., Trinath, T. & Oeltermann, A. (2001), 'Neurophysiological investigation of the basis of the fMRI signal', *Nature* **412**(6843), 150–157. 26, 27, 28

Lu, Z. L. & Sperling, G. (1995), 'The functional architecture of human visual motion perception.', *Vision research* **35**(19), 2697–722. 45

Mather, G. (1980), 'The movement aftereffect and a distribution-shift model for coding the direction of visual movement', *Perception* **9**(4), 379–392. 19, 23, 54

Mather, G. & Moulden, B. (1980), 'A simultaneous shift in apparent direction: further evidence for a "distribution-shift" model of direction coding', *Q J Exp Psychol* **32**(2), 325–333. 19

Mather, G., Verstraten, F. & Anstis, S. M. (1998), *The motion aftereffect : a modern perspective*, MIT Press. 87

Maunsell, J. H. R. & Van Essen, D. C. (1983*a*), 'Functional properties of neurons in middle temporal visual area of the macaque monkey . I . Selectivity for stimulus direction , speed , and orientation', *Journal of neurophysiology* **49**(5), 1127–1147. 8

Maunsell, J. H. & Van Essen, D. C. (1983*b*), 'Functional properties of neurons in middle temporal visual area of the macaque monkey . II . Binocular interactions and sensitivity to binocular disparity', *Journal of neurophysiology* **49**(5), 1148–1167. 47, 138

McKeefry, D. (2001), 'Motion adaptation in chromatic motion-onset visual evoked potentials', *Documenta Ophthalmologica* **103**(3), 229–251. 17

McKeefry, D. J., Laviers, E. G. & McGraw, P. V. (2006), 'The segregation and integration of colour in motion processing revealed by motion after-effects.', *Proceedings of the Royal Society, Biological sciences* **273**(1582), 91–9. 17

Mineault, P. J., Khawaja, F. A., Butts, D. A. & Pack, C. C. (2012), 'Hierarchical processing of complex motion along the primate dorsal visual pathway.', *Proceedings of the National Academy of Sciences of the United States of America* **109**(16), E972–80. 7

Moran, J. & Desimone, R. (1985), 'Selective attention gates visual processing in the extrastriate cortex', *Science* **229**, 781–784. 24

Morgan, M., Chubb, C. & Solomon, J. A. (2006), 'Predicting the motion after-effect from sensitivity loss', *Vision Research* **46**(15), 2412–2420. 9, 21, 22, 58, 74, 84, 135

Morgan, M., Dillenburger, B., Raphael, S. & Solomon, J. (2012), 'Observers can voluntarily shift their psychometric functions without losing sensitivity.', *Attention, perception and psychophysics* **74**, 185–193. 11, 21, 83

Morgan, M. J. (2011), 'Wohlgemuth was right: Distracting attention from the adapting stimulus does not decrease the motion after-effect', *Vision research* **51**(20), 2169–2175. 24, 46, 75, 82, 136

Morgan, M. J. (2012), 'Motion adaptation does not depend on attention to the adaptor', *Vision Research* **55**, 47–51. 46, 51

Morgan, M. J. & Chubb, C. (1999), 'Contrast facilitation in motion detection: evidence for a Reichardt detector in human vision.', *Vision research* **39**(25), 4217–31. 15

Morgan, M. J., Chubb, C. & Solomon, J. A. (2008), 'A 'dipper' function for texture discrimination based on orientation variance.', *Journal of vision* **8**(11), 9.1–8. 58, 66

Morgan, M. J., Chubb, C. & Solomon, J. A. (2011), 'Evidence for a subtractive component in motion adaptation', *Vision Research* **51**, 2312–2316. 9, 22, 58, 84, 135

Morgan, M. J., Hauperich, A. & Solomon, J. A. (2017), 'Adaptation can overcome change blindness', *Manuscript in preperation* . 87, 136, 138

Morgan, M. J., Melmoth, D. & Solomon, J. A. (2013), 'Linking hypotheses underlying Class A and Class B methods.', *Visual neuroscience* **30**(5-6), 197–206. 21, 22

Morgan, M. J., Raphael, S., Tibber, M. S. & Dakin, S. C. (2014), 'A texture-processing model of the 'visual sense of number'', *Proceedings of the Royal Society B: Biological Sciences* **281**(1790), 20141137–20141137. 24

Morgan, M. J. & Ward, R. (1980), 'Interocular Delay Produces Depth in Subjectively Moving Noise Patterns', *Quarterly Journal of Experimental Psychology* **32**(3), 387–395. 35

Morrone, M. C., Burr, D. C. & Vaina, L. M. (1995), 'Two stages of visual processing for radial and circular motion', *Nature* **376**, 507–509. 68

Motter, B. C. (1993), 'Focal attention produces spatially selective processing in visual cortical areas V1, V2, and V4 in the presence of competing stimuli.', *Journal of neurophysiology* **70**(3), 909–19. 24

Movshon, J., Adelson, E. H., Gizzi, M. S. & Newsome, W. T. (1985), The analysis of moving images, *in* 'Pattern recognition mechanisms', ontificiae edn, Vatican Press, Rome, pp. 117–151. 7

Mullen, K. T. & Baker, C. L. J. (1985), 'A motion aftereffect from an isoluminant stimulus', *Vision Research* **25**(5), 685–688. 17

Mulligan, S. J. & MacVicar, B. A. (2004), 'Calcium transients in astrocyte endfeet cause cerebrovascular constrictions', *Nature* **431**(7005), 195–199. 28

Newsome, W. T., Britten, K. H. & Movshon, J. A. (1989), 'Neuronal correlates of a perceptual decision', *Nature* **341**(6237), 52–54. 35

Nieder, A. (2005), 'Counting on neurons: the neurobiology of numerical competence', *Nature Reviews Neuroscience* **6**(3), 177–190. 25

Nieder, A. & Dehaene, S. (2009), 'Representation of Number in the Brain', *Annual review of neuroscience* **32**, 185–208. 25

Nieder, A., Freedman, D. J. & Miller, E. K. (2002), 'Representation of the Quantity of Visual Items in the Primate Prefrontal Cortex', *Science* **297**(5587), 1708–1711. 24

Nikolova, N. & Morgan, M. J. (2013*a*), Changes resulting from adaptation to radial motion., *in* 'British Neuroscience Assiciation Abstracts', p. 664. 142

Nikolova, N. & Morgan, M. J. (2013*b*), Discrimination functions for radial motion and orientation., *in* 'Perception (S)', p. 184. 142

Nikolova, N. & Morgan, M. J. (2013*c*), Mechanisms for discrimination following adaptation to radial motion., *in* 'Neuroscience Meeting Planner', p. 458. 142

Nikolova, N. & Raphael, S. (2012), The reference frame of the motion aftereffect examined using velocity adjustments., *in* 'Perception (S)', p. 180. 142

Nishida, S. & Ashida, H. (2000), 'A hierarchical structure of motion system revealed by interocular transfer of flicker motion aftereffects', *Vision Research* **40**(3), 265–278. 46

Nishida, S., Ashida, H. & Sato, T. (1994), 'Complete interocular transfer of motion aftereffect with flickering test', *Vision Research* **34**(20), 2707–2716. 20

Nishida, S., Motoyoshi, I., Andersen, R. A. & Shimojo, S. (2003), 'Gaze modulation of visual aftereffects.', *Vision research* **43**(6), 639–49. 89, 100

Nishimoto, S., Huth, A. G., Bilenko, N. Y., Gallant, J. L., Feinberg, D., Adriany, G. & Yacoub, E. (2017), 'Eye movement-invariant representations in the human visual system', *Journal of Vision* **17**(1), 11. 101

Noory, B., Herzog, M. H. & Ogmen, H. (2015), 'Spatial properties of non-retinotopic reference frames in human vision', *Vision Research* **113**, 44–54. 137

Norman, K. A., Polyn, S. M., Detre, G. J. & Haxby, J. V. (2006), 'Beyond mind-reading: multi-voxel pattern analysis of fMRI data', *Trends in Cognitive Sciences* **10**(9), 424–430. 139

O'Craven, K. M., Rosen, B. R., Kwong, K. K., Treisman, A. & Savoy, R. L. (1997), 'Voluntary attention modulates fMRI activity in human MT-MST', *Neuron* **18**(4), 591–598. 29, 141

Ogawa, S., Lee, T. M., Kay, A. R. & Tank, D. W. (1990), 'Brain magnetic resonance imaging with contrast dependent on blood oxygenation.', *Proceedings of the National Academy of Sciences of the United States of America* **87**(24), 9868–9872. 26

Ogawa, S., Menon, R. S., Kim, S.-G. & Ugurbil, K. (1998), 'On the characteristics of functional magnetic resonance imaging of the brain', *Annu. Rev. Biophys. Biomol. Struct* **27**, 447–474. 26

Ogawa, S., Tank, D. W., Menon, R., Ellermann, J. M., Kim, S. G., Merkle, H. & Ugurbil, K. (1992), 'Intrinsic signal changes accompanying sensory stimulation: Functional brain mapping with magnetic resonance imaging', *Proceedings of the National Academy of Sciences of the United States of America* **89**(13), 5951–5955. 27

Oostende, S. V., Sunaert, S., Hecke, P. V., Marchal, G. & Orban, G. A. (1997), 'The Kinetic Occipital (KO) Region in Man : An fMRI Study', *Cerebral Cortex* **7**, 690–701. 29

Orban, G. A., Lagae, L., Verri, A., Raiguel, S., Xiao, D., Maes, H. & Torre, V. (1992), 'First-order analysis of optical flow in monkey brain.', *Proceedings of the National Academy of Sciences of the United States of America* **89**(7), 2595–9. 7, 8, 104

Paradiso, M. A., Meshi, D., Pisarcik, J. & Levine, S. (2012), 'Eye movements reset visual perception.', *Journal of vision* **12**(13), 11. 138

Pelli, D. G. (1997), 'The Video Toolbox software for visual psychophysics: Transforming numbers into movies'. 34, 48, 77

Peppiatt, C. & Attwell, D. (2004), 'Neurobiology: feeding the brain.', *Nature* **431**(7005), 137–138. 28

Perrone, J. A. (1986), 'Anisotropic responses to motion toward and away from the eye', *Perception & Psychophysics* **39**(1), 1–8. 133, 134, 137

Peterson, W. W., Birdsall, T. G. & Fox, W. C. (1954), 'The theory of signal detectability.', *Proceedings of the IRE Professional Group on Information Theory* **4**, 171–212. 9

Prins, N. & Kingdom, F. A. A. (2009), 'Palamedes: Matlab routines for analyzing psychophysical data'. 38

Ptito, M., Kupers, R., Faubert, J. & Gjedde, A. (2001), 'Cortical Representation of Inward and Outward Radial Motion in Man', *NeuroImage* **14**(6), 1409–15. 133, 137

Qian, N., Andersen, R. A. & Adelson, E. (1994), 'Transparent Motion Perception as Detection of Unbalanced Motion', *Physiology* **14**, 7367–7380. 15

Raichle, M. E. & Mintun, M. A. (2006), 'Brain Work and Brain Imaging', *Annual Reviews in Neuroscience* **29**(1), 449–476. 27

Raidvee, A., Averin, K. & Allik, J. (2012), 'Visibility versus accountability in pooling local motion signals into global motion direction', *Attention, Perception, & Psychophysics* **74**(6), 1252–1259. 66

Raidvee, A., Averin, K., Kreegipuu, K. & Allik, J. (2011), 'Pooling elementary motion signals into perception of global motion direction', *Vision Research* **51**(17), 1949–1957. 66, 85

Raphael, S. & Morgan, M. J. (2016), 'The computation of relative numerosity, size and density', *Vision Research* **124**(June), 15–23. 65

Raphael, S., Morgan, M. J. & Dillenburger, B. C. (2010), The effect of attentional modulation on adaptation to transparent expanding/contracting motion, *in* 'Society for Neuroscience Meeting Planner', number 12, p. 17. 23, 76, 82, 90, 136

Raymond, J. (1993), 'Complete interocular transfer of motion adaptation effects on motion coherence thresholds', *Vision Research* **33**(13), 1865–1870. 54

Raymond, J. E. & Braddick, O. (1996), 'Responses to Opposed Directions of Motion:', *Vision Research* **36**(13), 1931–1937. 54

Read, H. L. & Siegel, R. M. (1997), 'Modulation of responses to optic flow in area 7a by retinotopic and oculomotor cues in monkey.', *Cerebral cortex* **7**(7), 647–61. 8

Rees, G., Friston, K. & Koch, C. (2000), 'A direct quantitative relationship between the functional properties of human and macaque V5.', *Nature Neuroscience* **3**(7), 716–723. 28, 59, 104

Rees, G., Frith, C. D. & Lavie, N. (1997), 'Modulating irrelevant motion perception by varying attentional load in an unrelated task', *Science* **278**(5343), 1616–1619. 46, 75

Rees, G., Frith, C. & Lavie, N. (2001), 'Processing of irrelevant visual motion during performance of an auditory attention task', *Neuropsychologia* **39**(9), 937–949. 24

Reichardt, W. (1961), *Sensory Communication*, ed. rosenb edn, MIT Press/Wiley, New York. 12

Rezec, A., Krekelberg, B. & Dobkins, K. R. (2004), 'Attention enhances adaptability: evidence from motion adaptation experiments', *Vision Res* **44**(26), 3035–3044. 46, 75, 82, 136

Ross, J. (2003), 'Visual discrimination of number without counting.', *Perception* **32**(7), 867–70. 59

Ross, J. & Burr, D. C. (2010), 'Vision senses number directly.', *Journal of vision* **10**(2), 10.1–8. 64, 136

Ross, J. & Ma-Wyatt, A. (2004), 'Saccades actively maintain perceptual continuity', *Nature Neuroscience* **7**(1), 65–69. 139

Ross, J. & Speed, H. D. (1991), 'Contrast adaptation and contrast masking in human vision', *Proceedings of the Royal Society of London B: Biological Sciences* **246**, 61–69. 58

Ross, J., Speed, H. D. & Morgan, M. J. (1993), 'The effects of adaptation and masking on incremental thresholds for contrast', *Vision Res* **33**(15), 2051–2056. 58, 84

Ruff, C. C., Blankenburg, F., Bjoertomt, O., Bestmann, S., Freeman, E., Haynes, J.-D., Rees, G., Josephs, O., Deichmann, R. & Driver, J. (2006), 'Concurrent TMS-fMRI and Psychophysics Reveal Frontal Influences on Human Retinotopic Visual Cortex', *Current Biology* **16**(15), 1479–1488. 6

Saito, H.-A., Yukie, M., Tanaka, K., Hikosaka, K., Fukada, Y., Lwai, E. & Iwai, E. (1986), 'Integration of Direction Signals of Image Motion in the Superior Temporal Sulcus of the Macaque Monkey', *Journal of Neuroscience* **6**(1), 145–157. 8, 104, 105, 132, 137

Saxe, R., Brett, M. & Kanwisher, N. (2006), 'Divide and conquer: A defense of functional localizers', *NeuroImage* **30**(4), 1088–1096. 131

Schaafsma, S. J., Duysens, J. & Gielen, C. C. (1997), 'Responses in ventral intraparietal area of awake macaque monkey to optic flow patterns corresponding to rotation of planes in depth can be explained by translation and expansion effects.', *Visual neuroscience* **14**(4), 633–46. 8

Sekuler, R. & Pantle, A. (1967), 'A model for after-effects of seen movement', *Vision Research* **7**(5), 427–439. 22

Sekuler, R. W. & Ganz, L. (1963), 'Aftereffect of seen motion with a stabilized retinal image', *Science* **139**(3553), 419–420. 22

Sereno, M. I. (1998), 'Brain mapping in animals and humans', *Current opinion in neurobiology* **8**(2), 188–194. 29

Sereno, M. I., Dale, A. M., Reppas, J. B., Kwong, K. K., Belliveau, J. W., Brady, T. J., Rosen, B. R. & Tootell, R. B. (1995), 'Borders of multiple visual areas in humans revealed by functional magnetic resonance imaging', *Science* **268**(5212), 889–893. 29, 44, 110, 117, 123, 129

Shirai, N., Birtles, D., Wattam-Bell, J., Yamaguchi, M. K., Kanazawa, S., Atkinson, J. & Braddick, O. (2009), 'Asymmetrical cortical processing of radial expansion/contraction in infants and adults', *Developmental Science* **12**(6), 946–955. 105, 133, 137

Shirai, N., Imura, T., Hattori, Y., Adachi, I., Ichihara, S., Kanazawa, S., Yamaguchi, M. K., Tomonaga, M., Tomoko, I., Hattori, Y., Ikuma, A., Ichihara, S., So, K., Yamaguchi, M. K. & Tomonaga, M. (2009), 'Asymmetric perception of radial expansion/contraction in Japanese macaque (Macaca fuscata) infants', *Experimental Brain Research* **202**(2002), 319–325. 133

Shirai, N., Kanazawa, S. & Yamaguchi, M. K. (2006), 'Anisotropic motion coherence sensitivities to expansion/contraction motion in early infancy', *Infant Behavior and Development* **29**(2), 204–209. 133, 134

Shirai, N. & Yamaguchi, M. K. (2004), 'Asymmetry in the perception of motion-in-depth', *Vision Research* **44**(10), 1003–1011. 133, 134

Singh, K. D., Smith, A. T. & Greenlee, M. W. (2000), 'Spatiotemporal Frequency and Direction Sensitivities of Human Visual Areas Measured Using fMRI', *NeuroImage* **12**, 550–564. 141

Sinha, D. (1952), 'An experimental study of a social factor in perception: The influence of an arbitrary group standard', *Patna University Journal* **7**(7), 16. 46, 51, 75, 82, 87, 136

Smith, A. T., Greenlee, M. W., Singh, K. D., Kraemer, F. M. & Hennig, J. (1998), 'The processing of first- and second-order motion in human visual cortex assessed by functional magnetic resonance imaging (fMRI).', *The Journal of neuroscience* **18**(10), 3816–30. 105

Smith, A. T. & Hammond, P. (1985), 'The pattern specificity of velocity aftereffects', *Experimental Brain Research* **60**(1), 71–78. 90

Smith, A. T., Wall, M. B., Williams, A. L. & Singh, K. D. (2006), 'Sensitivity to optic flow in human cortical areas MT and MST', *Eur. J. Neurosci* **23**(2), 561–569. 43, 47, 105

Smith, S. M., Jenkinson, M., Woolrich, M. W., Beckmann, C. F., Behrens, T. E. J., Johansen-Berg, H., Bannister, P. R., De Luca, M., Drobnjak, I., Flitney, D. E., Niazy, R. K., Saunders, J., Vickers, J., Zhang, Y., De Stefano, N., Brady, J. M. & Matthews, P. M. (2004), 'Advances in functional and structural MR image analysis and implementation as FSL', *NeuroImage* **23, Supple**, S208 – S219. 40

Snowden, R. J. & Milne, a. B. (1997), 'Phantom motion after effects–evidence of detectors for the analysis of optic flow.', *Current biology* **7**(10), 717–22. 89, 104

Snowden, R. J., Treue, S., Erickson, R. G., Andersen, R. A., Robertson, G., Goddard, J., Keough, R. & Marchetti, S. (1991), 'The response of area MT and V1 neurons to transparent motion', *The Journal of neuroscience* **11**(9), 2768–85. 19

Solomon, J. A. (2009), 'The History of Dipper Functions', *Attention, Perception, & Psychophysics* **71**(3), 435–443. 57, 66

Solomon, J. A., Chubb, C., John, A. & Morgan, M. (2005), 'Stimulus contrast and the Reichardt detector.', *Vision research* **45**(16), 2109–17. 16

Solomon, J. & Morgan, M. (2017), 'Numerosity as a summary statistic', *Manuscript submitted for publication* . 65

Somers, D. C., Dale, A. M., Seiffert, A. E. & Tootell, R. B. H. (1999), 'Functional MRI reveals spatially specific attentional modulation in human primary visual cortex', *Proceedings of the National Academy of Sciences USA* **96**(4), 1663–1668. 29

Spitz, H. H. (1966), 'Differential Effects of Central and Lateral Fixation on After-Effects of Expansion and', *The American Journal of Psychology* **79**(4), 618–622. 51, 57

Stoppel, C. M., Boehler, C. N., Strumpf, H., Heinze, H.-J., Noesselt, T., Hopf, J.-M. & Schoenfeld, M. A. (2011), 'Feature-based attention modulates direction-selective hemodynamic activity within human MT.', *Human brain mapping* **32**(12), 2183–92. 24

Strettoi, E., Novelli, E., Mazzoni, F., Barone, I. & Damiani, D. (2010), 'Complexity of retinal cone bipolar cells', *Progress in Retinal and Eye Research* **29**(4), 272–283. 2

Strong, S. L., Silson, E. H., Gouws, A. D., Morland, A. B. & McKeefry, D. J. (2017), 'Differential processing of the direction and focus of expansion of optic flow stimuli in areas MST and V3A of the human visual cortex', *Journal of Neurophysiology* **117**(6), 2209–2217. 8, 105, 131

Sunaert, S., Van Hecke, P., Marchal, G. & Orban, G. a. (1999), 'Motion-responsive regions of the human brain.', *Experimental brain research* **127**(4), 355–370. 29

Takeuchi, T. (1997), 'Visual search of expansion and contraction', *Vision Research* **37**(15), 2083–2090. 133, 134, 137

Tanaka, K., Fukada, Y. & Saito, H.-A. (1989), 'Underlying mechanisms of the response specificity of expansion/contraction and rotation cells in the dorsal part of the medial superior temporal area of the macaque monkey', *J Neurophysiol* **62**(3), 642–656. 8

Tanaka, K. & Saito, H.-A. (1989), 'Analysis of Motion of the Visual Field by Direction, Expansion/Contraction, and Rotation Cells Clustered in the Dorsal Part of the Medial Superior Temporal Area of the Macaque Monkey', *Journal of Neurophysiology* **62**(3), 626–641. 104, 105, 132, 137

Taya, S., Adams, W., Graf, E. & Lavie, N. (2009), 'The fate of task-irrelevant visual motion: perceptual load versus feature-based attention.', *Journal of Vision* **9**(12), 1–10. 46, 75, 82, 83, 136

Taylor, J. G., Schmitz, N., Ziemons, K., Grosse-Ruyken, M.-L. L., Gruber, O., Mueller-Gaertner, H.-W. W. & Shah, N. J. (2000), 'The network of brain areas involved in the motion aftereffect', *Neuroimage* **11**(4), 257–270. 20, 30

Taylor, M. M. (1963), 'Tracking the Decay of the After-Effect of Seen Rotary Movement', *Perceptual and Motor Skills* **16**(1), 119–129. 68

Taylor, W. R. & Smith, R. G. (2012), 'The role of starburst amacrine cells in visual signal processing.', *Visual neuroscience* **29**(1), 73–81. 3

Thompson, B., Deblieck, C., Wu, A., Iacoboni, M. & Liu, Z. (2016), 'Psychophysical and rTMS Evidence for the Presence of Motion Opponency in Human V5', *Brain Stimulation* **9**(6), 876–881. 141

Thompson, P. (1981), 'Velocity after-effects: The effects of adaptation to moving stimuli on the perception of subsequently seen moving stimuli', *Vision Research* **21**(3), 337–345. 90

Thomsen, K., Offenhauser, N. & Lauritzen, M. (2004), 'Principal neuron spiking: neither necessary nor sufficient for cerebral blood flow in rat cerebellum', *Journal of Physiology* **5601**, 181–189. 28

Thurstone, L. L. (1927), 'A law of comparative judgment.', *Psychological Review* **34**(4), 273–286. 85

Tokita, M. & Ishiguchi, A. (2009), 'Effects of feature types on proportion discrimination', *Japanese Psychological Research* **51**(2), 57–68. 66

Tolhurst, D. J., Tadmor, Y. & Chao, T. (1992), 'Amplitude spectra of natural images.', *Ophthalmic & physiological optics* **12**(2), 229–32. 33

Tootell, R. B., Dale, A. M., Sereno, M. I. & Malach, R. (1996), 'New images from human visual cortex', *Trends in Neurosciences* **19**, 481–489. 29

Tootell, R. B. H., Mendola, J. D., Hadjikhani, N. K., Ledden, P. J., Liu, A. K., Reppas, J. B., Sereno, M. I. & Dale, A. M. (1997), 'Functional Analysis of V3A and Related Areas in Human Visual Cortex', *Journal of Neuroscience* **17**(18), 7060–7078. 29

Tootell, R. B. H., Reppas, J. B., Dale, A. M., Look, R. B., Sereno, M. I., Malach, R., Brady, T. J. & Rosen, B. R. (1995), 'Visual motion aftereffect in human cortical area MT revealed by functional magnetic resonance imaging', *Nature* **375**(6527), 139–141. 30

Tootell, R. B. H., Reppas, J. B., Kwong, K. K., Malach, R., Born, R. T., Brady, T. J., Rosen, B. R. & Belliveau, J. W. (1995), 'Functional analysis of human MT and related visual cortical areas using magnetic resonance imaging', *Journal of Neuroscience* **15**(4), 3215–3230. 43, 105, 123

Tootell, R. B. H. & Taylor, J. B. (1995), 'Anatomical Evidence for MT and Additional Cortical Visual Areas in Humans', *Cerebral Cortex* **5**(1), 39–55. 29, 105

Treue, S. & Martínez Trujillo, J. C. (1999), 'Feature-based attention influences motion processing gain in macaque visual cortex.', *Nature* **399**(6736), 575–9. 24

Treue, S. & Maunsell, J. H. (1999), 'Effects of attention on the processing of motion in macaque middle temporal and medial superior temporal visual cortical areas.', *The Journal of neuroscience* **19**(17), 7591–602. 24

Turi, M. & Burr, D. (2012), 'Spatiotopic perceptual maps in humans: evidence from motion adaptation.', *Proceedings. Biological sciences / The Royal Society* **279**(1740), 3091–7. 101

Turner, R., Le Bihan, D., Moonen, C. T. W., Despres, D. & Frank, J. (1991), 'Echo-planar time course of MRI of cat brain deoxygenation changes', *Magnetic Resonance in Medicine* **22**, 159–166. 27

Van Essen, D. C., Lewis, J. W., Drury, H. A., Hadjikhani, N. A., Tootell, R. L. B. H., Bakircioglu, M. & Miller, M. I. (2001), 'Mapping Visual Cortex in Monkeys and Humans Using Surface-based Atlases', *Vision Research* **41**, 1359–1378. 29, 116

Van Essen, D. C., Newsome, W. T. & Maunsell, J. H. (1984), 'The visual field representation in striate cortex of the macaque monkey: asymmetries, anisotropies, and individual variability.', *Vision research* **24**(5), 429–48. 16

van Santen, J. P. H. & Sperling, G. (1985), 'Elaborated Reichardt detectors', *Journal of the Optical Society of America A* **2**(2), 300. 15, 16

Vautin, R. G. & Berkley, M. A. (1977), 'Responses of single cells in cat visual cortex to prolonged stimulus movement: neural correlates of visual aftereffects', *J Neurophysiol* **40**(5), 1051–1065. 20

Verstraten, F. A., Fredericksen, R. E. & Van De Grind, W. A. (1994), 'Movement aftereffect of bi-vectorial transparent motion.', *Vision research* **34**(3), 349–58. 54

Verstraten, F. A., van der Smagt, M. J., Fredericksen, R. E. & van de Grind, W. A. (1999), 'Integration after adaptation to transparent motion: static and dynamic test patterns result in different aftereffect directions', *Vision Res* **39**(4), 803–810. 20, 22

Vetter, P., Butterworth, B. & Bahrami, B. (2008*a*), 'Modulating Attentional Load Affects Numerosity Estimation: Evidence against a Pre-Attentive Subitizing Mechanism', *PLoS ONE* **3**(9), e3269. 25

Vetter, P., Butterworth, B. & Bahrami, B. (2008*b*), 'Modulating Attentional Load Affects Numerosity Estimation: Evidence against a Pre-Attentive Subitizing Mechanism', *PLoS ONE* **3**(9), 3269. 65

von Grunau, M. W. (2002), 'Bivectorial transparent stimuli simultaneously adapt mechanisms at different levels of the motion pathway', *Vision Res* **42**(5), 577–587. 89

Wade, N. J. (1994), 'A selective history of the study of visual motion aftereffects.', *Perception* **23**(10), 1111–34. 87

Wall, M. B., Lingnau, A., Ashida, H. & Smith, A. T. (2008), 'Selective visual responses to expansion and rotation in the human MT complex revealed by functional magnetic resonance imaging adaptation', *The European journal of neuroscience* **27**(10), 2747–2757. 24, 47, 105, 140

Wandell, B. A. (1999), 'Computational neuroimaging of human visual cortex', *Annual review of neuroscience* **22**, 145–73. 29

Wandell, B. a., Dumoulin, S. O. & Brewer, A. a. (2007), 'Visual field maps in human cortex.', *Neuron* **56**(2), 366–383. 123

Warren, P. A., Rushton, S. K., Lloyd, M., Wann, J., Harris, L. & Burr, D. (2009), 'Optic Flow Processing for the Assessment of Object Movement during Ego Movement', *Current Biology* **19**(18), 1555–1560. 104

Warren, W. H. & Hannon, D. J. (1988), 'Direction of self-motion is perceived from optical flow', *Nature* **336**(6195), 162–163. 104

Wässle, H. (2004), 'Parallel processing in the mammalian retina', *Nature Reviews Neuroscience* **5**(10), 747–757. 4

Watson, A. B. & Ahumada, A. J. J. (1983), 'A look at motion in the frequency domain', *NASA Technical Memorandum* (84352). 14

Watson, J. D. G., Myers, R., Frackowiak, R. S. J., Hajnal, J. V., Woods, R. P., Mazziotta, J. C., Shipp, S. & Zeki, S. (1993), 'Area V5 of the Human Brain: Evidence from a Combined Study Using Positron Emission Tomography and Magnetic Resonance Imaging', *Cerebral Cortex* **3**(2), 79–94. 105

Watt, R. J. & Andrews, D. P. (1981), 'APE: Adaptive probit estimation of psychometric functions', *Current Psychological Reviews* **1**(2), 205–213. 37

Watt, R. J. & Morgan, M. J. (1983), 'The recognition and representation of edge blur: Evidence for spatial primitives in human vision', *Vision Research* **23**(12), 1465–1477. 9

Weigelt, S., Singer, W. & Kohler, A. (2012), 'Feature-Based Attention Affects Direction-Selective fMRI Adaptation in hMT+', *Cerebral cortex* pp. 1–10. 121, 131

Werblin, F. S. & Dowling, J. E. (1969), 'Organization of the retina of the mudpuppy, Necturus maculosus. II. Intracellular recording.', *Journal of Neurophysiology* **32**(3). 4

Williams, D. S., Detrett, J. A., Leight, J. S. & Koretsky, A. P. (1992), 'Magnetic resonance imaging of perfusion using spin inversion of arterial water', *Proceedings of the National Academy of Sciences* **89**(1), 212–216. 26

Wohlgemuth, A. (1911), 'On the after-effect of seen movement', *British journal of psychology. Monograph supplements* **1**, 1–117. 46, 75, 82, 136

Woodworth, R. S. & Schlosberg, H. (1954), *Experimental psychology (Rev. ed.)*, Rinehart & Winston, New York: Holt. 36

Wunderlich, G., Marshall, J. C., Amunts, K., Weiss, P. H., Mohlberg, H., Zafiris, O., Zilles, K. & Fink, G. R. (2002), 'The importance of seeing it coming: a functional magnetic resonance imaging study of motion-in-depth towards the human observer', *Neuroscience* **112**(3), 535–540. 133

Wurtz, R. H. (2008), 'Neuronal mechanisms of visual stability.', *Vision research* **48**(20), 2070–89. 89

Wurtz, R. H. & Duffy, C. J. (1992), 'Neuronal correlates of optic flow stimulation.', *Annals of the New York Academy of Sciences* **656**, 205–19. 8

Yu, C. P., Page, W. K., Gaborski, R. & Duffy, C. J. (2010), 'Receptive Field Dynamics Underlying MST Neuronal Optic Flow Selectivity', *Journal of Neurophysiology* **103**(5), 2794–2807. 7

Zeki, S. M. (1974), 'Functional organization of a visual area in the posterior bank of the superior temporal sulcus of the rhesus monkey.', *The Journal of physiology* **236**(3), 549–573. 104

Zonta, M., Angulo, M. C., Gobbo, S., Rosengarten, B., Hossmann, K.-A., Pozzan, T. & Carmignoto, G. (2003), 'Neuron-to-astrocyte signaling is central to the dynamic control of brain microcirculation.', *Nature Neuroscience* **6**(1), 43–50. 28